Tesis para optar al título de
Doctor en Ingeniería
Del Instituto Tecnológico de Buenos Aires

Modelado matemático de procesos discontinuos de polimerización en masa de estireno utilizando iniciadores multifuncionales

Autor: Ing. Emilio Berkenwald

Directores: Dra. Diana A. Estenoz, Dr. Dardo Marqués

Buenos Aires, Argentina
Abril 2016

Modelado matemático de procesos discontinuos de polimerización en masa de estireno utilizando iniciadores multifuncionales

por

Ing. Emilio Berkenwald

En cumplimiento parcial de los requisitos
para optar al grado de

Doctor en Ingeniería
del
Instituto Tecnológico de Buenos Aires

Buenos Aires, Argentina Abril 2016

Mathematical modeling of discontinuous bulk styrene polymerization processes using multifunctional initiators

by

Emilio Berkenwald, Ch. E.

Submitted in partial fulfillment of the
requirements for the degree of

Doctor en Ingeniería

of the

Instituto Tecnológico de Buenos Aires

Buenos Aires, Argentina April 2016

Instituto Tecnológico de Buenos Aires

Departamento Doctorado

Los aquí suscriptos certifican que han asistido a la presentación oral de la Tesis

_____,

cuyo autor es _____, completando parcialmente, los requerimientos exigidos para la obtención del Título de Doctor en Ingeniería.

Fecha: _____

Directora _____

Ph. D.

Tribunal de Tesis _____

Ph. D.

_____

Ph. D.

_____

Ph. D.

Instituto Tecnológico de Buenos Aires

Departamento Doctorado

The undersigned attended the oral presentation of the thesis entitled

_____,

by _____, and recommend its approval.

It has been submitted in partial fulfillment of the requirements for the degree of Doctor en Ingeniería.

Date: _____

Tutor _____

Ph. D.

Members of the Board _____

Ph. D.

_____

Ph. D.

_____

Ph. D.

Agradecimientos

Deseo expresar mi más profundo agradecimiento a todos aquellos que me acompañaron en el transcurso de esta tesis.

A mi directora, Diana, por ser mi modelo profesional en lo académico y por brindarme la orientación, el apoyo y la amistad que me permitieron concretar este proyecto.

A mi co-director Dardo, por el estímulo, por creer en mí y por su participación en mi formación como ingeniero.

A los departamentos de Ingeniería Química y Doctorado del ITBA por haberme dado en el espacio y los colegas el mejor marco para este trabajo.

Al Grupo de Polímeros del INTEC y al Laboratorio de Síntesis de Polímeros del CIQA, por su apoyo, estímulo y calidez humana que me hacen apreciar aún más el ámbito académico.

Al ITBA, ANPCyT, CONICET al CIQA, por el apoyo económico.

A mis padres Alicia y Pedro, por su confianza y apoyo incondicional, y por motivarme siempre a seguir adelante con mis proyectos.

A mi hermano Mariano, mi abuela Sarita y mi tía Margarita, por su compañía y sus abrazos.

A mis amigos, mi familia de la vida, los que saben quiénes son, porque sin ellos no hay aspiración personal, profesional o académica que valga la pena.

A ellos y a todos los que no fueron mencionados anteriormente,

¡Muchas, muchas gracias!

Instituto Tecnológico de Buenos Aires

Resumen

Modelado matemático de procesos discontinuos de polimerización en masa de estireno utilizando iniciadores multifuncionales

por Emilio Berkenwald

Los poliestirenos son termoplásticos del tipo "commodity" que poseen una gran variedad de aplicaciones. La polimerización en masa del estireno por mecanismos de radicales libres es una de las rutas más utilizadas, tanto para la obtención de poliestirenos de uso general como para la de otros tipos de poliestirenos, tales como el poliestireno de alto impacto. La utilización de iniciadores químicos es un aspecto fundamental de este sistema de reacción, ya que posee un efecto directo sobre la productividad del proceso y las propiedades físicas del producto obtenido. El modelado matemático de este proceso de polimerización debe reproducir adecuadamente las características principales de este sistema complejo multivariable y puede ser utilizado para simulación, optimización y control.

En esta tesis, se estudia el uso de iniciadores multifuncionales para la polimerización en masa de estireno. El objetivo general es desarrollar modelos matemáticos detallados, y a la vez genéricos, que permitan describir la compleja fisicoquímica de estos procesos y predecir las variables principales de polimerización, la evolución de la estructura molecular y las características físicas del producto obtenido. La labor teórica se complementa con trabajos experimentales que permiten ajustar y validar los modelos propuestos.

Se introducen los procesos de polimerización de estireno iniciados químicamente y, en especial, se analiza el empleo de iniciadores multifuncionales. Se hace hincapié en el modelado matemático de dichos sistemas, sobre la base de cinéticas complejas e involucrando un gran número de ecuaciones diferenciales no lineales.

Se desarrolla un modelo matemático detallado para la polimerización del estireno en presencia de un iniciador trifuncional cíclico (TPDEC) a temperaturas donde la descomposición del iniciador es secuencial. Se estudia teórica y experimentalmente el efecto de las condiciones de polimerización sobre las características moleculares del producto y sobre la productividad del proceso.

El modelo desarrollado es extendido a fin de considerar rangos más amplios de temperatura, incluyendo el mecanismo de descomposición total del iniciador. Se simulan diferentes condiciones a efectos de determinar las de mayor interés tecnológico para el iniciador. Los resultados teóricos son ajustados y validados utilizando nuevos datos experimentales.

Se propone un modelo matemático genérico para la polimerización en masa discontinua de estireno empleando iniciadores multifuncionales. El modelo permite considerar iniciadores con distintas funcionalidades y estructuras moleculares. Se evalúa y compara teórica y experimentalmente la performance de diferentes iniciadores, tales como el trifuncional cíclico TPDEC, el bifuncional cíclico DPP y el bifuncional lineal L331.

Finalmente, se presenta un modelo matemático para la polimerización en masa de estireno en presencia de polibutadieno para la producción de poliestireno de alto impacto utilizando iniciadores multifuncionales. El modelo permite estimar la evolución y la estructura molecular del poliestireno libre, polibutadieno residual y copolímero de injerto, así como variables de interés para el procesamiento del material tales como el índice de fluidez (MFI). El modelo es ajustado y validado utilizando resultados experimentales.

Instituto Tecnológico de Buenos Aires

Abstract

Mathematical modeling of discontinuous bulk styrene polymerization processes using multifunctional initiators

by Emilio Berkenwald

Polystyrenes are commodity thermoplastics with a wide range of applications. Bulk polymerization of styrene by free-radical polymerization is one of the most widespread routes for obtaining both general purpose and other polystyrene types, such as high impact polystyrene. The use of polymerization initiators is a key feature of this reaction process, and has a direct effect on both process productivity and physical properties of the obtained product. The mathematical modeling of this process must adequately simulate the main features of this complex multivariable system and could be used for simulation, optimization and control purposes.

In this thesis, the use of multifunctional initiators for the bulk polymerization of styrene is examined. The general objective is to develop both detailed and generic mathematical models that describe the complex physics and chemistry of these processes, to predict the main polymerization variables, the evolution of the molecular structure and the physical characteristics of the obtained product. The theoretical labor is complemented with experimental work that allow to adjust and validate the proposed models.

An overview of chemically-initiated styrene polymerization systems and the problematic addressed by the use of multifunctional initiators is presented. Special emphasis is made on the modeling of said reacting systems, based on complex kinetics and a large number of non-linear differential equations.

A detailed mathematical model for the discontinuous bulk polymerization of styrene using a trifunctional cyclic initiator (DEKTP) is presented, considering temperatures where initiator decomposition is sequential. The effect of polymerization conditions on process productivity and the molecular characteristics of the obtained product is investigated.

The developed model is extended in order to consider wider temperature ranges, including the total decomposition mechanism of the initiator. Different conditions are simulated in order to determine the working zones of technological interest for the initiator. The theoretical results are adjusted and validated using new experimental data.

A generic mathematical model for the batch bulk polymerization of styrene using multifunctional initiators is presented. The model considers initiators with different functionalities and molecular structure. The performances of the initiators DEKTP (cyclic trifunctional), PDP (cyclic bifunctional), L331 (linear bifunctional) are evaluated and compared.

Finally, a mathematical model for the bulk polymerization of styrene in the presence of polybutadiene, for producing high impact polystyrene using multifunctional initiators is presented. The model allows estimating the evolution and molecular structure of free polystyrene, residual polybutadiene and graft copolymer, as well as variables related to the processing, such as the melt flow index (MFI). The model is adjusted and validated using experimental results.

Contents

List of Figures

List of Tables

Preface

Polystyrenes are extensively used materials, ranging from products of everyday use to engineering thermoplastics. Among the latter, high impact polystyrene (HIPS) has become one of the most important heterogeneous polymers. The presence of an elastomeric phase in HIPS provides an improved impact resistance, without a significant loss in mechanical and processing properties.

The industrial styrene polymerization processes aim at obtaining materials with a given set of final properties, while achieving a high productivity. To this end, the use of chemical initiators for triggering the chain polymerization reaction has been widely increased over the last few decades. The specialty chemicals used as initiators are the focus of research, with new compounds being continuously developed. In particular, multifunctional initiators have gained industrial relevance, since they have shown to be efficient to achieve high polymerization rates, high molecular weights and good reaction control.

Even though the technology employed in the synthesis of polystyrenes has been developed over the last six decades, there are still non-elucidated aspects regarding kinetics of complex systems, as well as structure-properties relationships. Mathematical models have been developed in order to theoretically study styrene polymerization processes. These models can be used for process simulation and control purposes, as well as for developing new recipes to obtain "tailor-made" materials. With the advent of improved numerical methods and reduced calculation times, the use of these models for simulation of industrial process has gained momentum and is nowadays a field of technological interest.

The use of new compounds as polymerization initiators, namely multifunctional initiators, can be studied with the aid of deterministic mathematical models. This approach

allows a better understanding of the physics and chemistry of the more complex polymerization processes and at the same time develops relevant tools to be used for industrial simulation purposes. Mathematical models involving certain multifunctional initiators are available, but there has been no attempt at developing a general framework or comprehensive models. In addition, no works address systems in which an initiator can simultaneously suffer two types of decomposition reactions. Finally, the effect of initiator functionality and molecular structure in styrene polymerization processes has not yet been thoroughly studied from a theoretical standpoint.

Considering all of the above, the development of mathematical models in the synthesis of polystyrenes using multifunctional initiators represents a challenge in the field of research. Therefore, the main objective of this thesis is to develop mathematical models for complex styrene polymerization processes using multifunctional initiators in order to study: i) the polymerization of styrene using a cyclic trifunctional initiator that can suffer two types of decomposition reactions, ii) the effect of initiator functionality and structure in a styrene polymerization process, and iii) the synthesis of high impact polystyrene using multifunctional initiators. The theoretical developments are complemented with experimental work in order to evaluate the performance of the multifunctional initiators and adjust and validate the mathematical models.

Chapter 1

Introduction

1.1 Styrene and polystyrene materials

Styrene (St), known commercially as styrene monomer (SM), is one of the simplest and most important unsaturated aromatic monomers [1]. It was initially isolated by distillation of a natural occurring resin [2] and is currently typically obtained from dehydrogenation of ethylbenzene, which is in turn obtained from benzene and ethylene, all derived from petroleum refining.

Global production of SM was $26 \cdot 10^6$ t in 2012 [3], with a market value of around 40 billion USD [4, 5]. Its manufacture consumes more than half the commercial benzene in the world. Asia accounts for the production of approximately 50% of the world St output, followed by Europe and North America [3]. SM is considered to be a commodity chemical, due to its large production volume and low cost [1].

Due to the presence of the vinyl group, St is highly reactive and can readily polymerize in air [2].

Styrene polymers include a broad range of types, from commodity plastics to engineering polymers. Polystyrene (PS) accounts for about 65% of St use and over $12 \cdot 10^6$ t of PS are commercialized each year [6]. PS homopolymer is easy to extrude and mold, it is one of the volumetrically least expensive thermoplastics [1]. In addition, the characteristics of St copolymers allow a wide range of applications. Due to the

high demand and expected growth of St polymers, there is an interest to improve and optimize the industrial production techniques.

1.1.1 General purpose polystyrene

General purpose polystyrene (GPPS) or crystal polystyrene are common names for the linear PS homopolymer. Due to its chemical structure, GPPS is an vitreous solid for temperatures up to the glass transition temperature T_g of around 100 °C [6]. GPPS possesses a high resistance to mechanical compression below the T_g, which allows it to be used for load bearing. Above the T_g, polystyrene behaves as a viscoelastic melt whose viscous properties are strongly related to the average molecular weight of the polymer, while the polydispersity greatly influences the shear compliance [7].

The main characteristics of GPPS as a material are stiffness, brilliance, gloss, hardness and a high refractive index. It is often used in audio/video cassettes packs, beakers, transparent food packagings, lamp covers, etc. [2].

1.1.2 Expanded polystyrene

Expanded polystyrene (EPS) is obtained from a polystyrene foam by addition of around 6% of a blowing agent (e.g. pentane) during the polymerization process [6]. These foams can then be molded into lightweight, closed-cell, low cost materials [2]. The density of an EPS foam can range from 10 to 30 kg/m^3, depending on its particular use [8].

The technical properties of EPS, such as low weight, rigidity and formability, allow a wide application range. It is widely used in packaging because of its good damping properties and as an insulator in the construction industry due to its very low thermal conductivity (0.03–0.004 W/m·K) [8]. It is additionally used in cold-storage refrigeration, cut ceiling ties [2] and for producing molded articles by “lost-foam” casting [8].

1.1.3 Heterogeneous styrene polymers

The addition of an elastomer or rubber can enhance some of the mechanical properties of St polymers [2] compared to the inherently brittle GPPS [9].

While GPPS and EPS are homopolymeric materials, high impact polystyrene (HIPS) and acrylonitrile butadiene styrene (ABS) are the most important heterogeneous St thermoplastics [10].

In the synthesis of HIPS, polybutadiene (PB) is the most commonly used rubber, although in some cases block copolymers consisting of St and butadiene (B) blocks are used. The final product consists essentially of a mixture of approximately 80% free PS, 18% B$-g-$St graft copolymer (GC) and 2% residual PB [11]. The microstructure of HIPS consists of a free PS matrix with a dispersed rubber phase (particles), which is in turn heterogeneous in nature. These rubber particles can present different morphologies as observed in a microscope, with the "salami" and "core-shell" types being those of most commercial interest (see Figure 1.1). In the former, particle diameter is around 2-5 μm and there are several free PS occlusions. In the latter, the particles have diameters smaller than 1 μm and present single occlusions [12]. Core-shell morphologies occur commonly in HIPS synthesized from diblock St, B copolymers [13] and allow obtaining transparent grades of HIPS (Transparent Impact Polystyrene, or TIPS). Other, less common morphologies have also been reported [14].

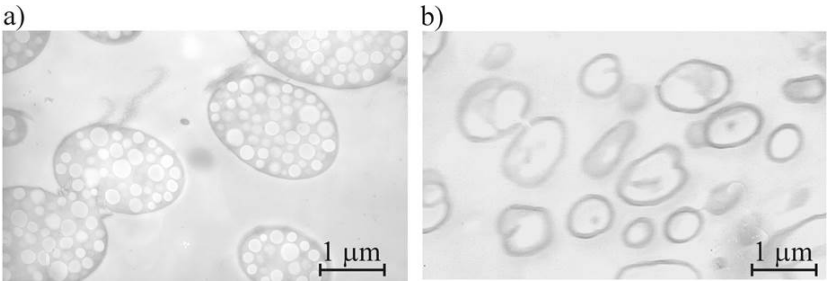

FIGURE 1.1: Typical HIPS morphologies: a) salami, b) core-shell [12].

ABS is a graft terpolymer, mainly synthesized by polymerizing a mixture of acrylonitrile (AN) and St in the presence of a rubber. The copolymerization generates a random copolymer of St and AN (SAN), of uniform chemical composition during the course of the reaction. The morphologies obtained in a bulk polymerization process are similar to those of HIPS, where the occluded rubber particles are dispersed in a vitreous SAN matrix [10].

Typical values for the properties of various St polymers (GPPS, SAN, HIPS and ABS) are presented in Table 1.1 [1, 2, 6]. With the exception of transparency and elastic modulus, it is observed that the increase in impact resistance does not necessarily result in a significant deterioration of other final properties [10].

Property	**GPPS**	**HIPS**	**SAN**	**ABS**
Density (kg/m^3)	1.05	1.03–1.05	1.07–1.25	1.04–1.21
Melt Flow Index[a] (g/10 min)	1–30	2–20	1–40	1–45
Elastic Modulus (MPa)	3000–3400	1400–2800	3400–3900	1800–3200
Yield Strength (MPa)	35–60	20–45	42–82	29–65
Rupture Elongation (%)	1.5–3.0	25.0–70.0	1.0–7.0	2.0–110.0
Impact Resistance[b] (kJ/m^2)	1–2	5–13	1–2	16–28
Softening Temperature[c] (°C)	78–102	75–97	107–111	91–108
Thermal Conductivity (W/m·K)	0.16–0.17	0.16–0.17	0.11–0.19	0.13–0.19
Transparency	Transparent	Opaque[d]	Transparent	Opaque[d]

[a]200 °C, 5 kg, [b]Charpy,[c]Vicat (50 °C/h, 5 kg). [d]Polymers with small particle diameters may be transparent.

TABLE 1.1: Mechanical properties of styrene polymers[1, 2, 6]

Due to its improved mechanical properties, HIPS is commonly used in packagings, household appliances, toys and construction, with packaging accounting for more than 30% of its use [2]. Due to the presence of the polar AN group, ABS provides a higher chemical resistance and good surface finishing. More than 50% of the global ABS production is used by the household appliances and automotive parts industries, namely for car bumpers and dashboard trim kits [15].

1.2 Polystyrene production processes

Currently, PS and HIPS materials are mainly produced by continuous polymerization processes [6], as expected for products with a high production volume and low value. The plant setup generally comprises a polymerization section, a devolatilization section and a pelletizing section. In the polymerization section, a continuous stirred-tank reactor (CSTR) is commonly used, and a second stirred-tank or tubular plug-flow reactor can be added to increase conversion. The removal of the heat of polymerization (around 71 kJ/mol [6]) and the handling of highly viscous melts are the most difficult aspects of the industrial operation [16].

The polymerization reactions commonly proceed via free-radical polymerization (FRP) mechanisms, which will be discussed in further detail below (see 1.3.1). Even though St polymerization occurs spontaneously at high temperature by thermal initiation [17], a polymerization initiator (see 1.3) is usually added to generate the radical species via chemical initiation, providing a better control of the polymerization rates, as well as the morphology in the case of heterogeneous materials [11].

1.2.1 Bulk polymerization

The bulk polymerization reaction can be carried in the monomer phase or in a highly concentrated monomer-containing solution. In the former case, the higher reagent concentration provides higher polymerization rates and better final properties, although high polymerization rates increase heat removal requirements. A solvent (e.g. toluene or ethylbenzene) may be added in small proportions (5–15%) to provide better control of the polymerization rate, melt viscosity and cross-linking reactions of the rubber phase, in the case of HIPS [11]. The solvent, as well as the unreacted monomer, are removed in the devolatilization (or degassing) section.

For HIPS production, the polymerization section is divided into a prepolymerization and a finishing stage, in a series of three to five reactors [11]. The morphology of the material is developed in the prepolymerization stage until around 15–30 % conversion. Higher conversions are reached in the finishing stage, commonly using non-stirred tower or tubular reactors, in order to preserve particle morphology. A flow diagram of different plant setups for HIPS production, according to technology owners, is presented in Figure 1.2.

In the CSTRs, heat removal is usually achieved by means of reflux cooling, using the evaporation of the monomer and condensers with a high surface area. Anchor stirrers, impellers, or helical ribbon agitators are commonly used for the effective mixing of the reactor contents. The reactor commonly operates at temperatures comprised between 100 and 170 °C and pressures of 0.5 to 2 bar [6].

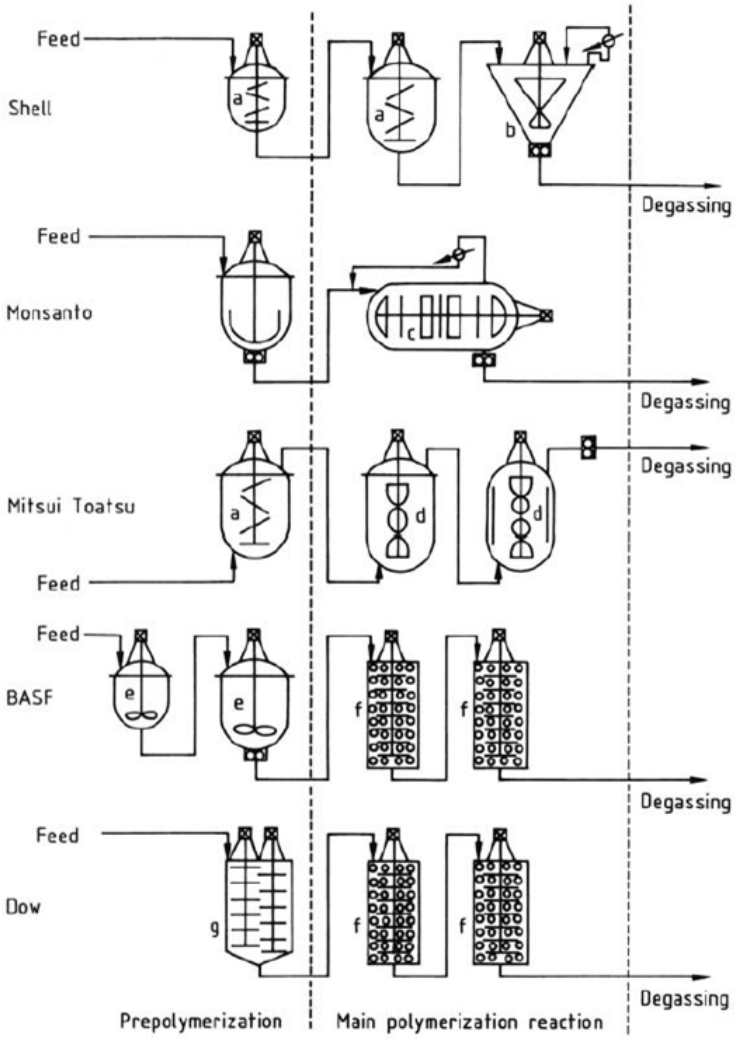

FIGURE 1.2: Plant configurations for HIPS production: a, b, d and g are stirred-tank reactors, c is a horizontal plug-flow reactor and f is a tower reactor [6].

1.2.2 Emulsion polymerization

Emulsion polymerization leads to the production of a fine dispersion of a polymer in a continuous medium (latex). This stable suspension has particle sizes in the order of 10–100 nm and particle concentrations of around 10^{14}–$10^{29}\mathrm{L}^{-1}$ [18].

Typically, emulsion polymerization is carried out in stirred-tank reactors, commonly operating in semi-batch mode. Batch and continuous operations are also possible [19].

As in batch emulsion polymerization, a monomer mixture is dispersed in water by means of a surfactant, which stabilizes the droplets, either by ionic (electrostatic) or non-ionic (steric) effects. The excess of surfactant forms micelles that are swollen with monomer. A free-radical polymerization reaction is chemically initiated with a water-soluble initiator.

The formed radicals enter the micelles and the reaction generates a polymer particle, either by homogeneous or heterogeneous nucleation.

Compared with bulk and solution polymerization, emulsion polymerization is advantageous because the low viscosity of the latex allows high heat removal rates. In addition, the water absorbs large amounts of heat with only a moderate increase in temperature. This allows combination of high polymerization rates and good temperature control [19].

Emulsion polymerization is the main production process for ABS, as well as other St and butadiene copolymers, such as Styrene-Butadiene Rubber (SBR). This type of polymerization allows better control of the particle morphology and presents a higher versatility for the incorporation of high amounts of rubber, compared to bulk processes [2].

Due to the lack of industrial processes employing emulsion polymerization for GPPS or HIPS production, this type of polymerization process is outside the scope of this thesis.

1.2.3 Suspension polymerization

In a suspension polymerization process, St is dispersed in water with addition of a suspension agent to stabilize the organic phase. Each of these droplets then acts as a microreactor (see Figure 1.3) where the reaction proceeds by addition of an initiator. Temperatures (80–110 °C) are usually lower than those involved in bulk processes [6].

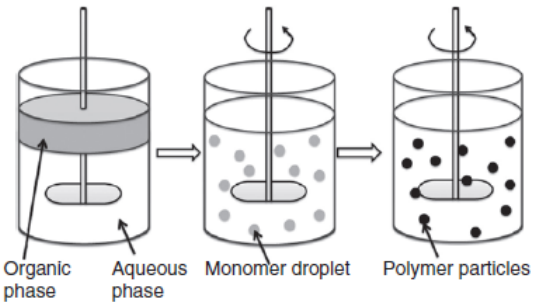

FIGURE 1.3: Schematic representation of suspension polymerization [18].

The effective viscosity of the reacting solution remains low during the polymerization process, so efficient agitation is possible [19]. This results in better temperature control, which has a direct effect on polymerization rates, molecular weights and copolymer composition.

Monomer droplets are converted to small polymer particles, with diameters in the order of 100 μm, which settle as soon as agitation is stopped. Particle size distribution is an important variable in suspension polymerization processes [20], and depends on the choice of the suspension agent, as well as reactor design. If the polymer is soluble in the monomer, such as PS, the suspension polymerization process will form "beads" or non-porous polymer particles. When the polymer is insoluble, irregular grains or particles are formed by precipitation, leading to a "powder" polymer [18].

Suspension polymerization is the main process used in the synthesis of EPS. In addition, the combined bulk-suspension process is sometimes used in HIPS production [6]. SAN copolymers are also largely produced using this type of polymerization process [19].

It should be noted that the kinetics of suspension polymerization are similar to that of bulk and solution polymerization [18], so that mathematical models developed for the latter can be used in suspension polymerization systems.

The main advantages and drawbacks of the different types of polymerization processes are summarized in Table 1.2. It should be noted, however, that the choice of a given process will also depend on t.he desired final properties for the synthesized material.

Process	**Advantage**	**Drawback**
Bulk	Simplicity, good product clarity.	Difficult temperature control, highly viscous materials.
Solution	Good temperature control.	Use of solvent reduces molecular weights and polymerization rates.
Bulk–Solution	Homogeneous product, good product clarity and color, low volatile species content.	Highly viscous materials.
Suspension	Excellent temperature control, simple reactors, high conversions.	Possible contamination with water and/or suspension agent.
Emulsion	Excellent temperature control, fast reactions.	Possible contamination with water and/or surfactant, poor product clarity and color, broad molecular weight distribution.

TABLE 1.2: Polystyrene production processes advantages and drawbacks [21].

1.3 Polymerization initiators

1.3.1 Free-radical polymerization

Since St is both a donor and acceptor of electrons, it can be polymerized by free-radical, anionic, cationic or coordination reactions. In spite of this versatility, GPPS, HIPS and ABS are industrially synthesized almost exclusively by free-radical polymerization (FRP) [10], given its simplicity and good reproducibility.

From an industrial stand-point, a major virtue of FRPs is that they can often be carried out under relatively undemanding conditions. In general, high molecular weight polymers can be produced without removal of the stabilizers present in commercial monomers, in the presence of trace amounts of oxygen, or in solvents that have not been rigorously dried or purified [22].

Free-radical polymerization, like other chain growth mechanisms, involves the sequential addition of monomers to an active center, i.e. radical species. In general, a bulk St FRP reaction involves steps of initiation, propagation, transfer and termination. In the traditional kinetic approach, each of these steps consists of a series of elementary chemical reactions [21]. The active centers that can start the polymerization reaction as a result of the initiation step are *initiating radicals*.

Styrene polymerizations can be initiated simply by applying heat [17, 23, 24]. In this case, the initiating radicals are derived from reactions involving only the monomer. Several mechanisms for spontaneous thermal St initiation have been proposed [23], with the Mayo and Flory mechanisms being the most widely accepted [24]. In the first mechanism, thermal initiation proceeds by a Diels-Alder dimerization of St, followed by assisted homolysis [22, 23] between the dimer and a third St molecule, generating two initiating monoradicals. For the second mechanism, Flory proposed that St dimerizes to form a diradical and a third St abstracts a hydrogen atom from the diradical to generate a initiating monoradical. Molecular modeling studies have found the Diels-Alder dimer to be the key intermediate for the reaction, thus favoring the mechanism proposed by Mayo [24].

Industrially, even though the controlled thermal polymerization would theoretically produce the highest molecular weights in a St FRP process, undesirable spontaneous polymerizations could clog production facilities [24]. In addition, as previously stated, if temperatures are low the polymerization rate would be too low for the process to be economically advantageous. In practice there must be a compromise between polymer productivity, mainly related to polymerization rate, and product quality, mainly related to molecular weight [18]. For these reasons, polymerization initiators are widely used in industrial polymerization processes [6, 22]. Removal of initiator residues from the finished product is not needed in most cases, avoiding possible purification steps [25].

Polymerization initiators are chemical species that contain thermally labile radical-generating functional groups. They are added to the recipe in a small proportion, usually $< 1\%$ by weight based on the monomer [26]. The use of chemical initiators has been found to increase the polymerization rates, while keeping molecular weights at acceptable levels.

The decomposition of a labile group in a polymerization initiator generates a primary radical, which adds to the St C–C double bond to form an initiating radical. This decomposition can be characterized by the rate of decomposition k_d or its half-life time, given by[1]

$$t_{1/2} = \frac{\ln 2}{k_d} \tag{1.1}$$

Most conventional polymerization processes require values of k_d in the range of $10^{-6} - 10^{-4}$ s^{-1}, i.e half-life times in the order of 1–100 h. Initiators typically have acceptable half-life times only within a relatively narrow temperature range, around 20–30 °C [22]. The dependance with pressure is very weak and should only be considered for very high pressure systems [19].

Given their technological value, polymerization initiators are the object of a number of patents and patent applications [27–33].

The two most important types of polymerization initiators contain azo or peroxide groups as labile groups. Due to their very limited use in industrial process, other types of polymerization initiators, such as carbon-carbon and photochemical initiators, will not be considered in this thesis.

[1] Equation 1.1 is strictly only valid for initiators that suffer unimolecular decomposition.

1.3.2 Azo compounds

Dialkyldiazenes and dialkyl hyponitrites are the main classes of azo initiators.

Dialkyldiazenes, of general formula R−N=N−R′ are sources of alkyl primary radicals. Most dialkyldiazenes employed as polymerization initiators are symmetrical, and their substituents are usually tertiary, which gives the generated radical greater stability. The most common compounds of this category include 2,2'-azobis(isobutyronitrile) (AIBN), 1,1'-azobis(cyclohexanecarbonitrile) (ACBN), 2,2'-azobis(2-methylbutanenitrile) and 4,4'-azobis(4-cyanovaleric acid), as shown in Figure 1.4. Asymmetrical dialkyldiazenes, such as triphenylmethyl-azobenzene yield radicals with different reactivities, and are frequently used in controlled polymerization reactions [22].

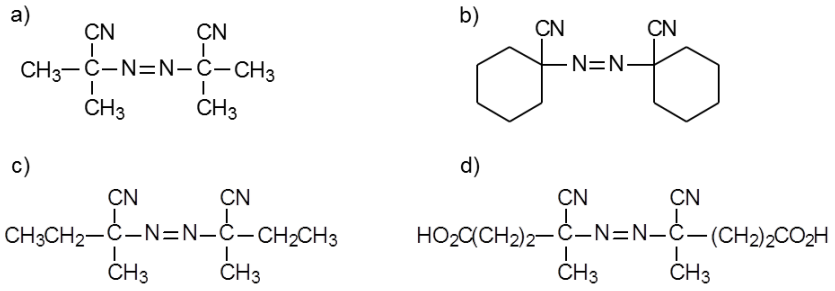

FIGURE 1.4: Symmetrical dialkyldiazene initiators: a) AIBN, b) ACBN, c) 2,2'-azobis(2-methylbutanenitrile) and d) 4,4'-azobis(4-cyanovaleric acid).

Hyponitrites, of general formula R−O−N=N−O−R′ and esters of hyponitrous acid (HO−N=N−OH), are sources of alkoxy or acyloxy primary radicals. Their use as polymerization initiators is limited because of their complex synthesis methods and low commercial availability [25].

The main characteristics of selected azo initiators are presented in Table 1.3. As the temperature ranges are in the lower values, these types of initiators are mainly used in suspension or emulsion polymerization systems. Water-soluble initiators, suitable for these types of polymerization, include 4,4'-azobis(4-cyanovaleric) acid and amidinium hydrochlorides. The byproducts of decomposition of certain dialkyldiazenes can be a concern and can require purification of the obtained polymer [22].

Arkema and DuPont are the main worldwide producers of azo initiators, although their market is small compared to that of peroxide initiators [1].

1.3.3 Peroxides

Peroxides, of general formula R−O−O−R′, are widely used as polymerization initiators. Among the most used peroxide types are diacyl peroxides, peroxycarbonates, peroxyesters, dialkyl peroxides, hydroperoxides and inorganic peroxides (e.g persulfate) [22]. Dibenzoyl peroxide (BPO) and dilauroyl peroxide (LPO) are among the most common diacyl peroxide initiators, which are sources of primary alkyl radicals (see Figure 1.5). The main characteristics of selected peroxide initiators are presented in Table 1.3. Given that some peroxides are suitable initiators in a higher value temperature range, peroxide initiators are suitable for bulk polymerization processes.

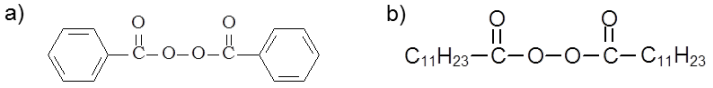

FIGURE 1.5: Peroxides initiators: a) BPO, b) LPO.

The relative ease of synthesis of peroxide type initiators compared to azo compounds makes their industrial use advantageous [25]. The leading producers of organic peroxide initiators are Arkema (with trade names such as Luperco, Luperox, Lupersol), Akzo (Trigonox, Perkadox) and Solvay. The worldwide market of peroxide initiators is about 10 times larger than the market for azo initiators [1]. It is worth around 1.5 billion USD and expected to have a growth of about 6.6 % until 2020 [34].

1.3.4 Multifunctional initiators

Multifunctional or polyfunctional initiators are chemical species with more than one radical-generating group. This category includes polyperoxides, polyazo compounds and azoperoxidic compounds. The chemical structure of the multifunctional initiators studied in this thesis are presented in Figure 4.1.

Multifunctional initiators may suffer two types of decomposition reactions.

Total or concerted decomposition can occur in initiators where radical generating labile groups are in appropriate proximity, such as in peroxyoxalate esters and α-hydroperoxy diazenes [22]. In addition, it may also occur in cyclic perketals [35] as well as cyclic multifunctional peroxide initiators [25, 36], depending on reaction temperature. In this decomposition mechanism, all labile groups decompose simultaneously.

Sequential or non-concerted decomposition- occurs when labile groups are sufficiently remote from each other [22] and generate radical species that may contain undecomposed labile groups. The labile groups decompose, generating new primary radicals and re-initiating the polymerization reaction. Bis-diazenes [22], azoperoxides [37, 38] and several polyperoxides [25, 39–41] present this decomposition behavior. Some cyclic compounds can be too sterically hindered for sequential decomposition to be possible, and thus fail to initiate the reaction [25]. Styrene polymerization was successfully achieved with certain cyclic peroxides [25, 36, 42] and it was found that the thermolysis of peroxide bonds in cyclic polyperoxide initiators involves diradical species [25]. The polymerization mechanism may cause the polymer species to contain these undecomposed labile groups, either at the chain end [39] or within the polymer chain [43]. The subsequent decomposition -second decomposition in the sequential mechanism- may form long chain radicals.

The use of multifunctional initiators has been increased in the recent decades, since they allow obtaining high polymerization rates and polymers with high average molecular weights, as a consequence of the sequential decomposition of the initiator [25, 39, 41]. Azoperoxidic compounds are also employed in the production of block and graft copolymers due to the different decomposition rates of the azo and peroxide groups [22, 44, 45].

Polyperoxide initiators are often categorized according to their "active oxygen content", [46–48] corresponding to the weight percentage of the active oxygen atoms (i.e. one per peroxide group) in the initiator molecule.

1.4 Modeling, optimization and control of styrene free-radical polymerization

Industrial bulk St polymerization process may optimized in order to maximize productivity or obtain a product with pre-specified final properties. Both productivity and physical properties are intimately related to the recipe and operating conditions (i.e. reaction temperature, reagent concentration, etc.) of the polymerization process. PS production processes are highly complex and involve a large number of interrelated variables.

TABLE 1.3: Main characteristics of St polymerization initiators.

Initiator	**Name**	**Type**	**Solvent**	**Temperature range** (°C)	**10 h $t_{1/2}$** (°C)	**Reference**
AIBN	2,2'-azobis(isobutyronitrile)	dialkyldiazene	benzene	37–105	65	[22]
ABCN	1,1'-azobis(cyclohexanecarbonitrile)	dialkyldiazene	toluene	80–100	88	[22]
ACVA	4,4'-azobis(4-cyanovaleric acid)	dialkyldiazene	water	60–80	70	[49]
BPO	Dibenzoyl peroxide	diacyl peroxide	benzene	38–80	78	[22]
LPO	Dilauroyl peroxide	diacyl peroxide	benzene	35–70	66	[22]
DBPOX	di-tert-butyl peroxalate	peroxyester	benzene	35–55	26	[22]
TBPO	ter-butyl peroctoate	peroxyester	benzene	70–100	74	[41]
DTBP	di-tert-butyl peroxide	dialkyl peroxide	benzene	100–135	125	[22]
$K_2S_2O_8$	potassium persulfate	inorganic peroxide	NaOH	50–90	69	[22]
L101	2,5-bis(tert-butylperoxy)-2,5-dimethylhexane	linear diperoxide	benzene	115–145	120	[49]
PDP	pinacolone diperoxide	cyclic diperoxide	styrene	100–130	107	[36]

From a process control stand-point, an industrial polymerization process generally presents a total of four control loops [50], as shown in Figure 1.6. A first inner loop considers the process variables that are measured and controlled, such as temperature, pressure, flow rate and reactor level. Said loop is usually closed by feedback controllers. A second, more external loop considers properties to be measured off-line, which specify product quality (e.g., average molecular weights, melt flow index, mechanical properties). Said loop is closed by the process engineer. A third loop is closed by consumers, which process the material and define the required properties. A fourth loop considers the final application of the product and is closed by global demand, usually by means of the adjacent inner loop [10, 50].

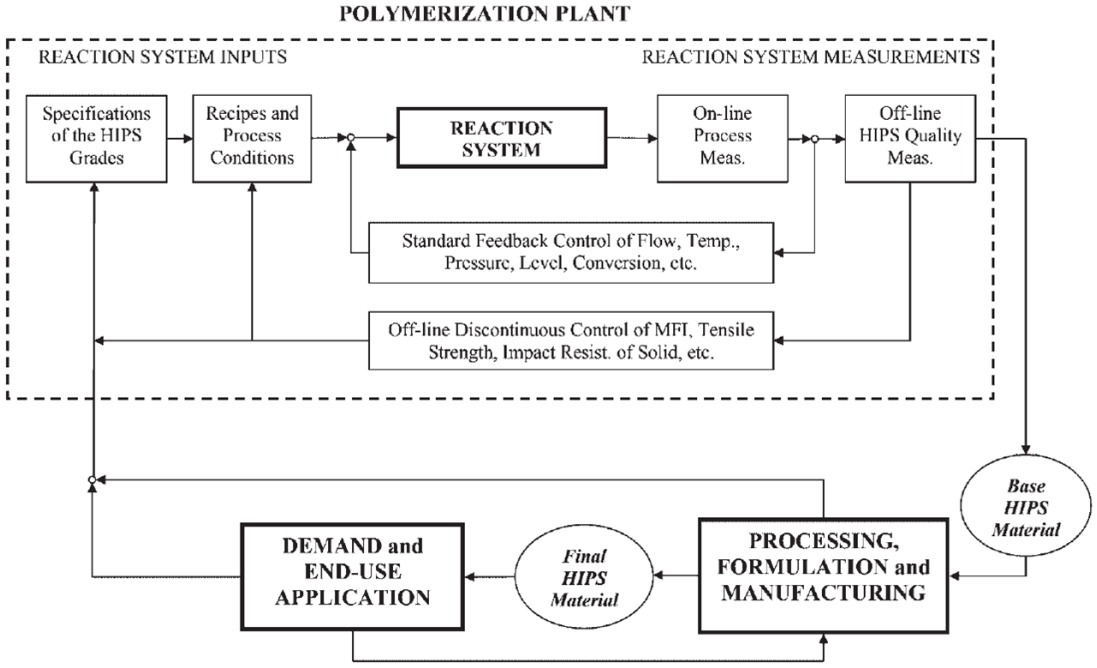

FIGURE 1.6: Control loops in an industrial HIPS polymerization process [50].

There are numerous molecular features that can have an impact on the final application properties of polymers. The molecular structure–properties relationships for most polymer materials remains poorly understood and relies heavily on empirical observation and testing [10]. In addition, as these relationships are very often strongly non-linear, advanced non-linear control techniques are to be used in many process applications [16].

Both optimization and process control generally rely on the availability of adequate mathematical models for the polymerization process [51]. Detailed models, which provide valuable information on how operation variables affect the molecular structure of produced polymer materials, are highly desirable for control of end-use properties.

For these reasons and due to the availability of better computational tools, the development of mathematical models for St polymerization processes has significantly grown over the last decades [18, 51–54]. Industrial applications of these models in the production of St polymers include simulation of an continuous industrial HIPS plant [11], determination of residence times in reactors using computational fluid dynamics [55], optimization of time between steady-state operations [56, 57], product grade transitions [50] as well as determining stability for open-loop control of a HIPS production process [58].

Most mathematical models that are suitable for optimization and control purposes are mechanistic -or deterministic- models, based on the mass balance equations for the polymerization system. For homogeneous systems, said equations are written as follows [11]:

$$\frac{d}{dt}\left([R_i]V\right) = \dot{Q}_{\text{in}}[R_i]_{\text{in}} - \dot{Q}_{\text{out}}[R_i]_{\text{out}} + \sum_j r_{ij}V \tag{1.2}$$

where $[R_i]$ is the volume average concentration of chemical species R_i in the reaction volume V, $\dot{Q}$ is the volume flow rate, subscripts "in" and "out" designate inlets and outlets and r_{ij} is the rate of reaction of species i in reaction j. The term involving the rates of reactions are derived from a kinetic mechanism for the polymerization reaction. In general, these mechanisms consist of a series of elementary reactions, for which the rate can be expressed as

$$r_{ij} = \nu_{ij} k_{ij} \prod_m [R_m]^{\alpha_m} \tag{1.3}$$

where ν_{ij} and k_{ij} are respectively the stoichiometric and kinetic coefficients for reaction j of species i, and the product involves all chemical species m in reaction j and α_m is the partial order of reaction with respect to that species.

The use of mechanistic models is justified when a basic understanding of the system is needed or when the state of the art is advanced enough to make a useful mechanistic model easily available [51].

Since every radical and polymer species must be considered in the balance equations, these mathematical models often consist of a very high number of ordinary differential equations. Because of the different orders of magnitude of the kinetic parameters, these systems are usually stiff and require specific numerical methods for their resolution.

In addition, polymerization processes have several characteristics that should be considered when developing detailed mathematical models. Volume contraction, a consequence of the differences in the densities of monomer and polymer, is accounted for by a linear decrease in reaction volume with increasing monomer conversion. This effect can generate a change in volume of up to 20 % in bulk St polymerization [19]. The gel effect, due to diffusion-controlled radical termination in a viscous medium, is also a major feature of bulk St polymerization systems. There are several different approaches to model this effect [17, 59, 60], it is generally accepted that the gel effect can be accounted for by appropriately reducing the value of the termination rate constant, either with increasing conversion [17] or average molecular weight [18], both of which are related to the increase in viscosity.

Mechanistic models for relatively simple St polymerization processes, e.g. thermal polymerization [17, 61–64], and polymerization using monofunctional initiators have been widely available. Said low-dimensionality systems can be successfully dealt with using analytical or simple differential methods [19]. Full information about the detailed molecular weight distribution (MWD) is readily available from the mass balances. Chemical species in these systems are usually characterized as R_n, where n is the kinetic chain length.

Systems involving more complex kinetics, e.g. using multifunctional initiators, usually yield higher-dimensional polymerization models. In particular, considering the sequential decomposition of a multifunctional initiator, polymers with undecomposed labile groups may form. If a mechanistic model is sought, a chemical species $R_n^{(i)}$ is characterized by chain length n as well as number of undecomposed labile groups i. Non-linear kinetics are also frequent in these types of systems [19]. It should also be noted that for cyclic multifunctional initiators, diradical species are expected to be involved in the polymerization mechanism [25].

Given the technological relevance of multifunctional initiators in St polymerization processes, they have been the subject of numerous theoretical and experimental works. The use of bifunctional initiators has been thoroughly studied [35, 39, 41, 43, 65–73], while works related to the use of initiators of a higher functionality are less numerous [25, 42, 74–79]. Several methods are used to overcome the mathematical complexity of these polymerization systems, with the method of moments being the most widely used.

This method reduces the dimension of the problem, leading to averaging in one of the dimension with the consequent loss of information about the full MWD [19]. Transform techniques, such as the probability-generating functions can also be applied in order to estimate the full MWD of the obtained polymer [73, 80, 81]. These polymerization systems have also been studied using stochastic techniques, namely the Monte Carlo method [82–84].

None of the mathematical models for St polymerization using multifunctional initiators available in the literature are "generic", as they cannot be readily applied to initiators of any given functionality. Theoretical studies of the influence of initiator functionality and structure are relatively scarce.

It should also be noted that no mathematical models consider both sequential and total decomposition mechanisms for multifunctional initiators. The predominance of either decomposition mechanism for a given initiator can be a function of reaction temperature. Since the sequential decomposition is generally considered the cause of the higher molecular weights provided by multifunctional initiators [39, 41], the decomposition mechanism of the initiator could define a temperature zone of technological interest for its use. It is generally accepted that initiators that decompose sequentially at a given temperature may decompose totally at higher temperatures [25, 36] If a temperature is selected such that initiator decomposition is total, its use will present little or no advantage over using a monofunctional one [26].

In the particular case of the synthesis of HIPS, bifunctional initiators have been theoretically and experimentally evaluated [41], while only experimental results for a trifunctional initiator are available [76]. Modeling a HIPS polymerization process involves complex co-polymerization kinetics and a much larger number of chemical species [41, 85, 86] and structure-properties relations may be needed in order adequately characterize the obtained material [10].

In view of the above, the general objective of this thesis is to theoretically and experimentally study bulk St polymerization processes using multifunctional initiators and to develop detailed mechanistic mathematical models that could suit industrial optimization purposes in the obtention of GPPS, HIPS and other St polymers.

The particular objectives are:

- To develop, adjust and validate a detailed mathematical model for bulk St polymerization using the cyclic trifunctional initiator DEKTP at temperatures of $120 - 130$ °C where decomposition is mostly sequential.

- To extend, re-adjust and re-validate the previous mathematical model to temperatures of $150 - 200$ °C in order to consider the total decomposition of DEKTP and develop a tool to evaluate the working zone of technological interest.

- To develop, adjust and validate a comprehensive detailed mathematical model for bulk St polymerization using multifunctional initiators of any given functionality and structure.

- To develop, adjust and validate a comprehensive detailed mathematical model for a HIPS polymerization system and predict product quality variables for process simulation purposes.

All theoretical developments are complemented with experimental work that allow to experimentally study the effect of the use of multifunctional initiators on polymer characteristics, as well as adjust and validate the mathematical models.

Chapter 2

Bulk styrene polymerization using the trifunctional cyclic initiator DEKTP at low temperatures (120–130 °C)

2.1 Introduction

The industrial use of multifunctional initiators in the bulk polymerization of St has been increased due to the possibility of obtaining high reaction rates and molecular weights simultaneously, as well as enhanced mechanical properties compared to PS obtained by using traditional initiators [41, 66, 69].

The use of peroxide type initiators has been preferred over the use of azo or C–C initiators, due to their relative ease of synthesis and lower rate of self-induced decomposition reactions [2, 35]. With the use of monofunctional initiators it is difficult to obtain an adequate balance between reaction rate, molecular weight, polydispersity and monomer conversion [39, 65, 70].

With the use of bifunctional initiators, it was possible to achieve optimization of polymerization processes, while enhancing the final properties of the product (i.e. molecular weight, monomer conversion and polydispersity) [39, 41, 65, 67, 69]. Both symmetrical

and asymmetrical initiators were used, showing that it was possible, under the right temperature and initiator concentration, to obtain high reaction rates and high molecular weights simultaneously. Reaction temperature affects the thermal stability of peroxide groups, while initiator concentration affects the rate of polymerization and reduces polymerization times without substantially lowering the molecular weight of the final product [39].

A few works have theoretically studied the synthesis of PS using bifunctional initiators. Mathematical models were developed, allowing prediction of reacting species concentrations, as well as molecular structure of the obtained polymer during the course of the polymerization reaction. Choi and Lei [69] and Kim and Choi [68] developed detailed kinetic models for the bulk St homopolymerization with symmetrical and asymmetrical diperoxyester initiators. They showed that operating at high temperatures, it is possible to obtain high reaction rates and molecular weights, with relatively narrow molecular weight distributions (MWDs). Villalobos [39] theoretically and experimentally investigated the polymerization of St with the following bifunctional initiators: 2,5-dimethyl-2,5-bis(2-ethylhexanol peroxy) hexane (Lupersol-256, L-256); 1,1-di(t-butyl-peroxy) cyclohexane, (Lupersol-331-80B); and 1,4-bis(t-butyl peroxycarbo) cyclohexane, (D-162). Compared to the standard monofunctional case, bifunctional initiators reduced polymerization times as much as 75%, without substantial changes in the final product properties. In Estenoz et al. [41] a detailed mathematical model was developed to simulate the synthesis of high impact polystyrene (HIPS) using symmetrical bifunctional initiators such as L-256 and L-118 [2,5-dimethyl-2,5-bis(benzoyl peroxyl) hexane]. High reaction rates and high molecular weights were observed, and the phase inversion periods were produced at lower conversions.

There are a number of works dealing with the use of multifunctional initiators [25, 42, 74–77, 82, 87–91]. Cerna et al. [89] studied the bulk polymerization of St using initiators with different functionalities (mono-, bi- and trifunctional initiators). The particular case of initiation by diethyl ketone triperoxide (DEKTP), a cyclic trifunctional peroxide initiator, at 120–130 °C, yielded polymers with high molecular weights (250,000–450,000 g/mol) at relatively short polymerization times (4–6 h). The obtained average molecular weights were higher than those obtained by using the bifunctional initiator pinacolone diperoxide (PDP), which has a close molecular structure to that of DEKTP. Two mechanisms have been proposed for the decomposition of DEKTP: a total decomposition of the

3 O–O groups at temperatures higher than 130 °C, and a sequential decomposition of the O–O groups at temperatures between 110–130 °C. In the latter case, Cerna et al. [89] were able to synthesize PS with undecomposed O–O in the polymer backbone. Sheng et al. [42] studied the use of the cyclic trifunctional initiator 3,6,9-triethyl-3,6,9-trimethyl-1,4,7-triperoxonane in the bulk polymerization of St. Experimental results showed that it was possible to produce polymers with higher molecular weights and lower polydispersities at a higher rate. The obtained PS had O–O bonds in the molecular chains. In Scorah et al. [74, 75], the bulk polymerization of St and methyl methacrylate in the presence of the tetrafunctional initiator polyether tetrakis(tert-butylperoxy carbonate) (JWEB50) was experimentally and theoretically studied. The developed model allowed the calculation of monomer conversion, average molecular weights and polymer structure and was validated with experimental results.

This chapter deals with the experimental and theoretical study of the bulk polymerization of St using the trifunctional cyclic initiator DEKTP. A mathematical model is developed to predict of the evolution of the reacting species concentration, monomer conversion and detailed polymer molecular structure. The effect of reaction conditions on process productivity and final product molecular characteristics is investigated.

The work presented in this chapter was reported in Berkenwald et al. [78], *"Mathematical model for the bulk polymerization of styrene using the symmetrical cyclic trifunctional initiator diethyl ketone triperoxide. I. Chemical initiation by sequential decomposition"*, J. Appl. Pol. Sci., 128, 1, 2013.

2.2 Experimental work

The experimental work consisted on the synthesis and characterization of the organic peroxide DEKTP and isothermal batch bulk polymerizations of St using the cyclic trifunctional initiator DEKTP. The selected polymerization temperatures are such that initiator decomposition is mostly sequential [89].

2.2.1 Synthesis of DEKTP

DEKTP initiator was synthesized according to the following procedure [89]: in a 250 mL Erlenmeyer flask 4.6 mL of hydrogen peroxide and 7.3 mL of sulfuric acid (70% v/v) were added and the temperature was kept at -10 °C. Then, 5.6 mL of diethyl ketone was added into the reaction medium and the reaction remained under agitation for 3 h. Thereafter, the organic phase was extracted with petroleum ether and dried with sodium sulfate for 12 hours. The petroleum ether was removed under distillation and the product was crystallized from methanol, yielding a white powder.

2.2.2 Polymerization reactions

Several bulk polymerizations of St were carried out in the presence of DEKTP at different temperatures and different initiator concentrations. In each experiment, a certain amount of DEKTP was dissolved in 2 mL of previously distilled St. The solution was placed in clean and dry test tubes, degassed by successive cycles of freezing-cooling from −180 °C (using liquid nitrogen) to room temperature, at reduced pressure. The tubes were sealed under vacuum and immersed in an oil bath. The selected polymerization temperatures were 120 °C, and 130 °C in order to ensure sequential decomposition of the initiator molecule. Preliminary studies show that at higher reaction temperatures (150–200 °C), the decomposition mechanism of the initiator is no longer sequential, and consists of a simultaneous decomposition of all three peroxide groups [89].

The first stage in the sequential decomposition reaction for DEKTP is presented in Figure 2.1, where only one peroxide group of the DEKTP molecule suffers a decomposition reaction. Further stages of the sequential decomposition arise as polymerization reaction generates polymer chains with undecomposed peroxide groups. Initiator concentrations were varied in the range of 0.005 and 0.02 mol/L. Monomer conversion was determined gravimetrically and molecular weights by gel permeation chromatography (GPC) at different reaction times. The equipment used was a Hewlett-Packard HPLC 1050 with software from Polymer Laboratories for Chemstation. Refraction Index and UV detectors were used, with ultrastyragel columns (10^3, 10^4, and 10^5 Å). Polystyrene

standards (580–3,900,000 g/mol) were used, at room temperature. To measure conversion, the obtained polymer was directly precipitated in methanol (volume ratio 1:10), filtered and dried under vacuum until constant weight (approximately 24 hours).

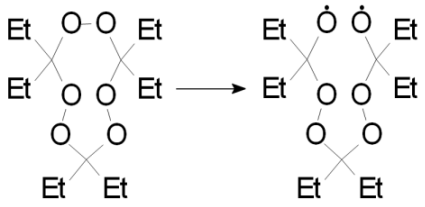

FIGURE 2.1: Sequential decomposition of DEKTP.

The experimental results are presented in Table 2.1, and Figures 2.2 and 2.3. It can be observed that initiation by DEKTP provides high reaction rates and high average molecular weights simultaneously. As expected, increasing the initiator concentration increases reaction rates. The existence of an initiator concentration that yields the highest molecular weights at a given polymerization temperature is also observed. An initiator concentration of 0.01 mol/L seems to be optimal for obtaining high reaction rates and molecular weights at a reaction temperature of 120 °C.

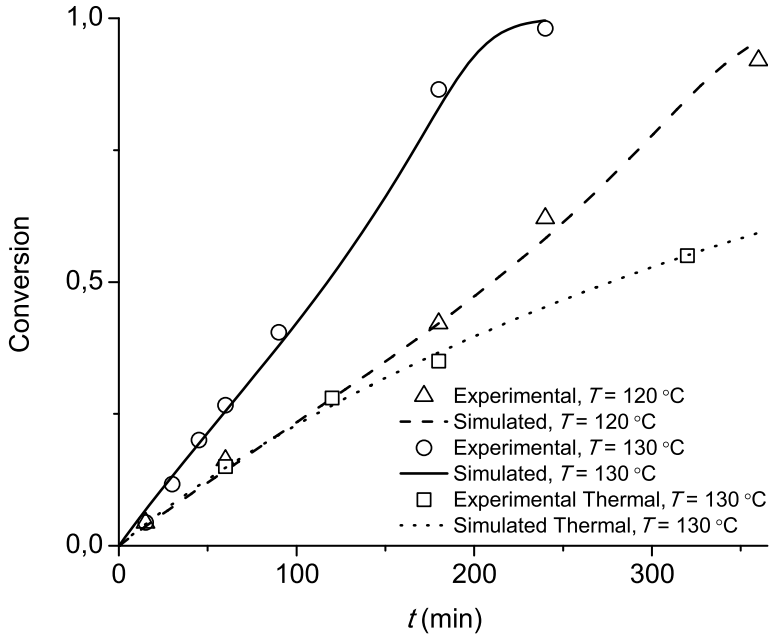

FIGURE 2.2: Conversion as a function of time for Experiments 2 and 4 of Table 2.1. The evolution of conversion for St thermal polymerization at 130 °C is also presented.

Experiment No.	T (°C)	$[I^{(3)}]_0$ (mol/L)	**Time** (min)	**Conversion** (%)	$\bar{M}_n \times 10^{-5}$ (g/mol)	$\bar{M}_w \times 10^{-5}$ (g/mol)
1	120	0.005	15	2.78 (3.05)	2.61 (1.84)	5.33 (3.58)
			60	13.05 (11.68)	2.17 (1.88)	4.27 (3.65)
			180	38.66 (33.03)	2.19 (1.99)	4.30 (3.88)
			240	42.58 (43.86)	2.39 (2.04)	4.57 (4.00)
			360	— (68.64)	2.28 (2.14)	4.46 (4.21)
2	120	0.01	15	4.35 (3.70)	2.32 (1.97)	3.60 (3.79)
			60	16.23 (14.30)	1.75 (2.01)	3.38 (3.87)
			180	42.14 (42.20)	2.00 (2.13)	3.81 (4.14)
			240	62.12 (58.32)	2.18 (2.19)	4.21 (4.27)
			360	92.05 (95.62)	2.50 (2.28)	5.32 (4.44)
3	120	0.02	15	3.83 (4.77)	2.23 (2.02)	4.30 (3.95)
			60	17.88 (18.47)	2.21 (2.05)	4.84 (3.98)
			180	55.16 (59.20)	1.94 (2.18)	3.65 (4.24)
			240	71.22 (87.39)	2.00 (2.23)	3.63 (4.34)
			360	98.22 (99.93)	1.74 (2.21)	3.16 (4.31)
4	130	0.01	15	4.42 (6.63)	1.86 (1.37)	3.52 (2.70)
			30	11.70 (13.26)	1.47 (1.39)	2.81 (2.73)
			45	20.04 (19.39)	1.41 (1.41)	2.61 (2.77)
			60	26.64 (25.53)	1.50 (1.42)	2.67 (2.81)
			90	40.48 (38.05)	1.47 (1.46)	2.67 (2.88)
			180	86.51 (82.94)	1.50 (1.55)	2.77 (3.08)
			240	98.10 (99.57)	1.57 (1.56)	3.30 (3.11)

TABLE 2.1: Experimental results and theoretical predictions for polystyrenes synthesized using DEKTP. Theoretical predictions are indicated in parenthesis.

Figures 2.2 and 2.3 show the evolution of conversion and average molecular weights for the reactions using a 0.01 mol/L concentration of DEKTP (experiments 2 and 4 in Table 2.1). The evolution of conversion for the thermal polymerization of St is also presented in Figure 2.2 for comparison purposes. In Figure 2.2, an increase in the polymerization rate is observed as temperature increases. For experiments 2 and 4, an inflection point in the conversion evolution curve can be observed, due to the sequential nature of the initiator decomposition. As expected, this inflection point does not appear in the case of purely thermal St polymerization. For the period of time evaluated, the molecular weights increase along the reaction (Figure 2.3). The calculated polydispersities are around 2 in agreement to the reported results for multifunctional initiators [39, 69]. As it was informed in Cerna et al. [89], these behaviors in the temperature range of 120–130 °C indicate that the initiator is decomposed by a sequential mechanism of decomposition

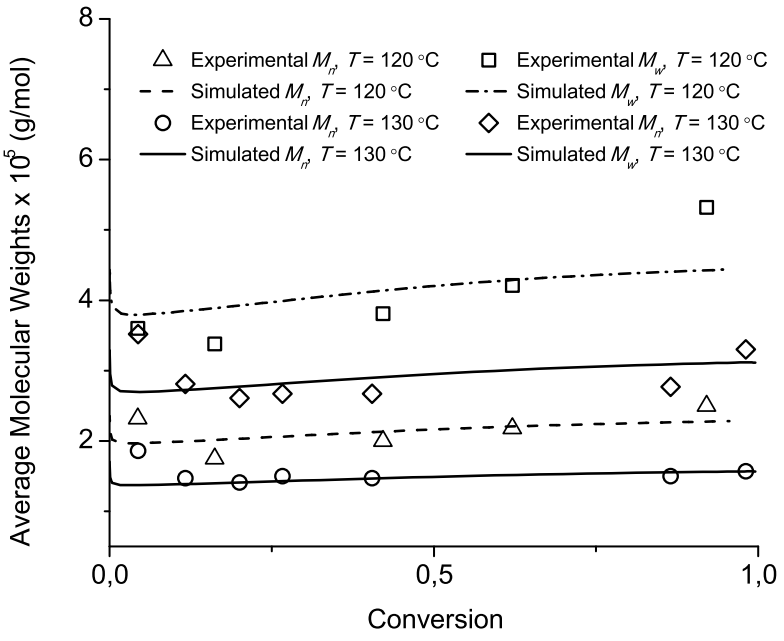

FIGURE 2.3: Average molecular weights as a function of conversion for Experiments 2 and 4 of Table 2.1.

of the peroxide groups, by which the diradicals formed by initiator decomposition have 2 undecomposed peroxide groups.

2.3 Mathematical model

2.3.1 Kinetic mechanism

The proposed kinetics involves initiation via a symmetrical cyclic trifunctional initiator, thermal initiation by the Mayo mechanism, propagation, transfer to the monomer, combination termination and re-initiation. Consider the global kinetic mechanism presented in Table 2.2. The following nomenclature is adopted:

$I^{(3)}$	Trifunctional initiator (DEKTP)
$\cdot I \cdot^{(2)}$	Initiator diradical with 2 undecomposed peroxide groups
$\cdot S_1 \cdot^{(2)}$	Monomer diradical with 2 undecomposed peroxide groups
$S_1 \cdot^{(0)}$	Monomer monoradical without undecomposed peroxide groups
$S_n \cdot^{(i)}$	PS monoradical of chain length n and i undecomposed peroxide groups
$\cdot S_n \cdot^{(i)}$	PS diradical of chain length n and i undecomposed peroxide groups
$S_n^{(i)}$	Polymer with n repetitive units of St and i undecomposed peroxide groups

Initiation

Chemical initiation

$I^{(3)} \cdot \xrightarrow{3k_{d1}} \cdot I \cdot^{(2)}$

$\cdot I \cdot^{(2)} + \mathrm{St} \cdot \xrightarrow{2k_{i1}} \cdot S_1 \cdot^{(2)}$

Thermal initiation

$3\mathrm{St} \xrightarrow{k_{i0}} 2 S_1 \cdot^{(0)}$

Propagation $(n = 1, 2, 3...; i = 0, 1, 2...)$

$S_n \cdot^{(i)} + \mathrm{St} \xrightarrow{k_p} S_{n+1} \cdot^{(i)}$

$\cdot S_n \cdot^{(i)} + \mathrm{St} \cdot \xrightarrow{2k_p} S_{n+1} \cdot^{(i)}$

Transfer to monomer $(n = 1, 2, 3...; i = 0, 1, 2...)$

$S_n \cdot^{(i)} + \mathrm{St} \xrightarrow{k_{fM}} S_n{}^{(i)} + S_1 \cdot^{(0)}$

$\cdot S_n \cdot^{(i)} + \mathrm{St} \xrightarrow{k_{fM}} S_n \cdot^{(i)} + S_1 \cdot^{(0)}$

Re-initiation $(n = 2, 3, 4...; m = 1, 2, ..., n-1; i = 1, 2...; j = 0, 1, ..., i-1)$

$S_n{}^{(i)} \xrightarrow{ik_{d2}} S_{n-m} \cdot^{(i-j)} + S_m{}^{(j-1)}$.

Combination Termination $(n, m = 1, 2, 3...; i, j = 0, 1, 2...)$

$\cdot S_n \cdot^{(i)} + \cdot S_m \cdot^{(j)} \xrightarrow{4k_{tc}} \cdot S_{n+m} \cdot^{(i+j)}$

$\cdot S_n \cdot^{(i)} + S_m \cdot^{(j)} \xrightarrow{2k_{tc}} S_{n+m} \cdot^{(i+j)}$

$S_n \cdot^{(i)} + S_m \cdot^{(j)} \xrightarrow{k_{tc}} S_{n+m}{}^{(i+j)}$

TABLE 2.2: St polymerization using DEKTP at low temperatures - Proposed kinetic mechanism.

The following has been assumed: a) at the considered reaction temperature, initiator decomposition is due exclusively to sequential decomposition [39, 89]; b) intramolecular termination is negligible [41]; c) disproportion termination is negligible [92]; d) all peroxide groups present in the trifunctional initiator and in the accumulated polymer exhibit the same thermal stability [41]; e) due to the short life time of radicals, decomposition of undecomposed peroxide groups cannot occur in radical molecules [41]; f) propagation

and transfer reactions are unaffected by chain length or conversion [41]; g) degradation reactions are negligible [17].

Note the following: i) when two monoradicals with i and j undecomposed peroxide groups terminate, the formed polymer will contain $i+j$ undecomposed peroxide groups; ii) diradicals only have an even number of peroxide groups, as they are generated only by propagation of the initiator diradical (with only 2 peroxide groups), and by combination termination of other diradicals, all of which have an even number of peroxide groups; iii) re-initiation involves the decomposition of a peroxide group within a polymer chain with undecomposed peroxide groups, which generates two monoradicals capable of further growing. Due to the molecular structure of the DEKTP molecule, only linear di- and mono radicals and linear polymer chains can be formed in the reaction system.

2.3.2 Homogeneous model

From the kinetics of Table 2.2 and assuming homogeneous bulk polymerization, the mathematical model of Appendix A was developed. This model is based on the mass balances for the chemical species present in the reaction system. In order to model the re-initiation reactions, polymeric chains were assumed to have uniformly distributed peroxide groups. A random chain scission can then be performed by using a uniformly distributed random variable (see Appendix A).

The mathematical model consists of two modules: the Basic module and the Distributions module. The Basic module allows the prediction of global chemical species evolution along the reaction (total mono- and diradicals, total polymer). The Distributions module allows simulation of the evolution of all chemical species characterized by their chain length and their number of undecomposed peroxide groups, and allows simulating the evolution of the molecular weight distribution -MWD- of each chemical species, characterized by the number of undecomposed peroxide groups.

The proposed model considers constant temperature, assuming that the reactor cooling/heating system is ideal in the sense that it is capable of providing/removing the exact amount of heat in order to keep the temperature constant. However, it is possible

Parameter	**Units**	**Arrhenius expression**	**Reference**
k_{d1}, k_{d2}	s^{-1}	$4.16 \cdot 10^{8} e^{-25506/RT}$	Adjusted in this work
k_{i0}	$\frac{L^2}{mol^2 S}$	$1.1 \cdot 10^{5} e^{-27340/RT}$	[93]
k_{i1}, k_p	$\frac{L}{mol\ s}$	$1.0 \cdot 10^{7} e^{-7067/RT}$	[39]
k_{fM}	$\frac{L}{mol\ s}$	$1.17 \cdot 10^{10} e^{-18651/RT}$	Adjusted in this work
k_{tc}	$\frac{L}{mol\ s}$	$1.26 \cdot 10^{9} e^{-(1667.3/RT)-2(C_1 x+C_2 x^2+C_3 x^3)}$ [a]	[17]
f		0.98	[25]

[a] $C_1 = 2.75 - 0.00505T; C_2 = 9.56 - 0.0176T; C_3 = -3.03 + 0.00785T$, with x monomer conversion

TABLE 2.3: St polymerization using DEKTP at low temperatures - Adopted kinetic parameters.

to simulate reactions at different temperatures through the use of Arrhenius expressions for the kinetic constants. The gel effect was indirectly considered by appropriately reducing the value of the termination kinetic constant with increasing conversion [17].

The Basic module is self-sufficient from the calculation point of view, and for its resolution equations A.1, A.2, A.4, A.7, A.8, A.16 and A.22, must be simultaneously solved. The equations of the Distributions module must be integrated using the Basic module results.

The Basic module is solved by a standard stiff differential equation numerical method based on a modified Rosenbrock formula of order 2. In the Distributions module, a large number of equations (more than 250,000) must be integrated. For this reason, an explicit forward Euler method was used, using the time intervals obtained from resolution of the Basic module. A typical simulation requires less than 1 second for the Basic module and about 5 minutes for the Distribution module using an Intel Core i3 based processor at 2.40 GHz.

2.3.3 Model adjustment and validation

The adopted kinetic parameters used for the simulation are presented in Table 2.3.

The expressions for k_{d1}, k_{d2} and k_{fM} were adjusted in this work. Since peroxide groups in the polymer chains were assumed to have the same thermal stability as peroxide groups in the initiator, $k_{d1} = k_{d2}$. Due to the short simulation times required, a fast interactive adjustment was possible. The adjusted values for k_{d1} are in agreement with the reported results for DEKTP decomposition [25, 89]. The value of k_{fM} is within the ranges reported for St polymerization [19]. The Basic module allowed the adjustment for k_{d1} and k_{d2} from the estimation of the monomer conversion from the experiments in Table 2.1. The parameter k_{fM} was adjusted to fit the experimental data of average molecular weights using the Distributions module.

The values for all other kinetic parameters were directly adopted from the literature [17, 39, 65, 94] and the value for f was obtained from experimental results by Cerna [25].

2.4 Simulation results

The model was used to simulate experiments 1 through 4 of Table 2.1. Simulated results are compared with experimental results in Table 2.1 and Figures 2.2 and 2.3. In general, a very good agreement between predicted and measured values is observed. Figures 2.2 and 2.3 show the simulation results corresponding to the evolution of conversion and average molecular weights for experiments 2 and 4 of Table 2.1. The change of the slope in the conversion curve in Figure 2.2 at approximately and 200 min at 120 °C and 150 min at 130 °C, is due to the combined effect of thermal and chemical initiation, which includes initiator decomposition and decomposition of unreacted peroxide groups within the polymer chains, together with the gel effect, globally producing an increase in the rate of polymerization. The re-initiation reactions within the polymer chains are also responsible for the high molecular weights observed experimentally and predicted by the model, as the scission of polymer chains can generate long chain monoradicals, capable of further growing by propagation reactions.

The mathematical model was also used to study the coupling effect of thermal and chemical initiation on the polymerization rate. In Figure 2.2, experimental and simulated conversion curves for polymerizations carried out at 130 °C in absence of initiator

were shown. Results indicate that at temperatures of 130 °C, thermal polymerization contributes on average to about 60% of the total rate of polymerization.

Aside from the prediction of experimental results presented in Table 2.1 and Figures 2.2 and 2.3, the model was used to simulate other variables. Model predictions are shown in Figures 2.4, 2.5, 2.6, 2.7.

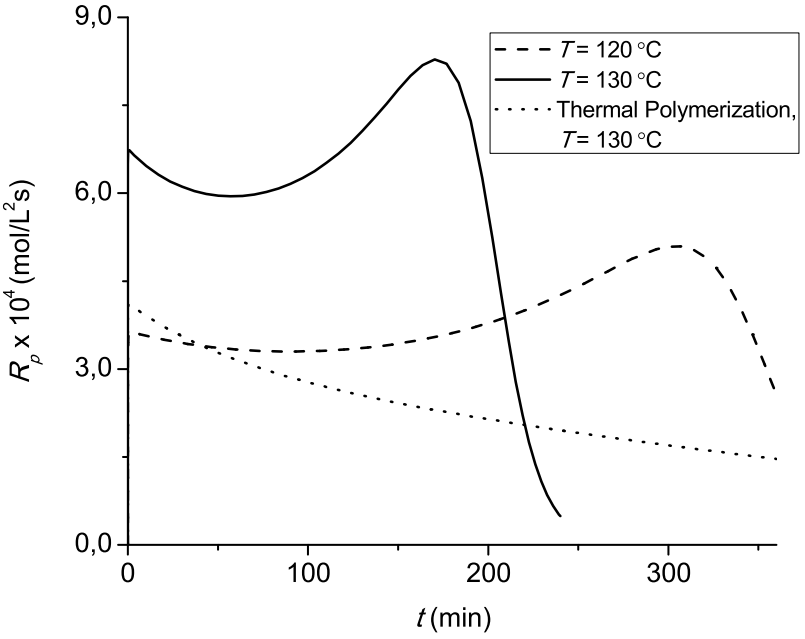

FIGURE 2.4: Rate of polymerization as a function of time for Experiments 2 and 4 of Table 2.1. The rate of polymerization for St thermal polymerization at 130 °C is also presented.

Figure 2.4 represents the evolution of the rate of polymerization R_p, as defined by Equation A.2, as a function of time, which can be computed using the Basic module of Appendix A [17]. Figure 2.1 shows that around 200 min at 200 °C and 150 min at 130 °C, the rate of polymerization increases as a result of chemical and thermal initiation, decomposition of peroxide groups within the formed polymer chains and gel effect, as explained for Figure 2.2. This increase in the rate of polymerization could also be observed indirectly in the change of the slope of the conversion curve in Figure 2.2. The drop in the value of the rate of polymerization at around 300 min at 120 °C and 200 min at 130 °C is due to monomer depletion. For comparison purposes, the evolution of the rate of polymerization in the absence of DEKTP initiation (that is, a purely thermal

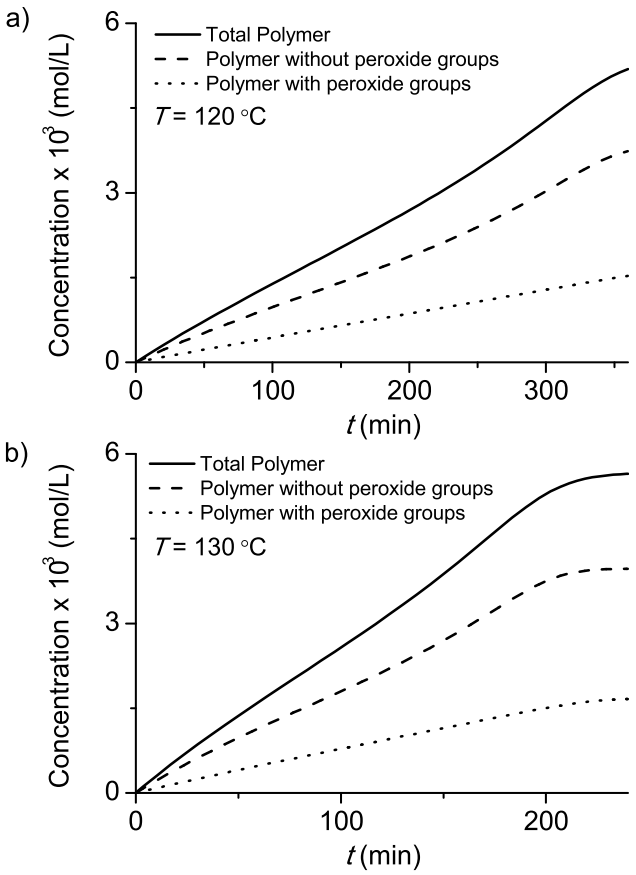

FIGURE 2.5: Evolution of total polymer, dead polymer and total polymer with undecomposed peroxide groups for: a) Experiments 2 and b) Experiment 4 of Table 2.1.

polymerization) is also represented. It can be seen that the rate of polymerization in this case is a monotonically decreasing function of time.

In Figure 2.5, the evolutions of the total polymer species molar concentration, as defined by Equation B.16 are presented. Total polymer consists of total dead polymer (i.e. without undecomposed peroxide groups) and total temporarily dead polymer (i.e. with undecomposed peroxide groups). Dead polymer concentration monotonically increases along the reaction time, exhibiting a slope that increases at around 200 min at 120 °C and 150 min at 130 °C coinciding with the time at which polymerization rate increases (as indicated for Figure 2.2 and Figure 2.5). The figure shows that the molar fraction of total polymer with undecomposed peroxide groups at the end of polymerization is close to about 30 %.

Figure 2.6 shows the evolutions of the different polymer species, characterized by the number of undecomposed peroxide groups within the polymeric chains. A logarithmic

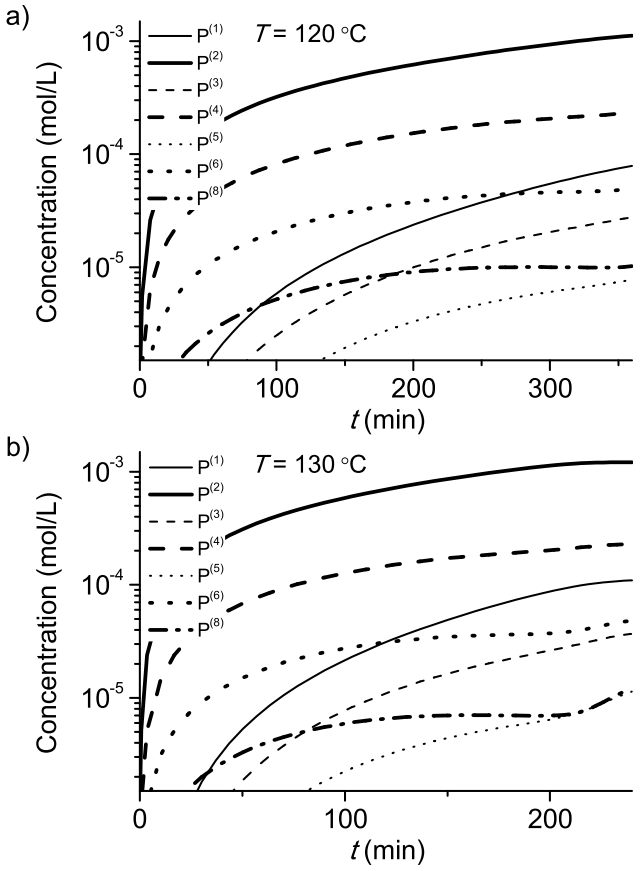

FIGURE 2.6: Evolution of total polymeric species characterized by the number of undecomposed peroxide groups for: a) Experiments 2 and b) Experiment 4 of Table 2.1.

scale was used in the concentration axis in order to show the differences in magnitudes. Only polymer chains with 1, 2, 3, 4, 5, 6 and 8 undecomposed peroxide groups are considered in the figure for clarity reasons. The evolution of the concentration of the different polymers species is highly dependent on the number of undecomposed peroxide groups, due to the fact that peroxide groups in the polymer are a result of propagation, transfer and termination of diradicals generated by initiator decomposition, but also to the decomposition of polymeric chains with a higher number of peroxide groups. A great number of monoradicals without peroxide groups is also produced by thermal initiation of the monomer at 120 and 130 °C, and in consequence dead polymer is the most abundant polymer species. It is possible to observe that the molar concentration of the polymer decreases with increasing peroxide group number per chain when considering polymers with even number of peroxide groups. The same can be stated for polymers with an odd number of peroxide groups. For polymers with an even number

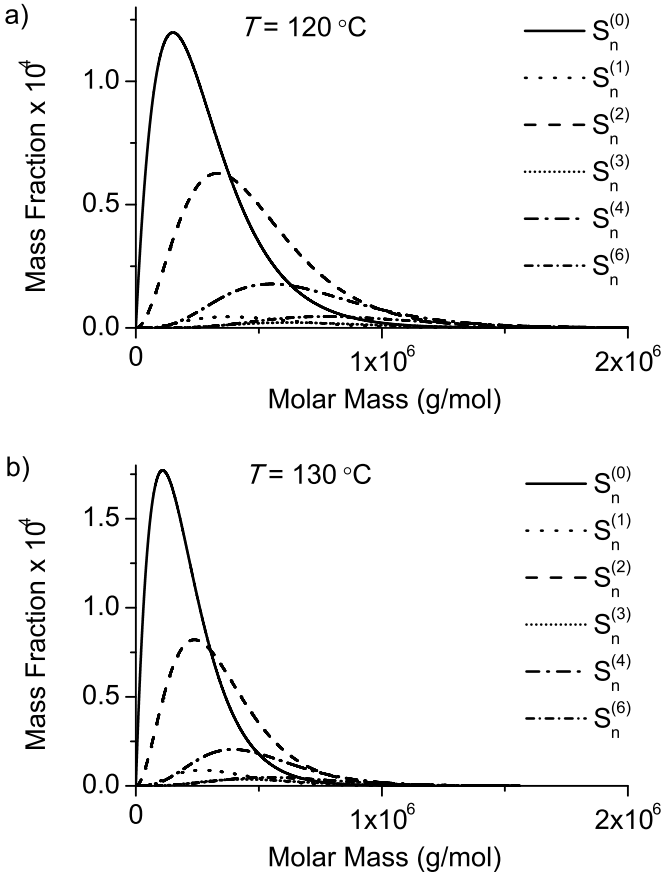

FIGURE 2.7: MWD of the polymeric species at the end of polymerization for: a) Experiments 2 and b) Experiment 4 of Table 2.1.

of peroxide groups, the concentrations show a similar evolution, indicating that most of the peroxide groups in polymer chains are generated by initiator decomposition. This is not the case for polymers with an odd number of peroxide groups, because radicals with an odd number of peroxide groups are generated only after polymer decomposition reactions. For this reason, polymers with an odd number of undecomposed peroxide groups are formed in the reaction system later than polymers with an even number of peroxide groups. These types of behaviors are a clear result of the sequential decomposition of the initiator molecule. The raise in polymer concentration for high peroxide group numbers (more than 3) at high reaction times can be explained as follows: when conversion is close to a value of 1, little monomer is left for thermal initiation reactions. However, initiator decomposition is still important, and all the radicals generated have 2 undecomposed peroxide groups. Re-initiation reactions also generate radicals with undecomposed peroxide groups and polymer generation is mostly by termination reactions between these radicals. These factors result in an increase in the concentration of

$[I^{(3)}]$ (mol/L)	$\bar{M}_n \times 10^{-5}$ (g/mol)	$\bar{M}_w \times 10^{-5}$ (g/mol)	$\bar{M}_n \times 10^{-5}$ (g/mol)	$\bar{M}_w \times 10^{-5}$ (g/mol)
	$T = 120$ °C		$T = 130$ °C	
0.001	2.14	4.22	1.50	2.99
0.002	2.16	4.26	1.53	3.07
0.005	2.22	4.36	1.56	3.11
0.01	2.28	4.44	1.57	3.11
0.02	2.21	4.31	1.56	3.08
0.05	2.12	4.02	1.49	2.86

TABLE 2.4: Theoretical study of the effect of initial initiator concentration in average molecular weights at total conversion for temperatures of 120 °C and 130 °C.

polymer with a high number of undecomposed peroxide groups towards the end of the polymerization.

Figure 2.7 shows the MWD of the formed polymer species at the end of the polymerization reaction. Only MWDs of a few polymeric species are represented in order to keep the picture clear but still representative. The obtained MWD shows that polymers with a high number of undecomposed peroxide groups have a wider distribution, over higher molecular weights. This is consistent with the fact that high peroxide group numbers arise from termination combination or transfer of monoradicals that have been generated by diradicals of initiator decomposition. These diradicals can propagate before terminating, so it is expected that termination of two diradicals will generate a long chain monoradical, which can itself terminate with another long chain monoradical. As expected, polymer chains with 1 undecomposed peroxide group are in average shorter than the ones from the polymer with 2 undecomposed peroxide groups, because the former is generated mostly by decomposition of the latter, after transfer to the monomer or termination with a radical without peroxide groups. Polymers with a greater number of peroxide groups have a relatively low mass fraction, but enough to significantly increase the average molecular weight. By comparing the MWDs obtained at different temperatures, it is possible to see that lower temperatures tend to increase the mass fraction of polymer with undecomposed peroxide groups compared to total polymer.

In Table 2.4, the effect of initiator concentration on average molecular weights is theoretically investigated. The model allowed calculating the average molecular weights for

total conversion as a function of initial initiator concentration. The simulated results indicate that at a given reaction temperature, there is an initiator concentration that yields the maximum values of the average molecular weights, indicating the presence of an optimum for initiator concentration. This fact was also observed experimentally at 120 °C as shown in Table 2.1 in experiments 1 through 3. The existence of this optimum can be interpreted as follows: at low initiator concentration, a low proportion of diradicals is generated by initiator decomposition. As these radicals propagate before generating a monoradical, which is capable of further propagation, the effect in average molecular weight is less significant. Increasing initiator concentration rises the proportion of diradicals, which results in an increase in average molecular weights. At high initiator concentrations, the dominating effect is the large number of active sites in the system, both by chemical and thermal initiation. This results in shorter polymer chains and lower average molecular weights. The value of this optimum concentration depends on the polymerization temperature, which also modifies the polymerization rate. For polymerization temperatures of 120–130 °C the optimum concentration is found to be 0.01 mol/L.

As it has been shown, the proposed mathematical model allows prediction of the concentration and MWD of polymer species with undecomposed peroxide groups at the end of the polymerization reaction. These variables could be used to study the evolution of polymer structure in the course of post-polymerization processes carried out at high temperatures, such as devolatilization, where decomposition of the remaining peroxide groups could take place, thereby modifying the values of final (processing and mechanical) properties.

In order to estimate the decrease in molecular weights due to decomposition of the remaining peroxide groups, the model was used to simulate the evolution of a polymer (obtained at 130 °C and with an initial DEKTP concentration of 0.01 mol/L) subjected to a process at temperatures of 180–200 °C with a residence time of 25 min. These values for the temperature and residence time are typical values for a devolatilization process [11, 95]. Simulation results indicate a decrease in molecular weights of about 30–40 % depending on process temperature. These results should be only considered estimative values, as the model does not include high temperature degradation reactions. In addition, in order to evaluate the performance of this initiator in an industrial polymerization process and the effect on final average molecular weights, it is required to consider not

only the polymerization reaction stage, but also the downstream post-reaction stages, for which the model developed in this work might not be appropriate.

2.5 Conclusions

This chapter experimentally and theoretically investigates the use of the symmetrical trifunctional initiator DEKTP in the bulk polymerization of St. The experimental work consisted of a series of isothermal batch polymerizations at different temperatures, in which conversion and average molecular weights were determined. For the theoretical analysis, a mathematical model was developed, allowing simulation the evolution of the chemical species characterized by the number of undecomposed peroxide groups within the chains, including di- and monoradicals as well as polymeric species. Re-initiation reactions are accounted for by using a uniformly distributed random variable in order to simulate random chain scission.

The main result is that the use of DEKTP allows obtaining high polymerization rates and high molecular weights simultaneously, because of its sequential decomposition. This leads to the formation of di- and monoradicals with undecomposed peroxide groups. These peroxide groups are then found in the polymeric chains, which are susceptible of re-initiation. Simulation of the proposed kinetic mechanism provides values which are in very good agreement with experimental results.

For a given polymerization temperature, experimental and simulation results show the existence of an optimum initiator concentration, for which the produced average molecular weights are highest.

The fact that undecomposed peroxide groups remain within the polymer chains is an important issue that should be taken into consideration for an industrial polymerization process. Simulation of the complete polymerization process would require an extension of the model, to account for high temperature reactions and other phenomena that could alter the polymer molecular structure in downstream post-reaction processes.

In the following chapters, the kinetic mechanism is extended to include the total decomposition of the initiator molecule at higher reaction temperatures and a generic model for multifunctional initiators is developed.

Chapter 3

Bulk styrene polymerization using the trifunctional cyclic initiator DEKTP at high temperatures (150–200 °C)

3.1 Introduction

It has been experimentally found that the compounds used as multifunctional initiators can suffer both sequential and total decomposition reactions [22, 25]. The total decomposition of DEKTP is presented in Figure 3.1. While the sequential decomposition mechanism can be used to explain the high molecular weighs obtained by the use of multifunctional initiators, total decomposition of a multifunctional initiator is often undesirable, since the beneficial effect on molecular weights is lost [6].

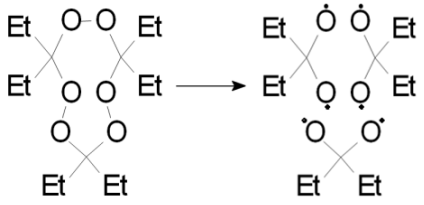

FIGURE 3.1: Total decomposition of DEKTP.

There are no works in the available literature containing mathematical models including both sequential and total decomposition mechanisms for multifunctional initiators. In Chapter 2, a detailed mathematical model, also reported in Berkenwald et al. [78], for the bulk polymerization of St in the presence of DEKTP was developed, considering reaction temperatures at which the initiator decomposition is mostly sequential (120–130 °C). This model allowed obtaining the complete MWD, but had limited validity when considering polymerization temperatures higher than 130 °C.

This chapter deals with the experimental and theoretical study of the bulk polymerization of St using DEKTP at temperatures of 150–200 °C, where initiator decomposition consists of two parallel decomposition reactions (sequential and total decomposition). A mathematical model is developed, based on an extended kinetic mechanism considering both decomposition reactions, allowing the prediction of the evolution of the reacting species concentration, monomer conversion and detailed polymer molecular structure. The effect of reaction temperature on process productivity and final product molecular characteristics is investigated.

The work presented in this chapter was reported in Berkenwald et al. [79], *"Mathematical model for the bulk polymerization of styrene chemically initiated by sequential and total decomposition of the trifunctional initiator diethyl ketone triperoxide"*, Pol. Eng. Sci., 55, 1, 2015.

3.2 Experimental work

The experimental work consisted on initiator synthesis and bulk polymerizations of St using DEKTP at different reaction temperatures, using the procedures described in the previous chapters. The selected polymerization temperatures were 150 °C and 200 °C. Initiator concentration was 0.01 mol/L, previously found to be the optimal initiator concentration for bulk polymerization of St using DEKTP [78].

The experimental results are presented in Figure 3.2. Results for temperatures of 120–130 °C are included for comparison purposes. As stated in the previous chapter, it can be observed that initiation by DEKTP allows for high reaction rates and high average molecular weights simultaneously at a polymerization temperature of 120–130 °C. For polymerization temperatures of 150 and 200 °C, polymerization rates are higher, but the

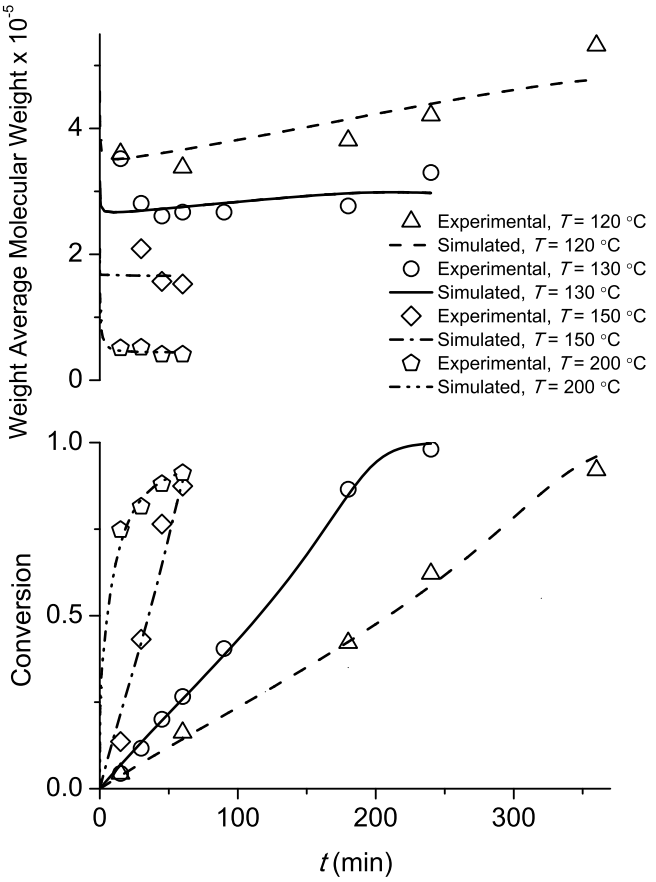

FIGURE 3.2: Conversion and Weight-Average Molecular Weight as a Function of Time for $T = 120$ °C, $T = 130$ °C, $T = 150$ °C and $T = 200$ °C.

produced average molecular weights are lower. The polydispersity of the obtained product is approximately 2, which is expected for these types of initiators at temperatures higher than 130 °C [25]. On the other hand, an increase in the rate of polymerization is observed as temperature increases from 120, 130 to 150 °C. At 200 °C, the rate of polymerization is high at the beginning of the reaction, but it becomes lower than the one at 150 °C after a short period of time (about 30 min). Molecular weights increase along the reaction for polymerization temperatures of 120–130 °C. At higher temperatures, molecular weights remain relatively constant (150 °C) or decrease along the reaction (200 °C).

3.3 Mathematical model

3.3.1 Kinetic mechanism

The proposed kinetics involves initiation via a symmetrical cyclic trifunctional initiator by sequential and total decomposition reactions, thermal initiation, propagation, transfer to the monomer, combination termination and re-initiation. Consider the global kinetic mechanism presented in Table 3.1, which is an extension of the kinetic mechanism from the previous chapter. In addition to the nomenclature from the preceding chapter, the following nomenclature is adopted:

$\cdot I \cdot^{(0)}$	Initiator diradical without undecomposed peroxide groups
$\cdot S_1 \cdot^{(0)}$	Monomer diradical without undecomposed peroxide groups
$\cdot S_n \cdot^{(0)}$	PS diradical of chain length n and i undecomposed peroxide groups
α_n	Stoichiometric coefficient corresponding to a PS monoradical of chain length n generated by total decomposition of a polymer with undecomposed peroxide groups
β_n	Stoichiometric coefficient corresponding to a PS diradical of chain length n generated by total decomposition of a polymer with undecomposed peroxide groups

The following has been assumed: a) at the considered reaction temperatures, initiator decomposition consists of two parallel reactions: sequential and total decomposition [22, 25]; b) intramolecular termination is negligible [41]; c) disproportion termination is negligible [92]; d) all peroxide groups present in the trifunctional initiator and in the accumulated polymer exhibit the same thermal stability [41]; e) due to the short life time of radicals, decomposition of undecomposed peroxide groups cannot occur in radical molecules [41]; f) propagation and transfer reactions are unaffected by chain length or conversion [41]; g) degradation reactions are negligible [17].

Note the following: i) when two monoradicals terminate, if one of then has a number of undecomposed peroxide groups greater than zero, the formed polymer will contain undecomposed peroxide groups; ii) diradicals only have either zero or an even number of peroxide groups, as they are generated only by propagation of the initiator diradical (either without or with only 2 peroxide groups), and by combination termination of other diradicals, all of which have zero or an even number of peroxide groups; iii) due to assumption c), polymeric chains may suffer both sequential decomposition reactions or

Initiation

Chemical Initiation

by sequential decomposition

$I^{(3)}. \xrightarrow{3k_{d1}} \cdot I.^{(2)}$

$\cdot I.^{(2)} + \mathrm{St}\cdot \xrightarrow{2k_{i1}} \cdot S_1.^{(2)}$

by total decomposition

$I^{(3)}. \xrightarrow{3k_{dt}} 3 \cdot I.^{(0)}$

$\cdot I.^{(0)} + \mathrm{St}\cdot \xrightarrow{2k_{i1}} \cdot S_1.^{(0)}$

Thermal Initiation

$3\mathrm{St} \xrightarrow{k_{i0}} 2S_1.^{(0)}$

Propagation $(n = 1, 2, 3...; i = 0, 1, 2...)$

$S_n.^{(i)} + \mathrm{St} \xrightarrow{k_p} S_{n+1}.^{(i)}$

$\cdot S_n.^{(i)} + \mathrm{St}\cdot \xrightarrow{2k_p} S_{n+1}.^{(i)}$

Transfer to monomer $(n = 1, 2, 3...; i = 0, 1, 2...)$

$S_n.^{(i)} + \mathrm{St} \xrightarrow{k_{fM}} S_n{}^{(i)} + S_1.^{(0)}$

$\cdot S_n.^{(i)} + \mathrm{St} \xrightarrow{k_{fM}} S_n\,.^{(i)} + S_1.^{(0)}$

Re-initiation $(n = 2, 3, 4...; m = 1, 2, ..., n-1; i = 1, 2...; j = 0, 1, ..., i-1)$

$S_n{}^{(i)} \xrightarrow{ik_{d2}} S_{n-m}.^{(i-j)} + S_m{}^{(j-1)}\,.$

$\mathrm{S}_n{}^{(i)} \xrightarrow{ik_{dt}} \sum_{l=1}^{n-1} \alpha_l \mathrm{S}_l.^{(0)} + \sum_{k=1}^{n-1} \beta_{ik} \cdot \mathrm{S}_k.^{(0)}$

where $\alpha_l = 1, 2$ and $\beta_{ik} = 1, 2, ...i-1$ with $\sum_{k=1}^{\infty} \beta_{ik} = i - 1$.

Combination termination $(n, m = 1, 2, 3...; i, j = 0, 1, 2...)$

$\cdot S_n.^{(i)} + \ \cdot S_m.^{(j)} \xrightarrow{4k_{tc}} \cdot S_{n+m}.^{(i+j)}$

$\cdot S_n.^{(i)} + S_m.^{(j)} \xrightarrow{2k_{tc}} S_{n+m}.^{(i+j)}$

$S_n.^{(i)} + S_m.^{(j)} \xrightarrow{k_{tc}} S_{n+m}{}^{(i+j)}$

TABLE 3.1: St polymerization using DEKTP at high temperatures - Proposed kinetic mechanism.

total decompositions reactions. In the former, two monoradicals which may contain undecomposed peroxide groups are generated. In the latter, the chain may fragment itself in both monoradicals and diradicals (depending on the position of the peroxide groups within the chains) without undecomposed peroxide groups; (iv) due to the molecular structure of the DEKTP molecule, only linear di- and mono radicals and linear polymer chains can be formed in the reaction system.

3.3.2 Homogeneous model

From the kinetics of Table 3.1 and assuming homogeneous bulk polymerization, the mathematical model of Appendix B was developed. This model is based on the mass balances for the chemical species present in the reaction system. In order to model the re-initiation reactions, polymeric chains were assumed to have uniformly distributed peroxide groups. Two random chain scission can then be performed by using two uniformly distributed random variables, corresponding to both sequential and total decomposition of peroxide groups.

The mathematical model consists of two modules: the Basic module of Appendix B.1 and the Distributions module of Appendix B.2. The Basic module allows the prediction of global chemical species evolution along the reaction (monomer, initiator, total mono- and diradicals). The Distributions module allows simulation of the evolution of all chemical species characterized by their chain length and their number of undecomposed peroxide groups, and allows estimating the evolution of the molecular weight distribution -MWD- of each species, characterized by their number of undecomposed peroxide groups.

The proposed model considers constant temperature, assuming that the reactor cooling/heating system is ideal in the sense that it is capable of providing/removing the exact amount of heat in order to keep the temperature constant. However, it is possible to simulate reactions at different temperatures through the use of Arrhenius expressions for the kinetic constants. The gel effect was indirectly considered by appropriately reducing the value of the termination kinetic constant with increasing conversion.[17]

The Basic module is self-sufficient from the calculation point of view, and for its resolution equations B.1, B.2, B.4, B.5, B.13, B.14, B.19, must be simultaneously solved.

Parameter	**Units**	**Arrhenius expression**	**Reference**
k_{d1}, k_{d2}	s^{-1}	$1.87 \cdot 10^8 e^{-25500/RT}$	Adjusted in this work
k_{dt}	s^{-1}	$1.53 \cdot 10^3 0 e^{-67549/RT}$	Adjusted in this work
k_{i0}	$\frac{L^2}{mol^2 S}$	$2.19 \cdot 10^5 e^{-27340/RT}$	[17]
k_{i1}, k_p	$\frac{L}{mol\ s}$	$1.051 \cdot 10^7 e^{-7082/RT}$	[17]
k_{fM}	$\frac{L}{mol\ s}$	$3.84 \cdot 10^9 e^{-17836/RT}$	Adjusted in this work
k_{tc}	$\frac{L}{mol\ s}$	$1.225 \cdot 10^9 e^{-(1667.3/RT)-2(C_1 x+C_2 x^2+C_3 x^3)}$ [a]	[17]
f		0.98	[25]

[a] $C_1 = 2.75 - 0.00505T; C_2 = 9.56 - 0.0176T; C_3 = -3.03 + 0.00785T$, with x monomer conversion

TABLE 3.2: St polymerization using DEKTP at high temperatures - Adopted kinetic parameters.

The equations of the Distributions module must be integrated using the Basic module results.

The Basic module is solved by a standard stiff differential equation numerical method based on a modified Rosenbrock formula of order 2. In the Distributions module, a large number of equations (more than 300,000) must be integrated. For this reason, an explicit forward Euler method was used, using the time intervals obtained from resolution of the Basic module. A typical simulation requires less than 1 second for the Basic Module and about 5 minutes for the Distribution module using an Intel Core i3 based processor at 2.40 GHz.

3.3.3 Model adjustment and validation

The adopted kinetic parameters are presented in Table 3.2.

The adjusted parameters correspond to initiator decomposition (k_{d1}, k_{d2} and k_{dt}) and transfer to monomer reactions (k_{fM}). Since all peroxide groups (in the initiator or in the polymer chains) were assumed to have the same thermal stability, $k_{d1} = k_{d2}$. All other kinetic parameters were taken from the literature and are valid in a temperature

range of 100-230 °C [17]. The Basic module allowed the adjustment for k_{d1} and k_{dt} from the estimation of the monomer conversion. The parameter k_{fM} was adjusted to fit the experimental data of average molecular weights using the Distributions module. A sensitivity analysis was performed by decreasing and increasing the adjusted values for the kinetic parameters and checking that the model response is within the acceptable range for this type of system

3.4 Simulation results

The model was used to simulate the experiments described in the previous section. Simulated results are compared with experimental measurements in Figure 3.2. Note that experiments at 120–130 °C were re-simulated using the extended model. As expected, theoretical predictions for these experiments are very similar to those reported in the previous chapter.

A very good agreement between predicted and measured values for high temperature experiments (150–200 °C) is observed. Figure 3.2 shows the simulation results corresponding to the evolution of conversion and average molecular weights. The simulated polydispersity of the formed polymer is around 2, in agreement with the experimental value. As stated in the preceding chapter, the change of the slope in the conversion curve in Figure 3.2 at approximately 200 min at 120 °C and 150 min at 130 °C, is due to the combined effect of thermal and chemical initiation, which includes initiator decomposition and decomposition of unreacted peroxide groups within the polymer chains, together with the gel effect, globally producing an increase in the rate of polymerization. The re-initiation reactions within the polymer chains are also responsible for the high molecular weights observed experimentally and predicted by the model at temperatures of 120–130 °C, where initiator decomposition is mostly sequential. The change of the slope in the conversion curves at 150 °C is less noticeable. At this temperature, the molecular weights are lower than in the previous temperature, and do not significantly increase along the reaction. At 200 °C, initiator decomposition is completely total, and its behavior is similar to the one of a classic monofunctional initiator, rather than a multifunctional initiator. The slope of the conversion curve decreases with reaction time, as the initiator is fully consumed after approximately 1 min, with the remaining initiation reactions due exclusively to thermal initiation. At this polymerization temperature,

simulation results predict the existence of a limiting conversion which may be lower than unity, indicating a polymerization mechanism corresponding to a "dead-end" polymerization, where radicals are rapidly consumed by termination and transfer reactions, resulting in short polymer chains [96, 97]. This behavior and its relation to the initiator decomposition reaction will be discussed in detail below. At 150 °C, both decomposition mechanisms coexist, but the total decomposition of the initiator does not generate polymer chains with undecomposed peroxide groups, therefore reducing the amount of re-initiation reactions that contribute to the increase of the rate of polymerization. As expected, thermal initiation at these high temperatures accounts for 80 to nearly 100% of total initiation (thermal and chemical), depending on the system temperature and reaction time.

Aside from the prediction of experimental results presented in Figure 3.2, the model was used to simulate other variables. Other model predictions are shown in Figures 3.3 through 3.7 and Table 3.3.

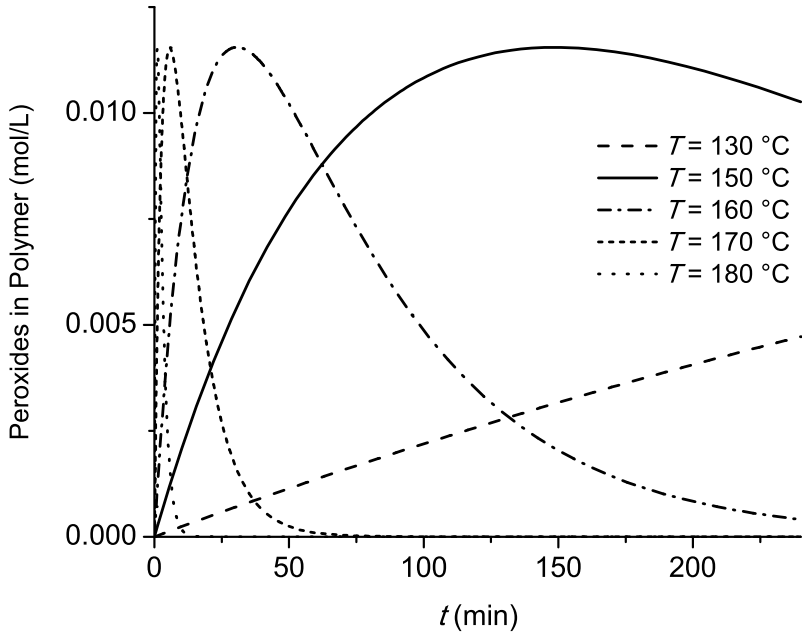

FIGURE 3.3: Evolution of peroxide groups in the polymer for different reaction temperatures.

Figure 3.3 represents the evolution of the concentration of the peroxide groups within the polymer chains for different reaction temperatures. For a polymerization temperature of 130 °C, sequential decomposition of the initiator generates polymeric chains with

undecomposed peroxide groups. As initiator decomposition is relatively slow, there is initiator left in the system throughout the polymerization reaction. For this reason, the rate of generation of peroxide groups within the polymer chains exceeds their rate of decomposition, resulting in an increasing function of time until the end of the polymerization reaction. Note that peroxide groups within the polymer chains still decompose and generate long chain monoradicals, which result in high average molecular weights predicted by the model for temperatures of 120–130 °C. If temperature is increased above 130 °C, initiator decomposition increases due to both thermal activation and total decomposition. In this case, the concentration of peroxide groups in the polymer might decrease with time in the course of the polymerization reaction. Total decomposition of the initiator molecule becomes comparable with the sequential decomposition at temperatures of approximately 150 °C. For this reason, even though the obtained R_p are high, the obtained molecular weights are low and do not increase along the reaction, as opposed to the case in the previous temperature range of 120–130 °C. At higher temperatures (170, 180 °C), initiator decomposition becomes very rapid, with a small contribution of sequential decomposition. This contribution increases the concentration of peroxides in polymer, which then decreases as a result of the decomposition undecomposed peroxide groups in polymer chains. At a temperature of 200 °C, initiator decomposition is mostly total and the concentration of peroxide groups in the polymer becomes zero almost instantaneously after the beginning of the reaction. These groups decompose so rapidly that the effect on molecular weights and average rate of polymerization is negligible. For this reason, at temperatures of 200 °C, the initiator behaves as a traditional monofunctional initiator, and while high R_ps are obtained, high average molecular weights might be difficult to achieve.

Comparing the conversion curves for 150 and 200 °C in Figure 3.2, it can be observed that the slope of the conversion curve (related to the rate of polymerization) is almost constant at 150 °C, whereas at 200 °C, conversion reaches a high value in a short period of time, and the slope of the curve largely decreases after said period. This behavior is common to "dead-end" polymerization, which is caused by an extremely rapid consumption of the initiator [96, 97]. In this system, such behavior arises due to the total decomposition mechanism, which has a high activation energy and becomes important at high temperatures.

From the experimental and theoretical results, it can be seen that both systems (150 and

T (°C)	$\bar{R}_{p0.9}$ (mol/(L · min))
130	0.0401
150	0.131
170	0.673
180	1.030
185	0.140
190	0.125
200	0.149

TABLE 3.3: Theoretical study of the effect of temperature on average rates of polymerization up to 90% conversion.

200 °C) reach about 90% conversion in about the same period of time, despite their large temperature difference (50 °C). This indicates a similar average rate of polymerization. The average rate of polymerization to attain a given conversion value can be theoretically calculated using Equation B.26, for different reaction temperatures.

Table 3.3 shows the average rates of polymerization predicted by the model for different reaction temperatures for a conversion value of 90%. It can be seen that the average rate of polymerization increases with temperature up to a temperature of 180 °C. At 185 °C, a drastic decrease in the average rate of polymerization is observed. The rapid decomposition of the initiator and the lack of peroxide groups in polymer chains to re-initiate the reaction (due to total decomposition), generate a decrease in the polymerization rate. This decrease is not compensated by the increase in thermal initiation of styrene. For temperatures higher than 190 °C, a slight increase in polymerization rate can be observed. This is due to the increase of St thermal initiation, which is the main radical generation mechanism at 190 °C and higher temperatures, where there is almost no contribution from peroxide groups.

To better illustrate the change in rate of polymerization, the conversion curves corresponding to 180, 190 and 200 °C at short polymerization times are represented in Figure 3.4, together with the evolution of total peroxide groups, as defined by B.19. It can be observed that the decrease between the rate of polymerization at 180 °C and the rate of polymerization at 190 °C is due to the rapid decomposition of total peroxide groups, generating a large number of radicals at very short reaction times. For a temperature of 190 °C, the system becomes exclusively thermally activated for a time of around

7 minutes, in agreement with the time in which peroxide groups throughout the system are totally consumed. For a lower temperature of 180 °C, the total peroxides are not fully consumed within the time at which the reaction reaches full conversion, the polymerization rate is almost constant up to high conversion values.

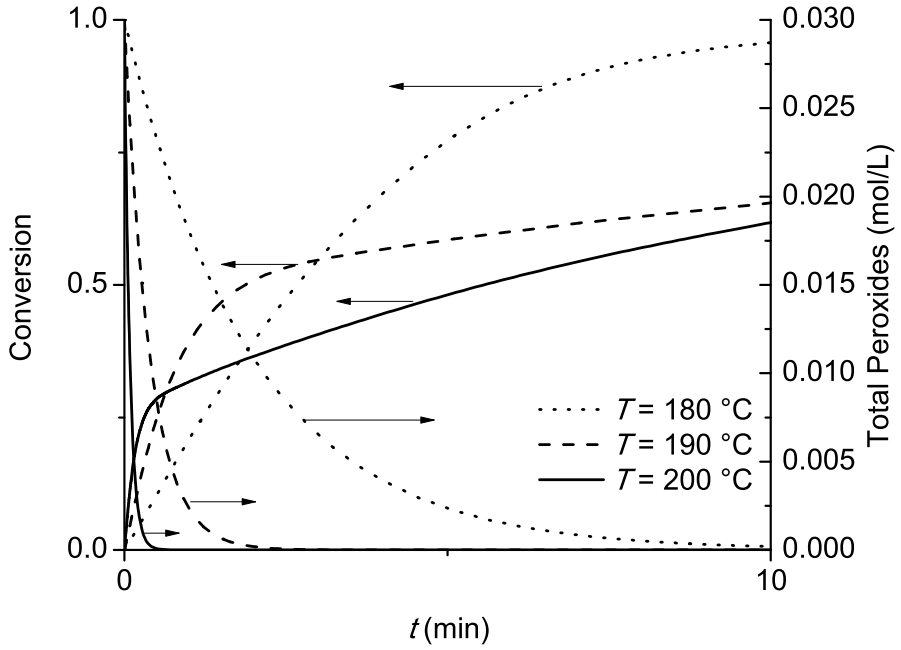

FIGURE 3.4: Theoretical conversion and evolution of total peroxide groups for $T = 180$ °C, $T = 190$ °C and $T = 200$ °C.

Figure 3.5 shows the theoretical MWDs of all formed polymer species at the end of the polymerization reaction. Only MWDs of a few polymeric species are represented in order to keep the picture clear but still representative. The polymeric species are characterized by both their chain length and number of undecomposed peroxide groups, as calculated by the Distributions module of the mathematical model (see Appendix B.2). When the polymerization temperature is such that the initiator decomposition is mostly sequential (130 °C), polymeric chains with undecomposed peroxide groups remain in the obtained product. Polymers with two undecomposed peroxide groups have higher concentration than polymers with a higher number of undecomposed peroxide groups, because these are the main products of an initiator diradical that propagated and terminated to form a polymeric chain. As the reaction temperature increases the fraction of polymers with undecomposed peroxide groups decreases. When the polymerization temperature is such that the initiator is consumed by both sequential and total decomposition (150 °C) this

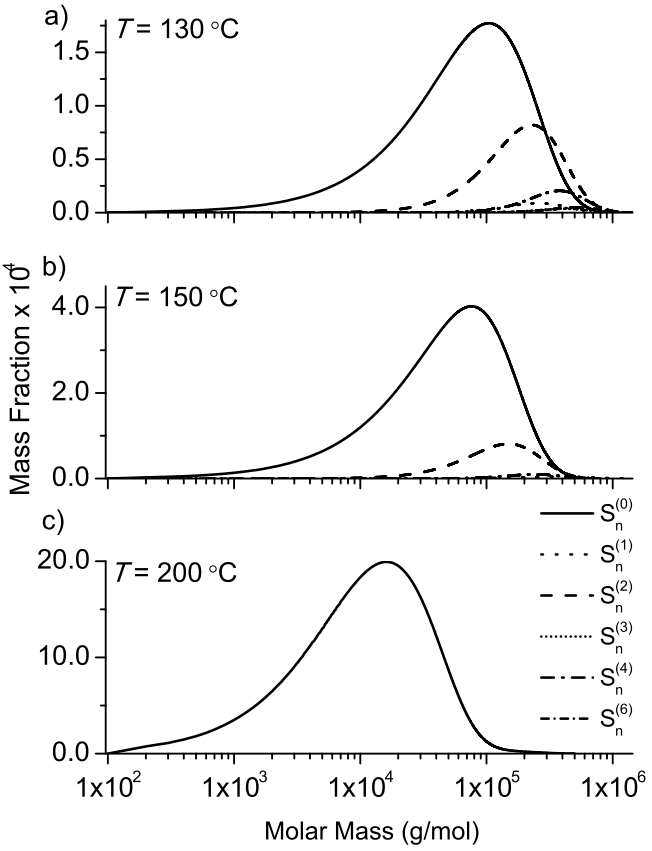

FIGURE 3.5: Theoretical MWD of the polymeric species at the end of polymerization for: a) $T = 130$ °C, b) $T = 150$ °C and c) $T = 200$ °C.

fraction is lowered, and when the polymerization temperature is such that initiator decomposition is mostly total (200 °C), there are no polymeric species with undecomposed peroxide groups at the end of the polymerization reaction. In this case, the simulated molecular structure of the obtained product is analogous to the one obtained in the bulk polymerization of St using a traditional monofunctional initiator. It can be seen that polymers with undecomposed peroxide groups have longer chains than the polymer with no undecomposed peroxide groups for a temperature of 130 °C, where initiator decomposition is mostly sequential. This is not the case for a temperature of 150 °C, due to the similar contribution of both decomposition mechanisms.

Figure 3.6 shows the comparison between experimental and simulated normalized MWDs of the total polymer (i.e. the sum of all polymeric species over number of peroxide groups) at the end of the polymerization reaction for different reaction temperatures. The mass fraction is normalized by dividing by the maximum mass fraction in order to

represent the MWDs for temperatures of 130, 150 and 200 °C in the same figure. A good agreement between experimental and simulated values is observed.

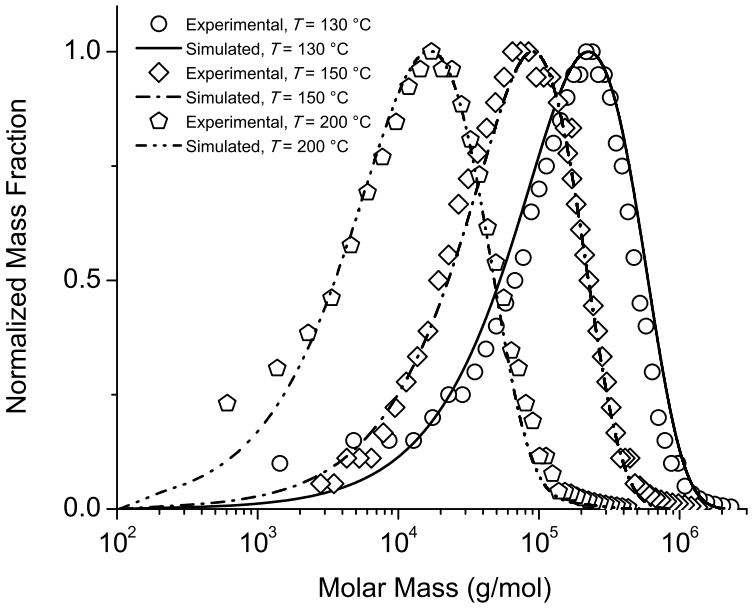

FIGURE 3.6: Experimental and theoretical MWDs of the total polymer for $T = 130$ °C, $T = 150$ °C and $T = 200$ °C.

The experimental and theoretical results for the bulk polymerization of St using DEKTP indicate that the initiator decomposition reaction can determine the behavior of the polymerization system, in terms of rates of polymerization and final properties of the obtained polymer (average molecular weight, presence of undecomposed peroxide groups). These different behaviors can be related to the reaction temperature.

Figure 3.7 shows the fraction of the rate of chemical initiation by total decomposition as a function of temperature. This fraction ia defined by Equation B.29 which involves the kinetic parameters for sequential (k_{d1}) and total decomposition (k_{dt}). Figure 3.7 consists of four different "working zones", each of them determined by the polymerization temperature. For each of these working zones, the polymerization system has different characteristics.

In Zone I (120–130 °C), initiator decomposition is mostly sequential, since the value for k_{d1} is about one order of magnitude greater than the one for k_{dt} (about 3 to 10% chemical initiation by total decomposition). In this region, high rates of polymerization (0.024–0.040 mol·L^{-1}min^{-1}) and high molecular weights (450,000–297,000 g/mol) are

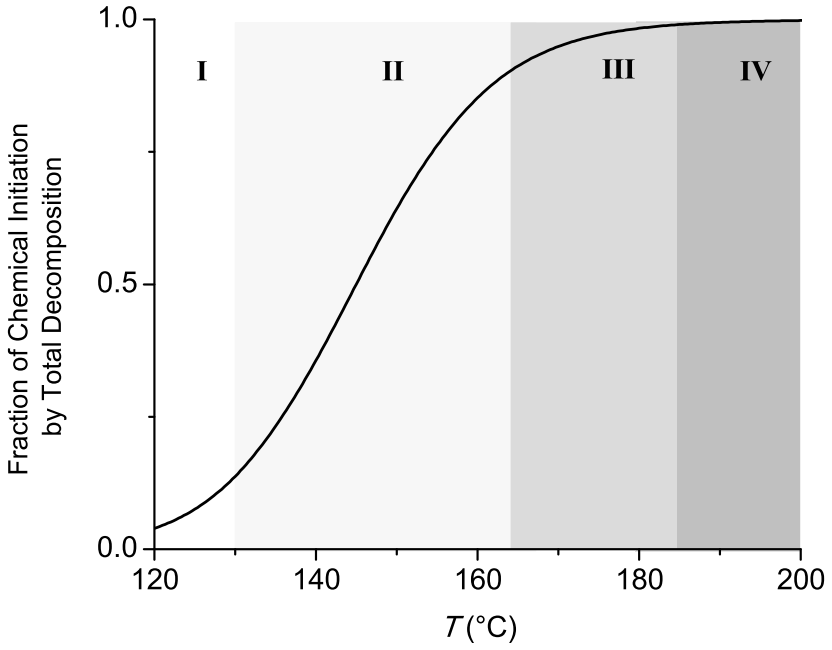

FIGURE 3.7: Fraction of chemical initiation by total decomposition of DEKTP and working zones as functions of temperature.

simultaneously obtained. Average molecular weights increase along the reaction, and the final product is a polymer containing undecomposed peroxide groups.

In Zone II (130–165 °C), initiator decomposition consists of both sequential and total decomposition mechanism, since both kinetic parameters have values in the same order of magnitude. This zone covers a wide range of temperatures for which the fraction of chemical initiation by total decomposition ranges from 10 to about 90%. In this working zone, polymerization rates are high (0.040 - 0.440 mol·L^{-1}min^{-1}), but the obtained molecular weights are significantly lower than those obtained in Zone I ($297,000-77,000$ g/mol), and it is observed that the average molecular weights remain constant or decrease along the reaction. Simulation results also show that polymers containing undecomposed peroxide groups might be obtained when the system reaches full conversion up to a temperature of 160 °C.

In Zone III (165–185 °C), the dominant decomposition mechanism is the total decomposition, as the value for k_{d1} is about one order of magnitude lower than the one for k_{dt} (90-95% chemical initiation by total decomposition). In this region, rates of polymerization are very high ($0.44-0.14$ mol·L^{-1}min^{-1}), but the average molecular weights

are low (77,000–48,000 g/mol) and decrease along the reaction. No polymers with undecomposed peroxide groups are obtained at the end of the reaction.

In Zone IV (185–200 °C), initiator decomposition is mainly total (more than 95% chemical initiation by total decomposition) and so rapid that the system behaves as a "dead-end" polymerization system, and exhibits a limiting value for conversion which can be lower than unity. In this region, the rates of polymerizations can be lower than those of Zone III (0.14–0.15 $mol \cdot L^{-1} min^{-1}$) and the obtained molecular weights are very low (48,000–44,000 g/mol).

Zone I is therefore the zone of technological interest, in which high polymerization rates and high average molecular weights can be obtained simultaneously. However, in industrial polystyrene processes where the final stages are carried out at high temperatures (above 180 °C), the effect of the decomposition of the undecomposed peroxide groups remaining within the polymer, and their effect on average molecular weights must be evaluated. In order to preliminarily estimate this effect, simulations were carried out considering only peroxide group decomposition at high temperatures, as in the previous chapter. Simulations results show a decrease of about 30–40 % in average molecular weight. Nevertheless, the obtained molecular weights are still comparable to those obtained in traditional radical styrene polymerization using monofunctional initiators, but the polymerization rates are higher, resulting in higher overall process productivity.

The working zones defined in this analysis can be directly related to the values of the kinetic parameters of the initiator decomposition reaction. This type of analysis can be performed for another multifunctional initiator, once the model parameters have been validated with experimental data, in order to find the zone of technological interest, for given reaction conditions and desired physical properties.

3.5 Conclusions

The bulk polymerization of St in the presence of DEKTP at temperatures of 150 and 200 °C was experimentally and theoretically investigated.

A mathematical model was developed, considering two simultaneous initiator decomposition mechanisms: sequential and total decomposition of DEKTP. The model allows the

prediction of the evolution of the reacting species concentration, monomer conversion and detailed polymer molecular structure.

The mathematical model can be applied to simulate polymerizations in a wide temperature range (120–200 °C), where experimental information shows that both decomposition mechanisms can be present.

Chemical initiation by DEKTP can be modeled as a set of two parallel reactions for temperatures of 120–200 °C. Experimental and theoretical results indicate a strong dependence of initiator decomposition kinetics with polymerization temperature. For polymerization temperatures of 120–130 °C, initiator decomposition is mostly sequential, resulting in high R_ps and high molecular weights simultaneously. For polymerization temperatures of 130–160 °C, where both decomposition mechanisms are present, higher rates of polymerization can be obtained, at the cost of reducing the average molecular weight of the final product. For polymerization temperatures higher than 160 °C, initiator decomposition is mostly total. The obtained polymers exhibit low molecular weights. In addition, no undecomposed peroxide groups remain within the polymer chains at these reaction temperatures. For temperatures higher than 185 °C, the system can behave as a "dead-end" polymerization system, with low average rates of polymerization and low molecular weights.

The mathematical model can be applied to choose the operating conditions in order to obtain a good balance between process productivity and quality of the obtained product. In addition, this approach could be extended to other multifunctional initiators or other polymers obtained via radical polymerization, as a tool for understanding the process kinetics and their interrelation with reaction conditions.

In the following chapter, a general mathematical model for the bulk polymerization of St for multifunctional initiators of different functionality and structure is presented.

Chapter 4

Bulk styrene polymerization using multifunctional initiators

4.1 Introduction

With the use of monofunctional initiators used in bulk St polymerization, it has been proven difficult to achieve an appropriate balance between residence times, polymerization rates, molecular weights and polydispersities, while also maintaining high conversions, the latter in order to maximize process productivity and minimize residual monomer concentration in the product [2, 65, 70].

As mentioned in Chapter 2, the use of multifunctional initiators provided a solution to the former problem. This type of initiators allows obtaining both high reaction rates and molecular weights, while also enhancing final properties of the product [39, 41, 43, 66, 69]. This improvement was attributed to the existence of additional radical-generating reactions given by the rupture of undecomposed labile groups, which are disseminated in the growing and temporarily dead polymer chains. These species can be involved in further initiation, propagation, chain transfer and termination reactions during the course of polymerization, leading to high average molecular weights. Several works have theoretically studied the synthesis of PS with bifunctional initiators and developed mathematical models to predict the reacting species concentrations and the molecular structure of the obtained polymer in the course of the polymerization reaction.

Kuchanov and Ivanova [87] studied different mono-, bi-, and trifunctional peroxide-type initiators of similar structures at a constant peroxide concentration and found similar polymerization rates that were independent of the initiator employed, provided the peroxide groups have a similar thermal stability. In Ivanov and Kuchanov [88], a statistical model was proposed for polymerization using multifunctional initiators. A few years later, the works of Choi and Lei [69], Kim and Choi [66] and Villalobos et al. [39] theoretically and experimentally investigated the polymerization of St with bifunctional initiators.

The majority of experimental and modeling works involved bifunctional initiators, specifically in the polymerization of St. Works involving experimental studies and modeling of polymerization systems using initiators with functionalities greater than two in free radical polymerization are less numerous [42, 75, 77, 89]. Cerna et al. [89] experimentally studied the bulk polymerization of styrene using initiators with different functionalities (monofunctional, bifunctional, and trifunctional initiators), while Scorah et al. [75] experimentally and theoretically studied the tetrafunctional initiator polyether tetrakis(tert-butylperoxy carbonate) (JWEB50). Works comparing monofunctional with bifunctional initiators can also be found in the literature [43, 65, 66, 69, 70] as well as works employing mixtures of mono- and bifunctional initiators [70].

With respect to initiator structure, it was observed that the use of cyclic multifunctional initiators (e.g. triperoxide cyclohexanone (CHTP), diethylketone triperoxide (DEKTP), acetone triperoxide (ATP), cyclohexanone diperoxide (CHDP) and pinacolone diperoxide (PDP)) in polymerization reactions represents a promising alternative [36, 42, 78, 79]. Sheng et al. [42] experimentally studied the use of the cyclic trifunctional initiator 3,6,9-triethyl-3,6,9-trimethyl-1,4,7-triperoxonane in the bulk polymerization of St, obtaining polymers with high molecular weights at high rates. In Berkenwald et al. [78], the use of diethyl ketone triperoxide (DEKTP), a cyclic trifunctional peroxide initiator, in the bulk polymerization of St was experimentally and theoretically studied. A mathematical model was developed to predict the evolution of the reacting species concentration, monomer conversion, and detailed polymer molecular structure. In this study, initiation by DEKTP at 120–130 °C yielded polymers with high molecular weights at relatively short polymerization times. In Berkenwald et al. [79] the bulk polymerization of styrene using DEKTP at higher temperatures (150–200 °C) was studied. Experimental and theoretical results are consistent with a total rupture of the initiator molecule at these

higher temperatures, resulting in lower average molecular weights. The working temperature zone of technological interest for the use of a multifunctional initiator is therefore that where initiator decomposition is mostly sequential.

From the works available in the literature that were previously discussed, it is observed that the theoretical determination of the detailed molecular structure of PS obtained in the bulk polymerization of St using multifunctional initiators is addressed by relatively few works, due to complexity of the polymerization system and the high calculation times involved in detailed species distributions. When considering cyclic multifunctional initiators, multiradical species may be generated and the polymer species will have undecomposed peroxide groups within their chains. Their position inside the chain should be estimated in order to evaluate the effect of the re-initiation reactions on the molecular weight distribution. Mathematical models based on moment equations can adequately predict the obtained average molecular weights, but fail to evaluate the full molecular weight distribution (MWD) [75]. If the mathematical models were used for simulating the complete industrial polymerization process, it is of importance that the detailed polymer MWD be simulated due to its effect on quality variables such as oligomer content, mechanical properties and processing properties [98]. Some works have used stochastic models, such as Dynamic Monte Carlo Simulation, in order to quantify the full MWD [82, 84]. These models can be mathematically complex and are not particularly well suited for optimization purposed. In addition, the mathematical models involving multifunctional initiators are limited to specific cases, in terms of initiator functionality and structure [65, 66, 69, 70, 75, 78, 79]. These models cannot be readily applied to initiators with other functionalities or structures, where more complex kinetics may be involved.

This objective of this chapter is to develop a general framework and a comprehensive mathematical model for a bulk styrene polymerization system initiated by multifunctional initiators. An advantageous feature of this model is that it allows the estimation of the evolution of the detailed MWD of each polymer species, and full information of the molecular structure of the obtained product. Additionally, this model is a comprehensive model, in the sense that it can be used to simulate any mono- or multifunctional initiator, either linear or cyclic. The model is adjusted and validated using new experimental results for the bulk polymerization of St using different peroxide initiators in

a batch reactor. The model is then used to theoretically study the use of multifunctional initiators and the effect of process conditions on polymerization rate and product quality.

The work presented in this chapter was reported in Berkenwald et al. [99], *"Bulk Polymerization of Styrene using Multifunctional Initiators in a Batch Reactor : A Comprehensive Mathematical Model"*, Int. J. Chem. React. Eng., 14, 1, 2016.

4.2 Experimental work

The experimental work consisted on the synthesis and characterization of the organic peroxide PDP and isothermal batch bulk polymerizations of St using the multifunctional initiators PDP and L331 at 0.01 mol/L. The experimental data for bulk polymerization of styrene using the trifunctional cyclic initiator DEKTP were taken from a previous work [78]. The selected polymerization temperatures are such that initiator decomposition is mostly sequential [36, 79, 89].

4.2.1 Reagents

Styrene (99%) was provided by Sigma-Aldrich and it was purified by vacuum distillation over sodium before use. 1,1-Bis(tert-butylperoxy)cyclohexane (Luperox-331M80) was supplied by Arkema and it was used as received. Ammonium chloride (NH4Cl, 99.5 %), 3-pentanone (99 %), 3,3-dimethyl-2-butanone (98 %), sodium sulfate anhydrous (Na_2SO_4, 99 %), petroleum ether (ACS reagent), methanol (99.8 %) and tetrahydrofuran (THF, 99 %) were supplied by Sigma-Aldrich and they were used without extra purification. Sulfuric acid (H_2SO_4, 98%) and hydrogen peroxide (H_2O_2, 50%) were purchased from J. T. Baker and they were used as received.

4.2.2 Synthesis of PDP

Pinacolone diperoxide (PDP) was obtained according to a method reported in the literature [36]. 50 mmol of 3,3-dimethyl-2-butanone were dripped into a stirred mixture of H_2O_2 (56 mmol) and H_2 SO_4 (195 mmol) at -15 to -20 °C. After 3 hours of reaction, the mixture was extracted with petroleum ether (3×25 mL). The organic layer was

freed of H_2O_2 by washing with a saturated solution of NH_4Cl (3×10 mL) and with water (3×10 mL). The organic layer was dried over Na_2SO_4 for 24 hours. The solution was filtered and the product was isolated by solvent evaporation. The obtained white solid was recrystallized twice from methanol and its purity was confirmed by nuclear magnetic resonance (NMR).

4.2.3 Polymerization reactions

A metal polymerization reactor was filled with 900 mL of St, and initiator was added in order to reach 0.01 mol/L for all initiators. The reaction mixture was de-gassed and blanketed with nitrogen and the reactor was heated to the selected temperature with a heating coil containing flowing hot oil. The employed peroxide initiators were:

- Cyclic trifunctional initiator diethyl ketone triperoxide (DEKTP) (IUPAC Name: 3,3,6,6,9,9-hexaethyl-1,2,4,5,7,8-hexaoxacyclononane)
- Cyclic bifunctional initiator pinacolone diperoxide (PDP) (IUPAC Name: 3,6-ditertbutyl-3,6-dimethyl-1,2,4,5-tetraoxacyclohexane)
- Linear bifunctional initiator Luperox-331M80 (L331) (IUPAC Name: 1,1-Bis(tert-butylperoxy)cyclohexane)

The chemical structures of the different polyperoxide initiators are presented in Figure 4.1.

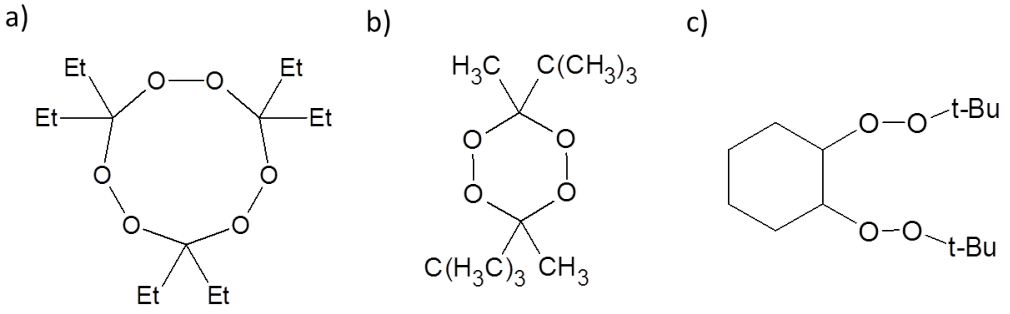

FIGURE 4.1: Chemical structures of multifunctional initiators: a) DEKTP b) PDP, c) L331.

The reaction conditions are summarized in Table 4.1. Note that polymerizations using DEKTP were taken from Berkenwald et al. [78]. The reaction temperature was monitored and controlled using a 4842 PID controller and an air-cooling system in order to

keep the temperature at the desired value. The stirring rate was 50 rpm. Samples were taken along the reaction using a sampling valve located at the bottom of the reaction vessel. The samples were then dissolved in 10 times their volume of toluene under agitation.

Initiator	**Concentration** (mol/L)	**Temperature** (°C)
DEKTP	0.01	120
DEKTP	0.01	130
PDP	0.01	110
PDP	0.01	120
L331	0.01	110
L331	0.01	116

TABLE 4.1: Reactions conditions for St polymerization using multifunctional initiators.

4.2.4 Analytical techniques

Cyclic peroxide initiator PDP was characterized by ^{1}H and ^{13}C NMR using a JEOL Eclipse-300 MHz spectrometer. $CDCl_3$ was used as solvent and analysis were performed at room temperature. The resulting NMR spectra are presented in Figure 4.2.

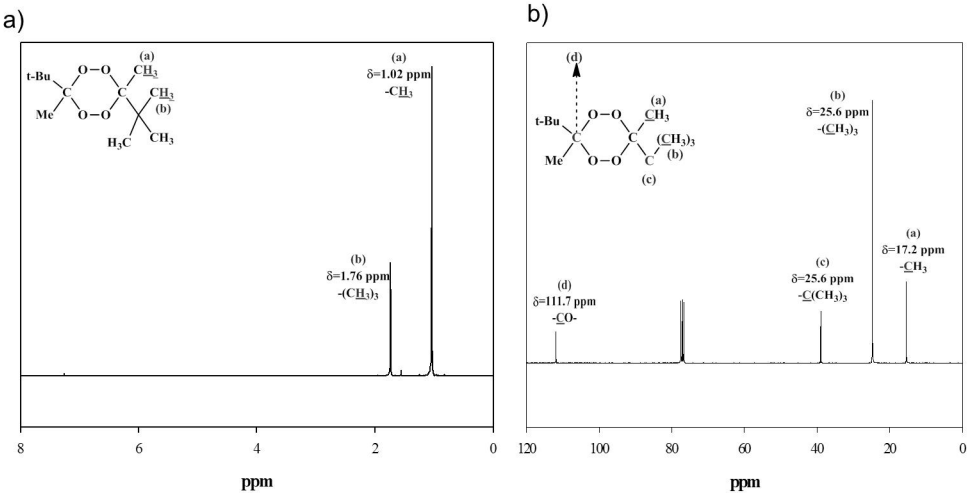

FIGURE 4.2: NMR spectra for synthesized PDP: a) ^{1}H NMR b) ^{13}C NMR.

Polymers were isolated from the samples by precipitation in methanol and filtration. Conversion was determined by gravimetric analysis from the weights of the samples and the weight of the filtered, dry polymer.

Molecular weights of polymer samples were determined by size exclusion chromatography (SEC) at 40 °C using a Hewlett-Packard instrument (HPLC series 1100) equipped with UV light and refractive index detectors. A series of three PLGel columns at porosities of 10^3, 10^5, and 10^6 Åwas used. Calibration was carried out with PS standards and THF (HPLC grade) was used as eluent at a flow rate of 1 mL/min.

4.2.5 Experimental results

The results for conversion and average molecular weights of the experiments of Table 4.1 are presented in Figure 4.3. Experimental results for the molecular weights distributions at the end of polymerization are presented in Figure 4.3.

The experimental results show that polymerizations rates are higher for PDP than for DEKTP at equivalent reaction temperature and initial initiator concentration. Further, initiation by L331 provides a higher initial polymerization rate than the one for PDP at the same temperature of 110 °C. As expected, increasing the reaction temperature increases the initial polymerization rate. It is observed that PDP initiation provides a greater initial R_p compared to DEKTP, indicating that the peroxide groups in PDP are less stable than those of DEKTP. The stability of peroxide groups inside the initiator molecules has been theoretically investigated using molecular simulations, which have shown that several stable conformers exist for DEKTP, while only two are stable in the case of PDP [100]. Similarly, the peroxide groups in L331 would be less stable than those in PDP. As regards the molecular weights, it can be seen that higher molecular weights are obtained when using DEKTP with respect to PDP and L331. This can be attributed to a higher stability -and lower decomposition rate- of peroxide groups in cyclic initiators, as well as the presence of diradicals in the reaction system.

4.3 Mathematical model

4.3.1 Homogeneous polymerization model

The mathematical model is based on the kinetic mechanism presented in Table 4.2, which includes initiation via a symmetrical cyclic or linear multifunctional initiator, thermal initiation, propagation, transfer to the monomer, combination termination and

re-initiation. In addition to the nomenclature from the preceding chapters, the following nomenclature is adopted:

$I^{(\phi)}$	Cyclic multifunctional initiator with ϕ undecomposed peroxide groups
$\bar{I}^{(\phi)}$	Linear multifunctional initiator with ϕ undecomposed peroxide groups
$\cdot I \cdot^{(i)}$	Initiator diradical with i undecomposed peroxide groups
$I \cdot^{(i)}$	Initiator monoradical with i undecomposed peroxide groups
$\cdot S_1 \cdot^{(i)}$	Monomer diradical with i undecomposed peroxide groups
$S_1 \cdot^{(i)}$	Monomer monoradical with i undecomposed peroxide groups

---

Initiation$(\phi = 1, 2, 3; i < \phi)$
Thermal Initiation
$3\text{St} \xrightarrow{k_{i0}} 2S_1 \cdot^{(0)}$
Chemical Initiation
$I^{(\phi)} \xrightarrow{\phi k_{d1}} \cdot I \cdot^{(\phi-1)}$
$\bar{I}^{(\phi)} \xrightarrow{\phi k_{d1}} \bar{I} \cdot^{(i)}$
$\cdot I \cdot^{(i)} + \text{St} \xrightarrow{2k_{i1}} \cdot S_1 \cdot^{(i)}$
$I \cdot^{(i)} + \text{St} \xrightarrow{k_{i1}} S_1 \cdot^{(i)}$

Propagation $(n = 1, 2, 3...; i = 0, 1, 2...)$
$S_n \cdot^{(i)} + \text{St} \xrightarrow{k_p} S_{n+1} \cdot^{(i)}$
$\cdot S_n \cdot^{(i)} + \text{St} \cdot \xrightarrow{2k_p} S_{n+1} \cdot^{(i)}$

Transfer to monomer $(n = 1, 2, 3...; i = 0, 1, 2...)$
$S_n \cdot^{(i)} + \text{St} \xrightarrow{k_{fM}} S_n{}^{(i)} + S_1 \cdot^{(0)}$
$\cdot S_n \cdot^{(i)} + \text{St} \xrightarrow{2k_{fM}} S_n \cdot^{(i)} + S_1 \cdot^{(0)}$

Re-initiation $(n = 2, 3, ...; m = 1, 2, ..., n-1; i = 1, 2...; j = 0, 1, ..., i-1)$
$S_n{}^{(i)} \xrightarrow{ik_{d2}} S_{n-m} \cdot^{(i-j)} + S_m{}^{(j-1)}$.

Combination termination $(n, m = 1, 2, 3...; i, j = 0, 1, 2...)$
$\cdot S_n \cdot^{(i)} + \cdot S_m \cdot^{(j)} \xrightarrow{4k_{tc}} \cdot S_{n+m} \cdot^{(i+j)}$
$\cdot S_n \cdot^{(i)} + S_m \cdot^{(j)} \xrightarrow{2k_{tc}} S_{n+m} \cdot^{(i+j)}$
$S_n \cdot^{(i)} + S_m \cdot^{(j)} \xrightarrow{k_{tc}} S_{n+m}{}^{(i+j)}$

TABLE 4.2: St polymerization using multifunctional initiators - Proposed kinetic mechanism

The following was considered: i) at the temperatures employed, the initiators decompositions are due exclusively to sequential decomposition [36, 39, 89]; ii) intra-molecular

termination is negligible [41]; iii) disproportion termination is negligible [92]; iv) all peroxide groups present in the initiator and in the accumulated polymer exhibit the same thermal stability [41]; v) because of the short lifetime of radicals, the decomposition of undecomposed peroxide groups does not occur in radical molecules [41]; vi) propagation and transfer reactions are unaffected by the chain length or conversion [41]; vii) degradation reactions are negligible [17].

Note the following: 1) when two mono-radicals with i and j undecomposed peroxide groups terminate, the formed polymer will contain $i+j$ undecomposed peroxide groups; 2) with a cyclic trifunctional initiator, diradicals only have an even number of peroxide groups, as they are generated only by propagation of the initiator diradical (with only two peroxide groups) and by the combination termination of other diradicals, all of which have an even number of peroxide groups; 3) re-initiation involves the decomposition of a peroxide group within a polymer chain with undecomposed peroxide groups, which generates two mono-radicals capable of further growth. Because of the molecular structure of the initiator molecules considered, only linear diradicals and mono-radicals and linear polymer chains can be formed in the reaction system.

At temperatures of 110–130 °C, peroxide groups in the initiators considered in this work decompose sequentially, and thus polymeric species containing undecomposed peroxide groups are generated. Said species can further decompose during the course of polymerization, adding to the complexity of the polymerization mechanism. Both the radical and polymer chain length distributions are modified by the rupture of one of these peroxide groups. Even though the values for the average molecular weights could be obtained by a moments-based mathematical model, a more detailed model is required in order to simulate the evolution of the full MWD.

A first-order, bi-dimensional, non-linear polymerization model was developed from the kinetic mechanism detailed in Table 4.2. The model consists of a set of non-linear differential equations, which are derived from the mass balances for the reacting species (see Appendix C), including the living radical species, dead and temporarily dead polymer species for all kinetic chain lengths and number of undecomposed peroxide groups.

The mathematical model consists of three modules:

- The Basic module (Appendix C.1), which allows the prediction of global chemical species evolution along the reaction (monomer, initiators, total radical species).
- The Moments module (Appendix C.2), consisting of equations for the evolution of the 0th, 1st and 2nd moments of the reacting species chain length distributions. Said moments can be used to estimate the evolution of average molecular weights during the course of polymerization.
- The Distributions module (Appendix C.3), which simulates the evolution of all chemical species, characterized by their chain length and number of undecomposed peroxide groups. The equations estimate the evolution of the complete MWD of each radical and polymer species. In order to consider the effect of reinitiation reactions in the MWDs, polymer chains were assumed to have uniformly distributed peroxide groups. A random-chain scission can be simulated with a uniformly distributed random variable. The uniform peroxide group distribution hypothesis is expected to be valid for cyclic initiators and for linear initiators with functionalities greater than two.

The proposed model considers an ideal cooling/heating system, which allows the polymerization temperature to be set at a specific value. However, the effect of temperature on reaction kinetics is considered through the use of Arrhenius expressions for the kinetic parameters. The gel effect was indirectly considered by appropriately reducing the value of the termination kinetic coefficient with increasing conversion [17].

The Basic module can be solved independently from the other two, and for its resolution, Equations C.1 to C.4, C.6, C.7, and C.15 to C.16 must be simultaneously solved. For predicting polymer molecular structure, the Moments module or alternatively the Distributions modules can be solved using the results from the Basic module, in order to estimate the average molecular weights or the detailed MWD of the polymer species, respectively. The Basic and Moments modules are solved by standard stiff differential equation numerical methods based on a second-order modified Rosenbrock formula, programmed in MATLAB v. 8.3. In the Distributions module, a large number of equations (more than 500,000) must be integrated. For this reason, an explicit forward Euler method was used, with the time intervals obtained from resolution of the basic module. A typical simulation requires less than 1 s for the Basic module, 1 min for the Moments

module and about 5 min for the Distributions module with an Intel Core i5 based processor at 2.40 GHz. These calculation times are considerably shorter than what has been reported with similar moments-based models for bifunctional initiators [84].

4.4 Simulation results

The model was adjusted using the experimental data in Figure 4.3 and Figure 4.4. Model parameter adjustment was sequential and consisted of two steps, using least-squares optimization algorithms. Firstly, k_{d1}, k_{dp}, f_1 and f_2 for each initiator were adjusted with the conversion data. Since all peroxide groups are assumed to have the thermal stability, $k_{dp} = k_{d1}$ and it was assumed that $f_1 = f_2$. Secondly, k_{fM} was adjusted with the average molecular weight data. The obtained values for the decomposition constants are in accordance with what has been reported for the decomposition rates of organic peroxides [89], and the values for the transfer constants are within the expected range reported in the literature [19]. All other values for the kinetic parameters were taken from the literature [17]. Model parameters are presented in Table 4.3.

Model parameter adjustment yields k_{d1} (L331) $>$ k_{d1} (PDP) $>$ k_{d1} (DEKTP), their differences being of orders of magnitude, which is in agreement with the experimental results. The higher value for L331 is related to the higher initial R_p, as discussed earlier. In addition, simulation results indicate that, in the case of L331 at 116 °C, the initiator is totally consumed at around 100 min, which is in agreement with the experimental results, as the slope of the conversion curve decreases at around 100 min at 116 °C. Once the initiator is fully consumed, the system becomes almost exclusively thermally activated and the R_p decreases.

As it can be observed in Figures 4.3 and 4.4, theoretical and experimental results are in very good agreement. The differences in molecular weights are, in all cases, within the experimental error range (below 10%). Note that the major differences in molecular weight values occur for the linear bifunctional initiator L331. The result is expected due to the uniform peroxide group distribution hypothesis. As an additional verification, simulations were carried out modifying the peroxide group distribution for the specific case of a bifunctional linear initiator, for which all peroxide groups are located

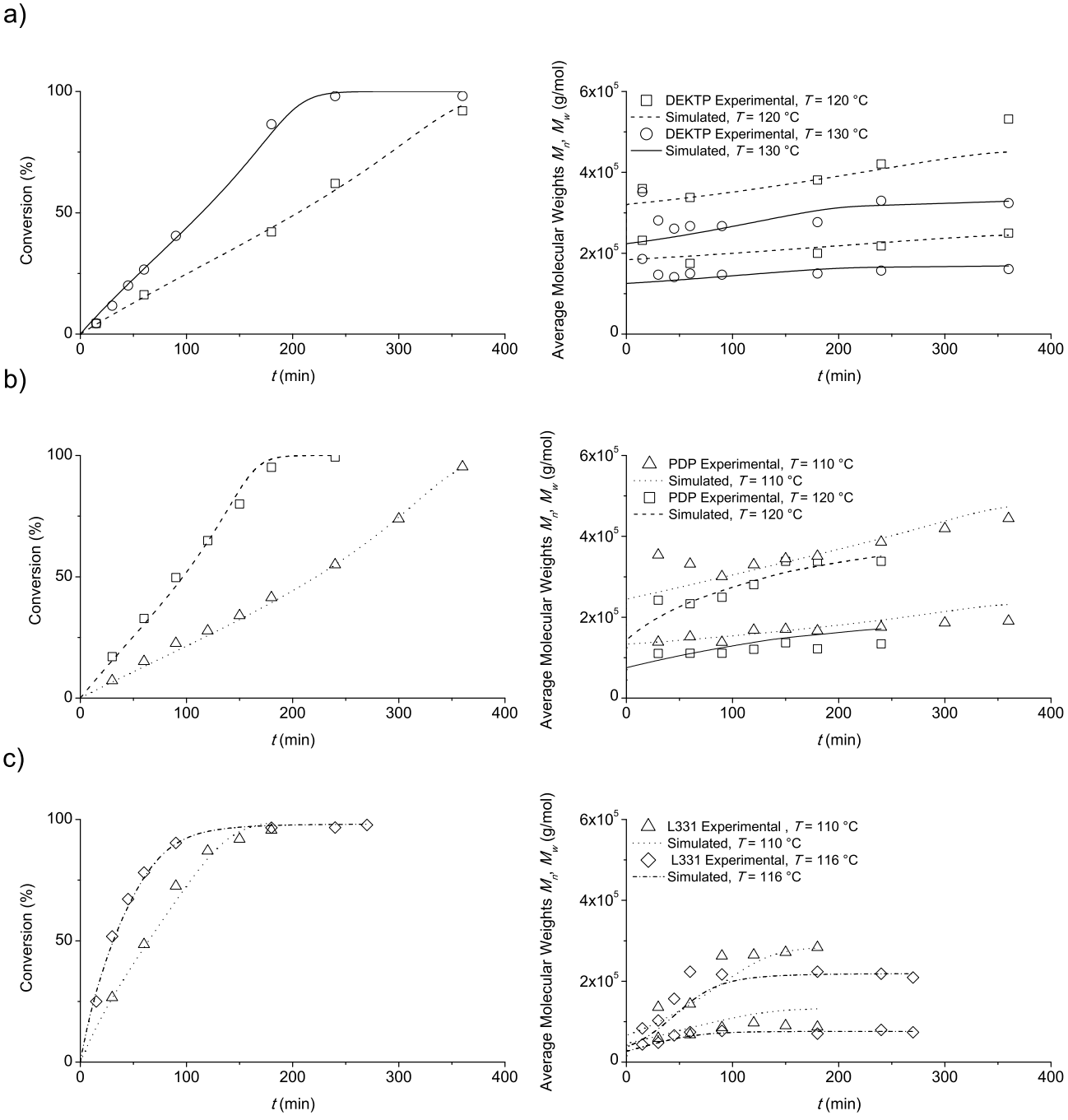

FIGURE 4.3: Conversion and average molecular weights as functions of time for a) DEKTP, b) PDP and c) L331.

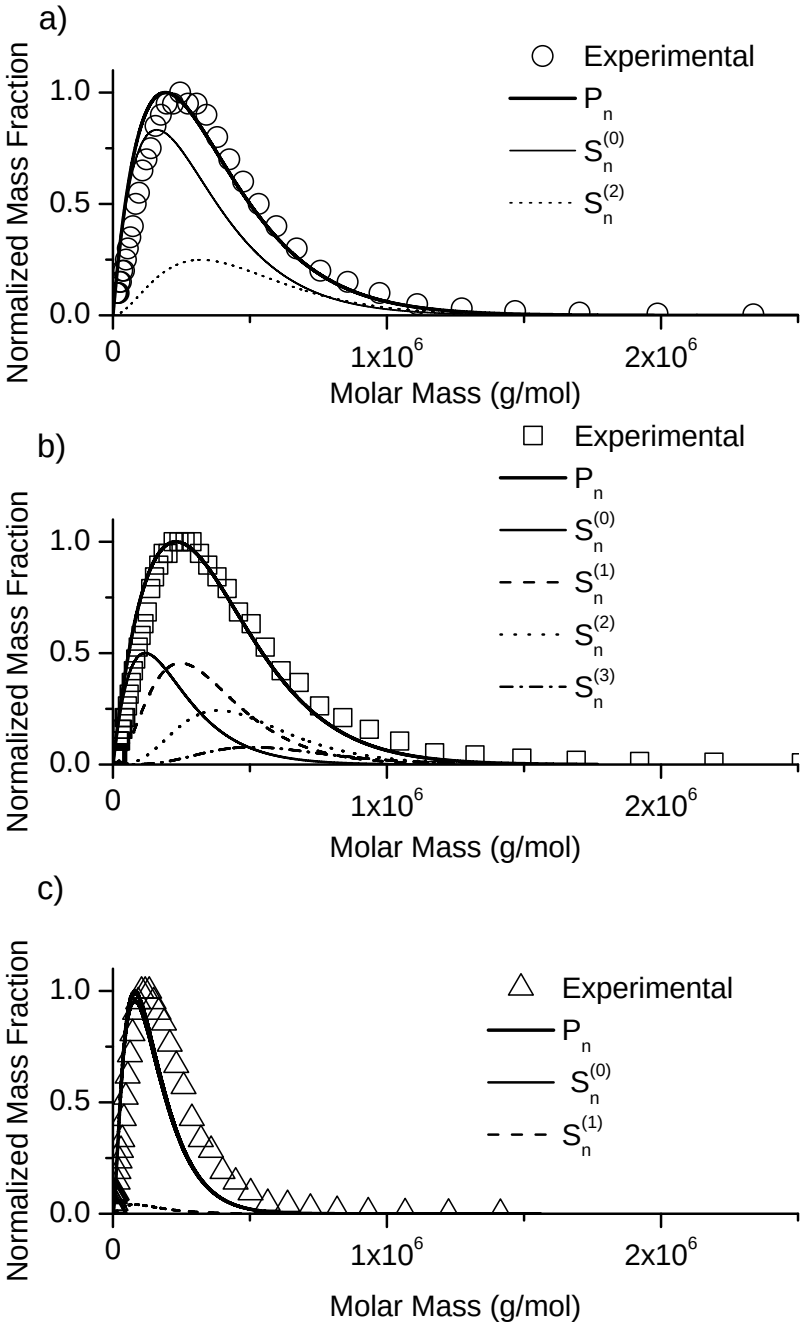

FIGURE 4.4: Experimental and theoretical MWDs for a) DEKTP, b) PDP and c) L331.

Parameter	**Units**	**Arrhenius expression**	**Reference**
k_{d1}, k_{dp} (DEKTP)	s^{-1}	$4.0e^{-5440/T}$	Adjusted in this work
k_{d1}, k_{dp} (PDP)	s^{-1}	$7.0 \cdot 10^{17}e^{-19761/T}$	Adjusted in this work
k_{d1}, k_{dp} (L331)	s^{-1}	$5.0 \cdot 10^{20}e^{-21331/T}$	Adjusted in this work
f_1, f_2 (DEKTP)		$0.03T - 11.29$	Adjusted in this work
f_1, f_2 (PDP)		$0.0025T - 0.708$	Adjusted in this work
f_1, f_2 (L331)		$0.0033T - 12.32$	Adjusted in this work
k_{i0}	$\frac{L^2}{mol^2 S}$	$2.19 \cdot 10^5 e^{-13810/T}$	[17]
k_{i1}, k_p	$\frac{L}{mol\ s}$	$1.051 \cdot 10^7 e^{-7082/RT}$	[17]
k_{fM}	$\frac{L}{mol\ s}$	$7.0 \cdot 10^{10} e^{-10185/T}$	Adjusted in this work
k_{tc}	$\frac{L}{mol\ s}$	$1.686 \cdot 10^9 e^{-(844/T)-2(C_1x+C_2x^2+C_3x^3)}$ [a]	[93]

[a] $C_1 = 2.75 - 0.00505T; C_2 = 9.56 - 0.0176T; C_3 = -3.03 + 0.00785T$, with x monomer conversion

TABLE 4.3: St polymerization using multifunctional initiators - Adopted kinetic parameters.

at chain ends (see Appendix C.3). In this case, as expected, a broader simulated MWD is obtained, which is in better agreement with the experimental values.

To confirm the consistency of the different modules, the following verifications were carried out:

- It was verified that the results from the Basic, Moments and Distributions modules were equivalent. Specifically, it was verified that average molecular weights calculated with the Moments module had the same values as the MWD averages obtained with the Distributions module, conversion calculated with Distributions module matched the one calculated with the Basic module and that peroxide group concentrations calculated by the Basic, Moments and Distributions modules are equivalent.

- It was verified that, when using the initiator L331 (linear bifunctional), polymers had a maximum of two undecomposed peroxide groups. When using a bifunctional linear initiator, polymer species with more than two peroxide groups are not generated in the course of polymerization.

Other simulation results using the model are presented in Figure 4.4, Figure 4.5 and Table 4.4.

Figure 4.5 shows the evolution of the total polymer species concentrations as functions of conversion, characterized by the number of (undecomposed) peroxide groups, as defined by Equation D.35. The simulated conditions correspond to the conditions in Table 4.1.

In Figure 4.5, it can be observed that species containing different numbers of peroxide groups are generated in the polymerization system. For these systems, the polymer without peroxide groups is the most abundant polymer species. This species is mainly generated by thermal initiation of the monomer.

In the case of the trifunctional cyclic initiator DEKTP and 130 °C, the species with two peroxide groups is the most abundant peroxide-containing species. This is because said polymer species is generated mostly by chemical initiation, and the primary initiator diradical contains two peroxide groups. The polymer with one peroxide group is generated at around 10% conversion, since the polymer with two peroxide groups must decompose for a growing chain containing one peroxide group to be generated. An analogous reasoning applies to polymers with a higher number of peroxide groups. It should be noted that polymers with an even number of peroxide groups are also generated by termination between two initiator diradicals and further propagation of the generated diradical (containing an even number of peroxide groups), accounting for their higher concentrations in the system. For the peroxide-containing species, the speed of generation exceeds that of decomposition, and their concentration increases with conversion.

In the case of the bifunctional cyclic initiator PDP at 120 °C, initiator decomposition generates a growing diradical with one undecomposed peroxide group. As the decomposition rate is higher than for the case of DEKTP, and the contribution of thermal initiation is lower, a larger number of peroxide containing species is generated. In the case of the species with a high number of peroxide groups (three or four), the rate of decomposition can exceed the rate of generation, and the polymer concentration can

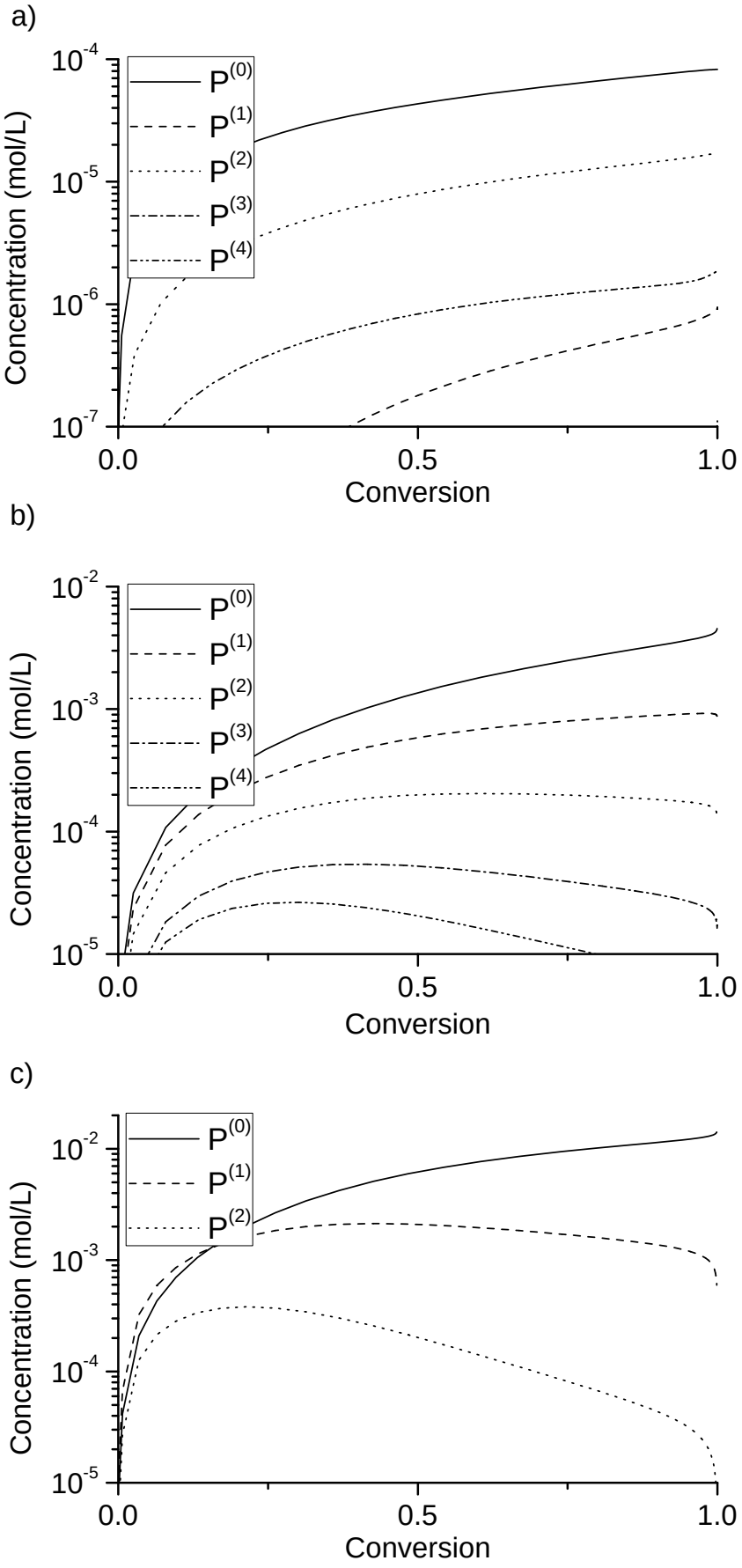

FIGURE 4.5: Evolution of the polymeric species for a) DEKTP, $T = 130$ °C, b) PDP, $T = 120$ °C, c) L331, $T = 116$ °C.

decrease with increasing conversion. Before the system reaches full conversion, the polymer with three peroxide groups is almost fully consumed and the polymer with four peroxide groups is fully consumed.

In the case of the linear bifunctional initiator L331 at 116 °C, the decomposition rate is highest, and the contribution of thermal initiation is lowest. The polymer containing one peroxide group, generated by propagation of the initiator radical, is in a larger proportion than the polymer without peroxide groups at very early stages in the polymerization. However, due to the decomposition of the peroxide groups, its concentration eventually decreases. The polymer with two peroxide groups is fully consumed before the system reaches full conversion. Due to the linear structure of the initiator molecule, polymers with a higher number of peroxide groups are not generated in this system.

In Figure 4.4, the MWDs of the most relevant molecular species, characterized both by chain length and number of peroxide groups, are presented. As expected, the polymer without peroxide groups is the most abundant species at the end of the polymerization for all initiators. As previously stated, in the case of DEKTP the polymer with two peroxide groups is the most abundant among these peroxide-containing species. In the case of PDP, due to the lower temperature and lower decomposition rate of the peroxides, a greater number of polymer species containing peroxide groups is present at the end of the polymerization. The polymer with one peroxide group, mainly generated from an initiator radical, is the most abundant peroxide-containing polymer species. In the case of L331, only a small fraction of polymer with one peroxide group remains in the system at the end of polymerization, due to the very high decomposition rate of the peroxide groups.

The model was also used to theoretically evaluate the influence of initiator functionality and structure in different polymerization processes. A series of simulations were carried out, corresponding to theoretical experiments, varying the initiator functionality and structure for given process conditions. In all of the simulations, it was assumed that the peroxide groups have a decomposition constant of $k_{d1} = k_{dp} = 4 \cdot 10^{-6}$ s^{-1} and $f_1 = f_2 = 0.5$ at a temperature of 120 °C. For the simulations, the functionality and structure of the initiators were varied, while the initial peroxide group concentration was set to 0.02 mol/L for all simulated initiators, so that the results can be compared. Simulation results are presented in Table 4.4.

Functionality	**Structure**	$\bar{R}_{p,100\%} \times 10^4$ (mol/L·s)	$\bar{M}_n \times 10^{-5}$ (g/mol)	$\bar{M}_w \times 10^{-5}$ (g/mol)
3	cyclic	3,19	2,80	5,31
3	linear	3,20	2,15	3,95
2	cyclic	3,19	2,77	5,20
2	linear	3,20	2,12	3,96
1	cyclic	3,19	2,73	5,37
1	linear	3,19	2,09	4,01

TABLE 4.4: Theoretical study of initiator functionality and structure in a St polymerization process.

As expected, all initiators provide equivalent rates of polymerization, if the same initial peroxide group concentration is used. The fact that the rate of initiation is independent of initiator functionality when all peroxides have the same thermal stability had been already experimentally verified in the work of Kuchanov and Ivanova [87]. It is also observed that higher average molecular weights are obtained when using initiators with higher functionalities, as the effect of re-initiation reactions on molecular weights is increased. A cyclic initiator provides higher average molecular weights than a linear one of the same functionality. This is explained by the fact that diradicals can propagate by their two ends, generating longer chain radicals. In addition, termination or transfer reactions of diradicals can form monoradicals, capable of further propagation and growth. The effect on polymerization rate of the diradicals containing two active reacting sites is small, since the concentration of monoradicals exceeds that of diradicals, due to thermal decomposition.

If a hypothetical family of initiators were to be synthesized, for which all peroxide groups had the same thermal stability, theoretical results show that:

- A cyclic initiator provides higher average molecular weights compared with a corresponding linear one, by about 30%. The structure of the initiator has little effect on the rate of polymerization
- At the same initiator concentration, an initiator of higher functionality provides higher polymerization rates and higher average molecular weights.

- At the same initial peroxide group concentration, an initiator of higher functionality provides higher average molecular weights while maintaining a high polymerization rate.

4.5 Conclusions

A comprehensive mathematical model was presented, which simulates the evolution of all the chemical species in the course of a bulk styrene polymerization process using multifunctional initiators.

The model was adjusted and validated using the experimental data from batch polymerization reactions using initiators DEKTP, PDP and L331. The proposed kinetic mechanism considers the re-initiation reactions due to undecomposed peroxide groups within the polymer chains, and the derived model can be used to evaluate the molecular structure of the obtained polymer. Theoretical and experimental results indicate that initiator structure and functionality are key variables determining initiator performance. An initiator of a high functionality and a cyclic structure provides polymers of high molecular weights, while maintaining high polymerization rates.

The model can be extended to simulate an industrial process with a polymerization initiator of a specific functionality and structure and for plant optimization purposes.

Chapter 5

Bulk styrene polymerization in the presence of polybutadiene using multifunctional initiators

5.1 Introduction

High impact polystyrene is a reinforced engineering thermoplastic, produced by bulk polymerization of St in the presence of a rubber (PB or butadiene copolymer). This heterogeneous material consists of a vitreous PS matrix, containing dispersed rubber particles. Said particles contain PS occlusions, which can have either salami or core-shell morphologies. HIPS properties depend not only on the recipe and operating conditions, but also on the technology employed in the production process [101, 102].

The industrial bulk process for the production HIPS involves four main stages: dissolution, prepolymerization, termination, and devolatilization [11]. In the first stage, the rubber is dissolved into the monomer at relatively low temperatures. The prepolymerization stage consists of the addition of a chemical initiator, under continuous stirring, reaching usually approximately 10–20 % conversion. In said stage, the morphology of the material is developed. Termination takes place at higher temperatures, in order to reduce the viscosity and promote the thermal initiation of the monomer. This stage is

carried out without stirring, to avoid destruction of the morphology. During the devolatilization stage, the unreacted monomer is removed, under vacuum and at elevated temperatures.

During the prepolymerization, the system is initially homogeneous. However, the thermodynamic incompatibility between PB and PS causes the system to separate into two phases: a continuous, rubber-rich phase and a dispersed, PS-rich phase [103, 104]. The reaction then proceeds with the generation of free PS, and graft copolymer (GC) [104, 105]. Towards the end of the prepolymerization stage, a crucial for the development of morphology takes place, known as phase inversion (PI). After the PI, the morphology remains almost unchanged during the following stages [12]. The PI is basically determined by the volume and viscosity of the phases, the presence of GC, and the stirring conditions [106, 107]. The PI phenomenon has been studied [108–112] but is still poorly understood.

The GC is generated by H-abstraction reactions involving the rubber and a free radical species, resulting in an active site from which a polymer chain can grow. Said radical species can be generated by chemical decomposition of an initiator molecule, which contains a certain number of labile groups, depending on its functionality. As in other industrial free-radical polymerization processes, with the use of monofunctional initiators it is difficult to achieve a good balance between process productivity and product properties [39].

Bifunctional initiators in processes for obtaining HIPS have been studied [41, 70, 113] both experimentally and theoretically. It was observed that said initiators allow high productivity and high molecular weights. The cyclic trifunctional initiator DEKTP has also been experimentally studied in the obtention of HIPS [76], obtaining products with adequate particle morphology and a good physical properties. It has been observed that the sequential decomposition of the initiators leads to significant increases in the rate of polymerization, high molecular weights and may introduce branching in the chains leading to improvements in the rheological and processing properties [74].

Most of the mathematical models of the bulk HIPS process assumed the reaction system to be homogeneous and allowed to simulate both batch [41, 94] as continuous industrial processes [11, 57, 113]. Except in Estenoz et al. [41] in which mono- and bifunctional initiators are considered, in all the above models are limited to the use of monofunctional

initiators. Even though multifunctional initiators are widely used in industrial HIPS processes, there are no available mathematical models to simulate a HIPS polymerization process using linear initiators with functionalities greater than 2 or cyclic multifunctional initiators.

This chapter is the first attempt to develop a comprehensive mathematical model for the bulk HIPS process using multifunctional initiators. The model allows the estimation of the evolution of the detailed MWD and molecular structure of the obtained products (free PS, GC and residual PB). This model can be used to simulate processes using any mono- or multifunctional initiator, either lineal or cyclic. The model is adjusted and validated using new experimental results for the bulk polymerization of St in the presence of PB using different peroxide initiators. The model is also used to theoretically study the use of multifunctional initiators and the effect of process conditions on polymerization rate and product quality.

The work presented in this chapter was reported in Berkenwald et al. *"Experimental and theoretical study of the use of multifunctional in the high impact polystyrene bulk process"*, submitted to Int. J. Chem. React. Eng., ID ijcre-2016-0069, 2016.

5.2 Experimental work

The experimental work consisted on the synthesis and characterization of high impact polystyrenes using three initiators with different functionalities: DEKTP (cyclic trifunctional), PDP (cyclic bifunctional) and L331 (linear bifunctional). The selected polymerization temperatures are such that initiator decomposition is mostly sequential [25, 36].

5.2.1 Reagents

Styrene (99 %) was provided by Sigma-Aldrich and it was purified by vacuum distillation over sodium before use. 1,1-bis(tert-butylperoxy)cyclohexane (Luperox-331M80) was supplied by Arkema and it was used as received. Sodium sulfate (Na_2SO_4, 99 %), petroleum ether (ACS reagent), methanol (99.8 %) and tetrahydrofuran (THF, 99 %) were supplied by Sigma-Aldrich and they were used without extra purification. Sulfuric acid (H_2SO_4, 98 %) and hydrogen peroxide (H_2O_2, 50 %) were purchased from J. T.

Baker and used as received. The medium cis-PB was provided by Dynastol Elastómeros S.A de C.V., Mexico ($\bar{M}_n = 215,000$g/mol, $\bar{M}_w = 410,000$g/mol). Cyclic initiators DEKTP and PDP were synthesized and characterized as indicated in Chapters 2 and 4.

5.2.2 Polymerization reactions

The polymerization reactions consisted of a series of bulk polymerizations of St in the presence of PB, with the main stages of an industrial HIPS process (dissolution, prepolymerization and finishing) using different multifunctional peroxide initiators. In the industrial process, the dissolution and prepolymerization take place in a series of continuously stirred tank reactors, while the finishing takes place in a series of non agitated reactors [11]. The peroxide initiators employed and reaction conditions, including initial initiator concentration of functionality ϕ $[I_0^{(\phi)}]$ and prepolymerization temperature T_{PP} are presented in Table 5.1.

Initiator	$[I_0^{(\phi)}]$ (mol/L)	T_{PP} (°C)
DEKTP	$1.56 \cdot 10^{-3}$	120
DEKTP	$1.56 \cdot 10^{-3}$	130
PDP	$1.56 \cdot 10^{-3}$	110
PDP	$1.56 \cdot 10^{-3}$	120
L331	$1.56 \cdot 10^{-3}$	110
L331	$1.56 \cdot 10^{-3}$	116

TABLE 5.1: Experimental conditions for HIPS polymerization using multifunctional initiators.

5.2.2.1 Dissolution

A metal polymerization reactor was filled with 64 g of PB and 736 g of St and was left under agitation at 70 rpm for 2 hours until a homogeneous mixture was obtained.

5.2.2.2 Prepolymerization

The selected peroxide initiator was added in order to reach a concentration of $1.56 \cdot 10^{-3}$ mol/L for all initiators. The reaction mixture was de-gassed and blanketed with nitrogen and the reactor was heated to the selected temperature with a heating coil containing

flowing hot oil. The reaction temperature was monitored and controlled using a 4842 PID controller and an air-cooling system in order to keep the temperature at the desired value. Samples were taken along the reaction using a sampling valve located at the bottom of the reaction vessel. In the industrial process, the prepolymerization stage proceeds until phase inversion. For the experimental setup, the prepolymerization time was set to 120 min in order to ensure phase inversion, which was visually verified.

5.2.2.3 Finishing

After the prepolymerization, 5 samples were taken from the reaction medium and placed into glass tubes, which are immersed in a bath of deionized water, in order to reach full conversion for 20 hours at a finishing temperature T_F of 150 °C.

5.2.3 Characterizations

5.2.3.1 Conversion

The samples taken at the prepolymerization stage were dissolved in 10 times their volume of toluene under agitation at room temperature until full dissolution. The polymer was then precipitated dropwise from methanol, filtered and dried under vacuum at 50 °C until constant weight.

5.2.3.2 Grafting efficiency

The grafting efficiency E_{GS} is defined as the ratio between the grafted PS mass and the total PS mass (free and grafted).

The free PS was isolated from the other polymer species (PB and GC) using the following solvent extraction technique: 0.5 g of each sample was dissolved in 25 mL of methyl ethyl ketone/dimethylformamide (MEK/DMF; 50 % in volume) mixture; under agitation at room temperature until full dissolution. The mixture was then centrifuged at 20,000 rpm at −20 °C for 4 h, and an insoluble precipitate and a soluble supernatant were obtained. The free PS from the soluble fraction was precipitated dropwise from methanol, filtered and dried under vacuum at 50 °C until constant weight. The precipitate, consisting of

the species PB and GC, was isolated from the soluble fraction and dried under vacuum at 50 °C until constant weight. The grafted PS was calculated by subtracting the initial PB mass to the PB and GC mass.

5.2.3.3 Molecular weights

The molecular weight distribution of the free PS and PB and the corresponding average molecular weights ($\bar{M}_n$ and $\bar{M}_w$) were determined by Size Exclusion Chromatography, using a Hewlett-Packer chromatograph with a series of three PLgel columns (nominal pore size 10^5, 10^4 and 10^3 Å). In all cases, a linear molecular weight calibration was obtained with either PS or PB standards. Tetrahydrofuran (THF, HPLC grade) was used as the eluent at a flow rate of 1 mL/min and the samples were analyzed at room temperature.

5.2.3.4 Morphology

The internal morphology of the obtained polymers was analyzed by Transmission Electron Microscopy (TEM) using a JEOL TEM. The measurements were carried out at 10 kV on sample cuts with a Leica Ultracut ultramicrotome and stained with osmium dioxide during 2 h. The sample cuts were performed at a temperature of −180 °C in the ultramicrotome chamber, yielding cuts of no more than 100 nm thickness.

5.2.3.5 Melt flow index

Melt flow index (in g/10 min) of the final polymers was determined as per ASTMD-1238-13, using a Dynisco Ph 800-322-2245 plastomer, a total charge of 5 kg and at a temperature of 200 °C.

5.2.4 Experimental results

The experimental results are presented in Figures 5.1 and 5.2, and Table 5.2. Figure 5.1 corresponds to the prepolymerization stage, while Table 5.2 presents the characteristics of final HIPS samples (at conversion ≈ 100 %). In Figure 5.2, the morphologies of the final HIPS samples as observed by TEM are presented.

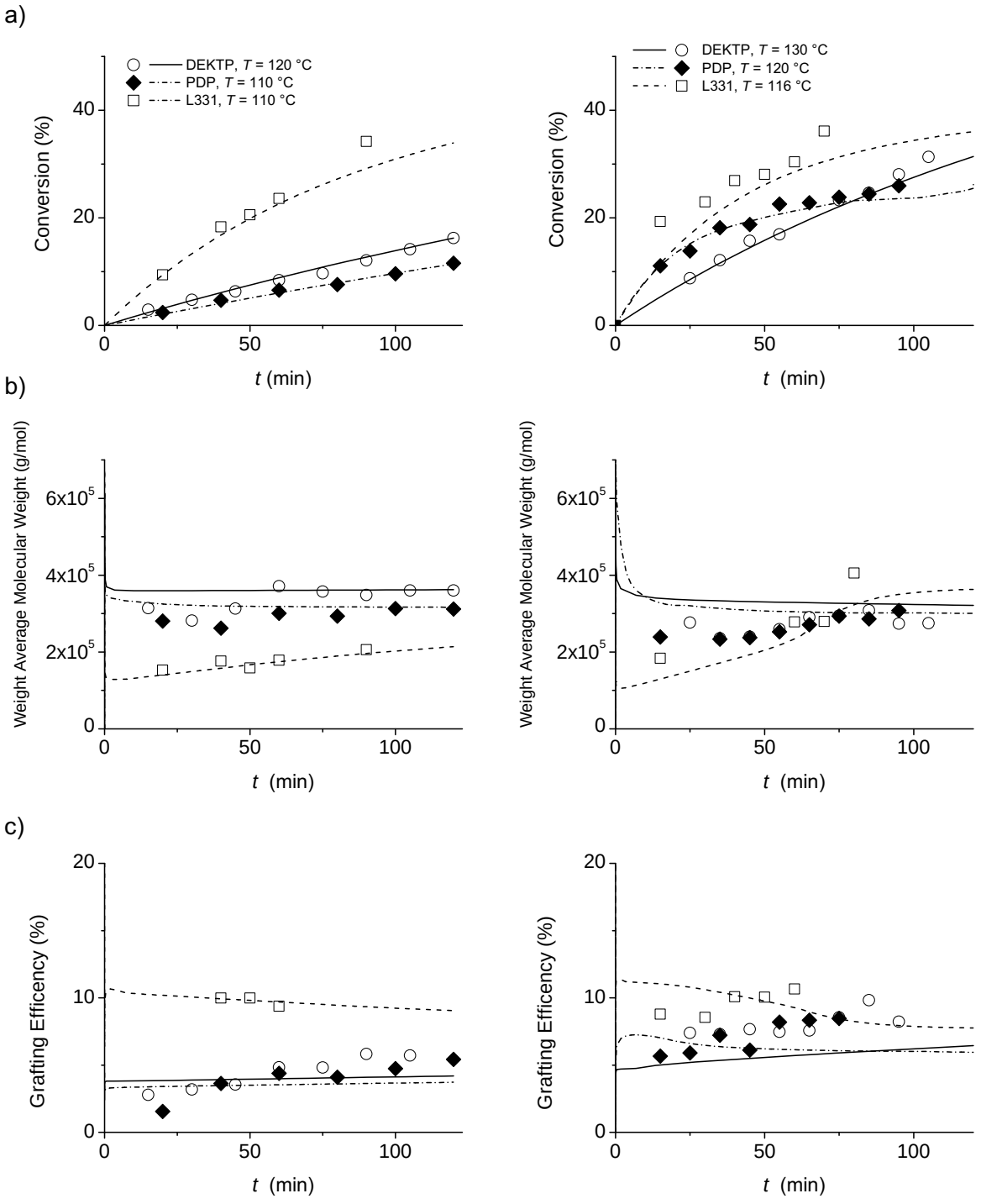

FIGURE 5.1: Experimental (points) and theoretical (continuous curves) results for HIPS prepolymerization stage using multifunctional initiators: a) conversion, b) free PS weight average molecular weight, and c) grafting efficiency.

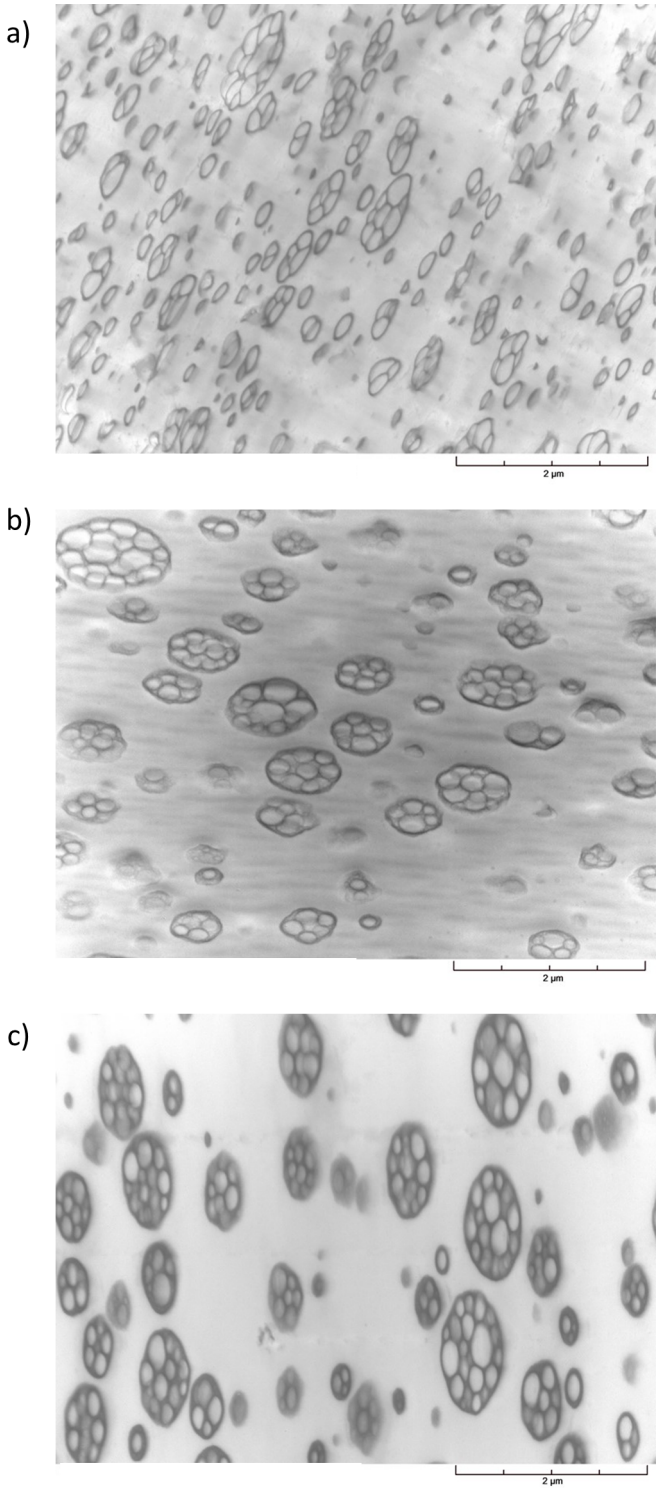

FIGURE 5.2: Morphologies as observed by TEM for HIPS synthesized with a) L331, b) PDP, and c) DEKTP.

Initiator	T_{PP} (°C)	T_F (°C)	$\bar{M}_{w,\mathrm{PS}}$ (g/mol)	E_{GS} (%)	MFI (g/10 min)
DEKTP	130	150	178712 (17640)	17 (15)	18 (10.7)
PDP	120	150	175762 (183090)	18 (17)	12 (9.2)
L331	116	150	299887 (275060)	20 (19)	2.0 (3.5)

TABLE 5.2: Final properties of the synthesized HIPS materials. Theoretical predictions are indicated in parenthesis.

The evolution of conversion with time during the pre-polymerization stage can be observed in Figure 5.1. From the slopes of the curves, the rate of polymerization R_p can be estimated. It can be seen that R_p(L331)> R_p(DEKTP)> R_p(PDP) for the lower temperature experiments. At higher temperatures, it is observed that R_p(PDP)> R_p(DEKTP) up to a prepolymerization time of about 75 min. This could be attributed to the different thermal stability of the peroxide groups of the initiators. Note that the R_p are not always determined at the same prepolymerization temperature.

The highest polymerization rates for L331 can be attributed to a higher decomposition rate of the peroxide, as well as higher initiator efficiency. The decompositions of peroxide groups in PDP appears to be more thermally activated than that of peroxide groups in DEKTP, which would explain the observed differences in relative R_p behavior at lower or higher temperatures.

As regards the molecular weights, it can be seen that in the case of the cyclic initiators DEKTP and PDP, molecular weights are approximately constant throughout the prepolymerization reaction, both at higher and lower temperatures. At lower temperatures, molecular weights obtained with L331 are slightly lower than those obtained using the cyclic initiators, in accordance with a higher decomposition rate of peroxide groups in L331. However, for the experiment at higher temperature, it can be observed that molecular weights increase along the reaction. At the end of the prepolymerization stage, average molecular weights obtained with L331 are higher than those obtained with cyclic initiators.

The behaviors observed for the evolution of conversion and free PS average molecular weights attributed to the higher stability of the cyclic initiators DEKTP and PDP are consistent with what was found in the previous chapter with respect to the different decomposition rates of these multifunctional initiators.

As regards the grafting efficiency, it should be noted that this variable is expected to have a large uncertainty due to the experimental technique employed for its determination [86]. The differences in experimental values are relatively small, although it can generally be seen that E_{GS}(L331)> E_{GS}(PDP)> E_{GS}(DEKTP). This can be attributed to a higher rate of H-abstraction reactions by initiator radicals, which generate grafting points in the PB chains. An increase in prepolymerization temperature promotes higher grafting efficiencies for the cyclic initiators DEKTP and PDP.

The different values for grafting efficiencies and number of grafting points during prepolymerization are also related to the differences in the observed morphologies for the final products of Figure 5.2. It can be observed that the product obtained with L331 presents a larger number of smaller particles, of an average diameter of approximately 290 nm and core-shell morphologies. In contrast, the product obtained with PDP and DEKTP presents a smaller number of larger particles, with average diameters of approximately 510 nm and 870 nm respectively, and salami morphologies.

With respect to the final properties of the HIPS samples in Table 5.2, it can be seen that the products synthesized with the cyclic initiators PDP and DEKTP present similar values for $\bar{M}_{w,\mathrm{PS}}$, E_{GS} and MFI. Initiation by DEKTP produces a product of higher molecular weight than the product obtained with PDP, in accordance with the values of the molecular weights during the prepolymerization stage. Additionally, the higher $\bar{M}_{w,\mathrm{PS}}$ and E_{GS} values observed in the case of L331 are consistent with the differences in values observed during the prepolymerization stage. The experimental results for the product synthesized with DEKTP show an unexpected behavior in the high MFI value, which is inconsistent with the higher molecular weight. This result can be attributed to the possible presence of small amounts of monomer in the melt.

5.3 Mathematical model

5.3.1 Pseudo-homogeneous polymerization model

The mathematical model is based on the kinetic mechanism presented in Table 5.3, which includes initiation via a symmetrical cyclic or linear multifunctional initiator,

thermal initiation, propagation, transfer to the monomer, transfer to the rubber, combination termination and re-initiation. In addition to the nomenclature from the preceding chapters, the following nomenclature is adopted:

$P^{(i)}$	Copolymer with i undecomposed peroxide groups in the grafted chain
$P_0{}^{\cdot(i)}$	Primary radical produced by attack to a butadiene repetitive unit (B) present in the residual PB or the $P^{(i)}$
$P_n{}^{\cdot(i)}$	Copolymer radical with i undecomposed peroxide groups and n repetitive units of St in the active branch

The following was considered: i) at the temperatures employed, the initiators decompositions are due exclusively to sequential decomposition [36, 39, 89]; ii) intra-molecular termination is negligible [41]; iii) disproportion termination is negligible [92]; iv) all peroxide groups present in the initiator and in the accumulated homo- and copolymers exhibit the same thermal stability [41]; v) because of the short lifetime of radicals, the decomposition of undecomposed peroxide groups does not occur in radical molecules [41]; vi) propagation and transfer reactions are unaffected by the chain length or conversion [41]; vii) degradation reactions are negligible [17].

Assuming a pseudo-homogeneous bulk polymerization [41], a mathematical model was developed from the kinetic mechanism detailed in Table 5.3. The model consists of a set of nonlinear differential equations, which are derived from the mass balances for the reacting species (see Appendix D), including the living radical species, dead and temporarily dead polymer and copolymer species for all kinetic chain lengths and number of undecomposed peroxide groups.

The mathematical model consists of three modules:

- The Basic module (Appendix D.1), which allows the prediction of global chemical species evolution along the reaction (monomer, initiators, total radical species, unreacted B units, grafting efficiency).
- The Distributions module (Appendix D.2), which simulates the evolution of all chemical species, characterized by their chain length and number of undecomposed peroxide groups. The equations estimate the evolution of the complete MWD of each radical and polymer species, including free PS, residual PB and GC. In order to consider the effect of re-initiation reactions in the MWDs, PS chains were

Initiation$(\phi = 1,2,3; i < \phi; j = 0,1,...)$

Thermal Initiation

$3\text{St} \xrightarrow{k_{i0}} 2S_1.^{(0)}$

Chemical Initiation

$I^{(\phi)} \xrightarrow{\phi k_{d1}} .I.^{(\phi-1)}$

$\bar{I}^{(\phi)} \xrightarrow{\phi k_{d1}} \bar{I}.^{(i)}$

$.I.^{(i)} + \text{St} \xrightarrow{2k_{i1}} .S_1.^{(i)}$

$I.^{(i)} + \text{St} \xrightarrow{k_{i1}} S_1.^{(i)}$

$.I.^{(i)} + P^{(j)} \xrightarrow{2k_{i2}} P_0.^{(j)} + I.^{(i)}$

$I.^{(i)} + P^{(j)} \xrightarrow{k_{i2}} P_0.^{(j)} + \bar{I}^{(i)}$

Propagation $(n = 1,2,3...; i = 0,1,2...)$

$S_n.^{(i)} + \text{St} \xrightarrow{k_p} S_{n+1}.^{(i)}$

$.S_n.^{(i)} + \text{St} \xrightarrow{2k_p} S_{n+1}.^{(i)}$

$P_0.^{(i)} + \text{St} \xrightarrow{k_p} P_1.^{(i)}$

$P_n.^{(i)} + \text{St} \xrightarrow{k_p} P_{n+1}.^{(i)}$

Transfer to monomer $(n = 1,2,3...; i = 0,1,2...)$

$S_n.^{(i)} + \text{St} \xrightarrow{k_{fM}} S_n{}^{(i)} + S_1.^{(0)}$

$.S_n.^{(i)} + \text{St} \xrightarrow{2k_{fM}} S_n.^{(i)} + S_1.^{(0)}$

$P_0.^{(i)} + \text{St} \xrightarrow{k'_{fM}} P^{(i)} + S_1.^{(0)}$

$P_n.^{(i)} + \text{St} \xrightarrow{k_{fM}} P^{(i)} + S_1.^{(0)}$

Transfer to rubber $(n = 1,2,3...; i,j = 0,1,2...)$

$S_n.^{(i)} + P^{(j)} \xrightarrow{k_{fG}} S_n{}^{(i)} + P_0.^{(j)}$

$.S_n.^{(i)} + P^{(j)} \xrightarrow{2k_{fG}} S_n.^{(i)} + P_0.^{(j)}$

$P_0.^{(i)} + P^{(j)} \xrightarrow{k_{fG}} P^{(i)} + P_0.^{(j)}$

$P_n.^{(i)} + P^{(j)} \xrightarrow{k_{fG}} P^{(i)} + P_0.^{(j)}$

Re-initiation $(n = 2,3,...; m = 1,2,...,n-1; i = 1,2...; j = 0,1,...,i-1)$

$S_n{}^{(i)} \xrightarrow{ik_{dp}} S_{n-m}.^{(i-j)} + S_m{}^{(j-1)}.$

$P^{(i)} \xrightarrow{ik_{dp}} P_{n-m}.^{(i-j)} + S_m{}^{(j-1)}.$

Combination termination $(n,m = 1,2,3...; i,j = 0,1,2...)$

$.S_n.^{(i)} + .S_m.^{(j)} \xrightarrow{4k_{tc}} .S_{n+m}.^{(i+j)}$

$.S_n.^{(i)} + S_m.^{(j)} \xrightarrow{2k_{tc}} S_{n+m}.^{(i+j)}$

$S_n.^{(i)} + S_m.^{(j)} \xrightarrow{k_{tc}} S_{n+m}{}^{(i+j)}$

$P_0.^{(i)} + P_0.^{(j)} \xrightarrow{k'_{tc}} P^{(i+j)}$

$P_0.^{(i)} + P_m.^{(j)} \xrightarrow{k'_{tc}} P^{(i+j)}$

$P_n.^{(i)} + P_m.^{(j)} \xrightarrow{k'_{tc}} P^{(i+j)}$

$P_0.^{(i)} + .S_m.^{(j)} \xrightarrow{2k''_{tc}} P_m.^{(i+j)}$

$P_n.^{(i)} + .S_m.^{(j)} \xrightarrow{2k''_{tc}} P_{n+m}.^{(i+j)}$

$P_0.^{(i)} + S_m.^{(j)} \xrightarrow{k''_{tc}} P^{(i+j)}$

$P_n.^{(i)} + S_m.^{(j)} \xrightarrow{k''_{tc}} P^{(i+j)}$

TABLE 5.3: HIPS polymerization using multifunctional initiators - Proposed kinetic mechanism.

assumed to have uniformly distributed peroxide groups. A random-chain scission can be simulated with a uniformly distributed random variable. The uniform peroxide group distribution hypothesis is expected to be valid for cyclic initiators and for linear initiators with functionalities greater than two [99].

- The Melt flow index module which estimates the MFI of the obtained polymer by considering the mass and momentum balances in a plastometer [57]. The MFI module inputs are the plastomer characteristics -dimensions and operating conditions- as well as the final HIPS characteristics.

The proposed model does not include an energy balance. However, non isothermal reactions can be simulated through the use of standard or modified Arrhenius expressions for the kinetic constants [17, 86]. When a temperature profile is imposed, the reactor cooling/heating system is considered ideal, in the sense that it is capable of exactly following said profile. The gel effect was indirectly considered by appropriately reducing the value of the termination kinetic coefficient with increasing conversion [17].

For the Basic module, Equations D.1 to D.4, D.8, D.9, and D.23 to D.24 must be simultaneously solved. The Distributions module is then solved using the results from the Basic module. Finally, the MFI module is solved using the weight average molecular weights calculated with the Distribution module. The Basic Module is solved by a standard stiff differential equation numerical method based on a second-order modified Rosenbrock formula, programmed in MATLAB v. 8.3. In the Distributions module, a large number of equations (more than 500,000) must be integrated. For this reason, an explicit forward Euler method was used, with the time intervals obtained from resolution of the basic module. The MFI module is solved using a Newton-Raphson method for solving a system of non-linear algebraic equations. A typical simulation requires less than 1 s for the Basic module, about 5 min for the Distributions module and less than 1 s for the MFI module with an Intel Core i5 based processor at 2.40 GHz. For the copolymer bivariate distribution, a very large number of differential equations must be solved, involving large variables in order to consider every possible number of St and B units. For this reason, a cruder numerical method was employed, considering for each time interval, the instantaneous chain length distribution (CLD) of the grafted St and number of grafting points estimated from the Basic module. It was assumed that the instantaneous CLD of the grafted PS chains is equal to the CLD the free PS [114].

5.4 Simulation results

The model was adjusted using the experimental data in Figure 5.1 and Table 5.2. Model parameter adjustment was sequential, using least-squares optimization algorithms. Firstly, k_{d1}, k_{dp}, k_{i2} f_1 and f_2 for each initiator were adjusted with the conversion and grafting efficiency data. Since all peroxide groups are assumed to have the thermal stability, $k_{dp} = k_{d1}$ and it was assumed that $f_1 = f_2$. Secondly, k_{fM} and k_{fG} were adjusted with the average molecular weight data. The obtained values for the decomposition constants as well as the rubber initiation constants are in accordance with what has been reported for the decomposition rates of organic peroxides [41, 89, 99], and the values for the transfer to monomer and transfer to rubber constants are within the expected range reported in the literature [41]. All other values for the kinetic parameters were taken from the literature [17]. Model parameters are presented in Table 5.4.

It was found that $f_1 k_{d1}$ (L331) $>$ $f_1 k_{d1}$ (PDP) $>$ $f_1 k_{d1}$ (DEKTP), which is in accordance to what was found in the previous chapter for St homopolymerization. In addition, it was found that k_{i2} (L331) $>$ k_{i2} (PDP) $>$ k_{i2} (DEKTP), indicating that the bifunctional linear initiator generates a higher number of grafting points at a given temperature. This result is in agreement with the lower grafting efficiencies observed for DEKTP and PDP compared to L331 and with the different morphologies observed in the final products.

Simulation results are compared to experimental results in Figure 5.1 and Table 5.2. In general, a fair agreement between experimental and predicted values is observed.

The predicted evolution of average molecular weights during the prepolymerization stage shows an increase in the values for linear initiator L331, while the molecular weights remain approximately constant for cyclic initiators PDP and DEKTP. This behavior is in agreement with the results from the previous chapter. As the temperature is increased to 150 °C for the finishing stage, the values of average molecular weights decrease.

Other simulation results using the model are presented in Figures 5.3. As shown, the model can be used to obtain smooth surfaces given by the values of $\bar{M}_n$ and E_{GS} at a given instant during the polymerization, as a function $[I^{(\phi)}]_0$ and T_{PP}. Given that the characteristics of the final product are greatly determined at the PI point, said point was chosen to evaluate the number average molecular weight of the free PS and the grafting efficiency. To estimate the PI point, the evolution of the volumes of hypothetical PS- and

Parameter	**Units**	**Arrhenius expression**	**Reference**
k_{d1}, k_{dp} (DEKTP)	s^{-1}	$3.4 \cdot 10^{42} e^{-43548/T}$	Adjusted in this work
k_{d1}, k_{dp} (PDP)	s^{-1}	$4.1 \cdot 10^{61} e^{-58622/T}$	Adjusted in this work
k_{d1}, k_{dp} (L331)	s^{-1}	$1.9 \cdot 10^{20} e^{-21034/T}$	Adjusted in this work
f_1, f_2 (DEKTP)	-	$0.034T - 12.7$	Adjusted in this work
f_1, f_2 (PDP)	-	$0.017T - 6.40$	Adjusted in this work
f_1, f_2 (L331)	-	$0.0073T - 1.96$	Adjusted in this work
k_{i0}	$\frac{L^2}{mol^2 S}$	$1.1 \cdot 10^{5} e^{-13810/T}$	[93]
k_{i1}, k_p	$\frac{L}{mol\ s}$	$1.051 \cdot 10^{7} e^{-7067/RT}$	[41]
k_{i2} (DEKTP)	$\frac{L}{mol\ s}$	$7.6 \cdot 10^{4} e^{-2115/T}$	Adjusted in this work
k_{i2} (PDP)	$\frac{L}{mol\ s}$	$8.3 \cdot 10^{8} e^{-6103/T}$	Adjusted in this work
k_{i2} (L331)	$\frac{L}{mol\ s}$	$1.8 \cdot 10^{3} e^{-492/T}$	Adjusted in this work
k_{fM}, k'_{fM}	$\frac{L}{mol\ s}$	$3.2 \cdot 10^{12} e^{-11698/T}$	Adjusted in this work
k_{fG}	$\frac{L}{mol\ s}$	$9.8 \cdot 10^{9} e^{-4892/RT}$	Adjusted in this work
k_{tc}, k'_{tc}, k''_{tc}	$\frac{L}{mol\ s}$	$1.686 \cdot 10^{9} e^{-(844/T)-2(C_1 x + C_2 x^2 + C_3 x^3)}$ [a]	[93]
A	-	1.8	[115]
B	-	1.35	[115]

[a] $C_1 = 2.75 - 0.00505T; C_2 = 9.56 - 0.0176T; C_3 = -3.03 + 0.00785T$, with x monomer conversion

TABLE 5.4: HIPS polymerization using multifunctional initiators - Adopted kinetic parameters.

PB-rich phases was calculated using the results from the model. It was assumed that the PI point is the point at which the volumes of both phases is equal [93]. The value of conversion at which PI occurs in the simulated conditions is found to be approximately 12 %, within the range reported in the literature [12].

For all initiators, it can be seen that increasing the prepolymerization temperature for a given initial concentration results in lower molecular weights at the PI, as expected. The effect of the initial initiator concentration at a given temperature depends on the choice of the initiator. For the cyclic peroxides DEKTP and PDP, it can be seen that $\bar{M}_{n,\mathrm{PS}}$

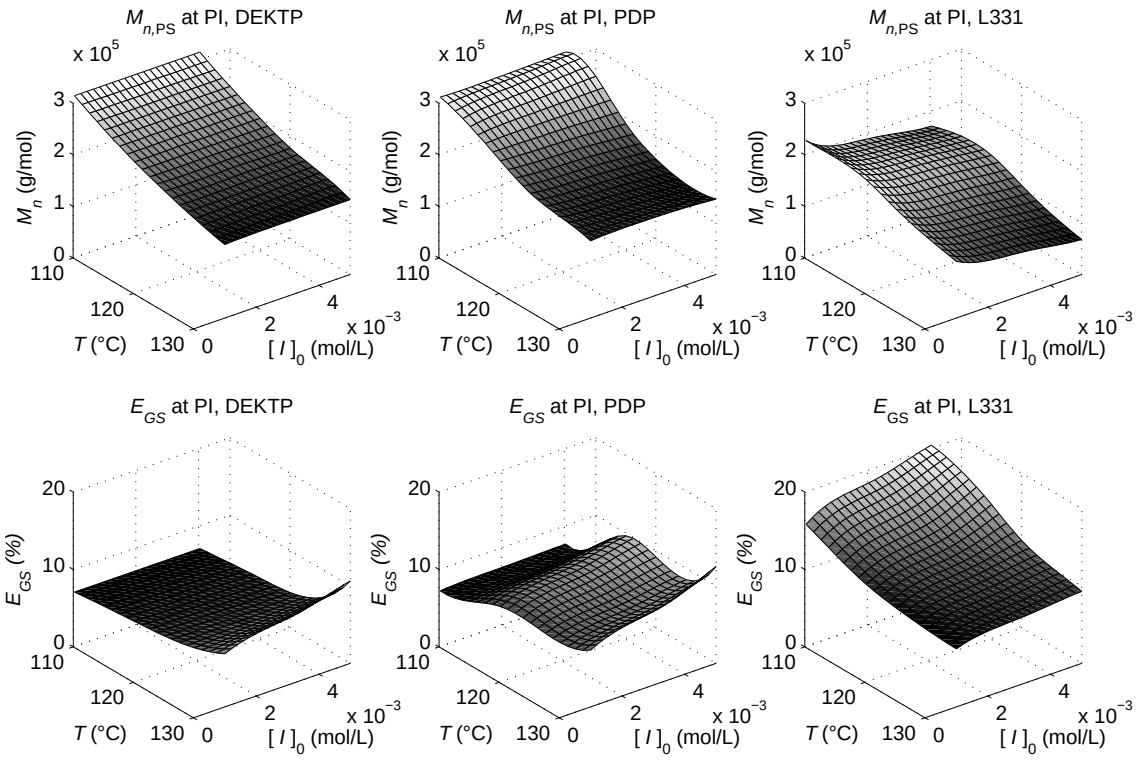

FIGURE 5.3: Theoretical simulations for HIPS Polymerization using multifunctional initiators.

at the PI point is very slightly dependent on initiator concentration. This has been experimentally verified in previous works [76] and is related to the higher stability and lower decomposition rate of the cyclic initiators. In the case of L331, molecular weights decrease with increasing initiator concentration, due to the higher decomposition rate which generates a higher number of active sites.

As regards grafting efficiencies at the PI point, it can be seen that cyclic initiators provide lower values than the linear initiator, indicating a lower selectivity toward grafting reactions with this type of initiators, as previously reported [76]. As expected, increasing initiator concentration increases the grafting efficiency. The effect of the prepolymerization temperature depends on the initiator: for cyclic initiators, an increase in grafting efficiency with increasing temperature is observed.

If the molecular structure at the PI point was correlated to the final product morphologies, this model could be used to find the optimum conditions of the prepolymerization stage (T_{PP}, $[I^{(\phi)}]_0$) to obtain a product with a pre-specified morphology. Analogously,

the model can also be used to obtain the optimum temperature profile during the finishing stage in order to obtain a pre-specified MFI. Simulations such as the ones shown in Figure 5.3 are a first step towards model inversion.

The model can also be used to estimate the molecular structure of the graft copolymer at the PI point. Figure 5.4 shows the detailed weight chain length distributions at the PI point obtained using the multifunctional initiators at a given prepolymerization temperature T_{PP} and an initial concentration of $1.56 \cdot 10^{-3}$ mol/L.

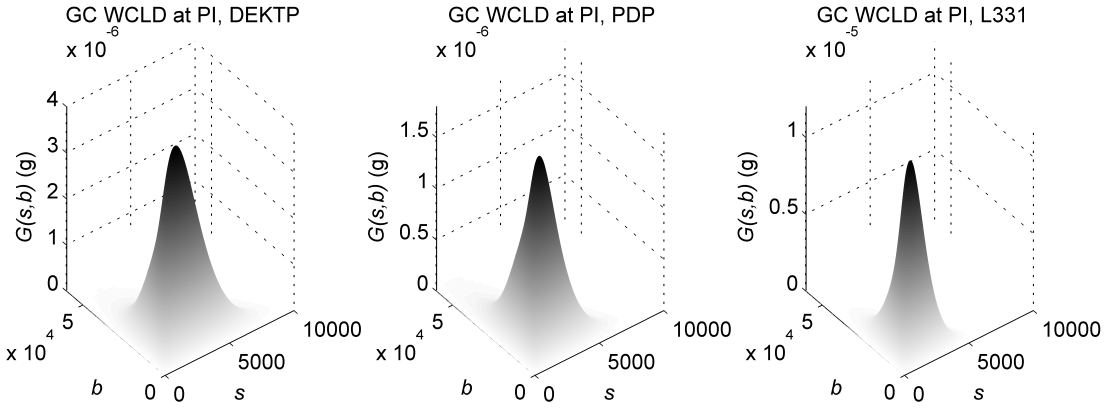

FIGURE 5.4: Copolymer bivariate distributions at the phase inversion point for HIPS polymerization using multifunctional initiators.

Initiator	T_{PP} (°C)	$\bar{M}_{n,\mathrm{C}}$ (g/mol)	$\bar{M}_{w,\mathrm{C}}$ (g/mol)	$\bar{\omega}_{\mathrm{St}}$	J (#/molecule)
DEKTP	130	196325	370403	0.49	0.64
PDP	120	206747	401301	0.50	0.64
L331	116	173727	315098	0.41	0.63

TABLE 5.5: Copolymer average molecular weights, chemical composition and number of grafted branches at the phase inversion point.

The average molecular characteristics of the graft copolymer (average molecular weights, average St mass fraction $\bar{\omega}_{\mathrm{St}}$ and average number of grafted St branches per reacted PB molecule J as estimated by the model are presented in Table 5.5. As expected, it can be observed the cyclic initiators provide higher copolymer average molecular weights. The chemical compositions and average number of St branches are within the ranges reported in previous works [41, 86].

5.5 Conclusions

A mathematical model for the bulk polymerization of styrene in the presence of polybutadiene using multifunctional initiators was presented. The model simulates the evolution of all the chemical species in the reaction system, consisting of a prepolymerization stage and a finishing stage and predicts the melt flow index of the obtained HIPS.

The model was adjusted and validated using the experimental data from batch HIPS polymerizations using initiators DEKTP, PDP and L331. The kinetic mechanism includes the re-initiation reactions due to undecomposed peroxide groups within the polystyrene chains and the derived model can be used to evaluate the detailed molecular structure of all polymer species, including free PS, residual PB and graft copolymer. Theoretical and experimental results indicate that the decomposition rates of the initiator functional groups are key variables in determining the characteristics of the final products, namely average molecular weights, grafting efficiency and particle morphology.

The model can be used to evaluate the influence of the recipe and operating conditions on the molecular and physical characteristics of the obtained polymer and find the conditions for synthesizing a polymer with a set of pre-specified properties.

Chapter 6

Concluding remarks

6.1 Main results

In the work described in the preceding chapters, mathematical models for complex styrene polymerization processes using multifunctional initiators were developed. The models were adjusted and validated using experimental data and were used to theoretically study the effect of recipe and operating conditions on the characteristics of the obtained materials.

In Chapter 2 and Chapter 3, the bulk polymerization of styrene in the presence of the cyclic trifunctional initiator DEKTP was experimentally and theoretically studied. A model considering the complex kinetics involving diradicals and re-initiation reaction was developed, in order to simulate the evolution of the chemical species in the course of polymerization and the detailed molecular structure of the obtained polymer. Chapter 2 considers the sequential decomposition of the initiator molecule at lower temperatures of $120 - 130$ °C. In Chapter 3, the kinetic mechanism was extended to include the total decomposition of the initiator at higher temperatures of $150 - 200$ °C. The extended model was used in the complete temperature range in order to find the working zone of technological interest for this initiator. It was found that a temperature of $120 - 130$ °C and an initial initiator concentration of 0.01 mol/L provide high polymerization rates and high molecular weights simultaneously.

In Chapter 4, a novel general approach was proposed for the bulk polymerization of St using multifunctional initiators of different functionalities and structures. A generic,

comprehensive model was developed, which allows studying the influence of initiator functionality and structure on the obtained materials. It was found that the decomposition rate of the peroxide groups is the key variable affecting initiator performance, and that a cyclic initiator provides molecular weights about 30 % than a corresponding linear one with equal thermal stability.

Chapter 5 presents a mathematical model for the bulk polymerization of styrene in the presence of polybutadiene using multifunctional. The model is an extension of the generic model from Chapter 4 to a HIPS polymerization process, considering the chemical species appearing due to the presence of the rubber, as well as different stages of a HIPS polymerization process (prepolymerization and finishing). In addition to the variables calculated by the previous model, the model provides full insight on the molecular structure of the different polymer species (free PS, residual PB and graft copolymer). Finally, the model was complemented with a melt flow index prediction module adapted for HIPS and was used to evaluate the influence of prepolymerization conditions on the molecular structure of the obtained materials.

6.2 Recommendation for future works

There is a wide range of possible works with the developed mathematical models. Two direct applications would be the static or dynamical optimization of a PS or HIPS production process. To this end, the current models could be adapted to continuous processes, and the possibility of initiator mixtures could be considered. For the static operation of a production process, the model could be used to obtain productivity maximization strategies that do not alter product quality. For the dynamic operation, the model would allow studying the dynamic evolution with changes in product grade of production levels, or combined changes in product grades in production levels.

It should be noted that the models available in the literature for continuous process do not include the modeling of the devolatilization stage, in which high temperatures are involved [95, 116]. In order to have a full mathematical description of a polymerization process, a model for the devolatilization stage should be developed. The model should consider the mass transfer phenomena that take place inside the devolatilization equipment, as well as the high temperature reactions that could alter the product

characteristics, including crosslinking reactions in the rubber particles [117], oligomer formation [95, 118] and possible decomposition reactions [119]. Specifically, with the use of multifunctional initiators, peroxide groups that could remain in the polymer chains could decompose at the high devolatilization temperatures, causing a decrease in molecular weight [78] with the consequent loss in mechanical properties.

In the particular case of the HIPS process, further research is needed in order to complete the yet poorly understood structure-properties relationships. In addition, the phenomenon of phase inversion should be adequately investigated and modeled, due to its crucial role in the development of the morphology [104, 109, 110].

The main long-term objective using the models for a continuous process would be to "invert" the model, in order to find the optimum recipe and operating conditions to obtain tailor made products in an industrial continuos process.

The presented models could also be extended to other St polymers, such as SAN and ABS, to which all improvements related to devolatilization and phase inversion apply.

Appendix A

Mathematical model for the bulk polymerization of styrene at 120–130 °C using DEKTP

The mathematical model is based on the kinetic mechanism of Table 2.2 and considers the mass balances for the chemical species in the reaction system.

A.1 Basic module

Balances for non-polymeric reagents and products

Initiator (DEKTP)

$$\frac{d}{dt}\left([I^{(3)}]V\right) = -3k_{d1}[I^{(3)}]V \tag{A.1}$$

Monomer (St)

Assuming the long chain hypothesis, by which propagation is the only monomer-consuming reaction:

$$\frac{d}{dt}\left([\mathrm{St}]V\right) = -R_pV = -k_p[\mathrm{St}]\left([R\cdot] + 2[\cdot R\cdot]\right)V \tag{A.2}$$

where R_p is the global St polymerization rate, and

$$[R\cdot] = \sum_{i=0}^{\infty}\sum_{n=1}^{\infty}[S_n\cdot^{(i)}] \tag{A.3a}$$

$$[\cdot R\cdot] = \sum_{i=0}^{\infty}\sum_{n=1}^{\infty}[\cdot S_n\cdot^{(i)}] \tag{A.3b}$$

represent the total concentrations of mono- and diradicals respectively.

Radical species

Consider the mass balances of all free radicals appearing in the global kinetics. Such balances provide:

$$\frac{d}{dt}\left([\cdot I\cdot^{(2)}]V\right) = \left(3fk_{d1}[I^{(3)}] - 2k_{i1}[\cdot I\cdot^{(2)}][\mathrm{St}]\right)V \tag{A.4}$$

$$\frac{d}{dt}\left([S_1\cdot^{(0)}]V\right) = \Big\{2k_i[\mathrm{St}]^3 - \Big(k_p[S_1\cdot^{(0)}] - k_{fM}\left([R\cdot] + 2[\cdot R\cdot]\right) + k_{fM}[S_1\cdot^{(0)}]\Big)[\mathrm{St}] - k_{tc}[S_1\cdot^{(0)}]\left([R\cdot] + 2[\cdot R\cdot]\right)\Big\}V \tag{A.5}$$

$$\frac{d}{dt}\left([\cdot S_1\cdot^{(2)}]V\right) = \Big\{\Big(2k_{i1}[\cdot \mathrm{I}\cdot^{(2)}] - 2k_p[\cdot S_1\cdot^{(2)}] - 2k_{fM}[\cdot S_1\cdot^{(2)}]\Big)[\mathrm{St}] - 2k_{tc}[\cdot S_1\cdot^{(2)}]\left([R\cdot] + 2[\cdot R\cdot]\right)\Big\}V \tag{A.6}$$

$$\frac{d}{dt}\left([\cdot S_n\cdot^{(i)}]V\right) = \Big\{2k_p[\mathrm{St}]\left([\cdot S_{n-1}\cdot^{(i)}] - [\cdot S_n\cdot^{(i)}]\right) - 2k_{fM}[\mathrm{St}][\cdot S_n\cdot^{(i)}] - 2k_{tc}\left([R\cdot] + 2[\cdot R\cdot]\right)[\cdot S_n\cdot^{(i)}] + 2k_{tc}\sum_{j=0}^{i}\sum_{m=1}^{n-1}[\cdot S_{n-m}\cdot^{(i-j)}][\cdot S_m\cdot^{(j)}]\Big\}V \quad (n \geq 2, i = 2, 4, 6...) \tag{A.7}$$

$$\frac{d}{dt}\left([S_n{}^{\cdot(i)}]V\right) = \left\{\left(k_p\left([S_{n-1}{}^{\cdot(i)}] - [S_n{}^{\cdot(i)}]\right) + k_{fM}\left(2[\cdot S_n{}^{\cdot(i)}] - [S_n{}^{\cdot(i)}]\right)\right)[\mathrm{St}]\right.$$
$$- k_{tc}\left([R\cdot] + 2[\cdot R\cdot]\right)[S_n{}^{\cdot(i)}] + 2k_{tc}\sum_{j=0}^{i}\sum_{m=1}^{n-1}[\cdot S_{n-m}{}^{\cdot(i-j)}][S_m{}^{\cdot(j)}]$$
$$\left. + k_{d2}\sum_{j=i+1}^{\infty}\sum_{m=n+1}^{\infty}p_{mj}(n,i)j[S_m^{(j)}]\right\}V$$
$$(n \geq 2, i = 0, 1, 2, 3...) \quad \text{(A.8)}$$

Where $p_{mj}(n,i)$ denotes the probability that a scission of a chain of dead polymer of length m and j peroxide groups yields a monoradical of chain length n with i peroxide groups. Adding this probability over all ns and is, the following can be proven:

$$\sum_{i=1}^{\infty}\sum_{n=1}^{\infty}\sum_{j=i+1}^{\infty}\sum_{m=n+1}^{\infty}p_{mj}(n,i)j[S_m^{(j)}] = 2\sum_{i=1}^{\infty}\sum_{n=1}^{\infty}i[S_n^{(i)}] = 2[\mathrm{Pe_P}] \quad \text{(A.9)}$$

where $[\mathrm{Pe_P}]$ is the concentration of peroxide groups in the polymer chains. The 2 in Equation A.16 arises from the fact that the scission of any polymer chain with peroxide groups produces 2 monoradicals.

From equations A.5 through A.16 the total concentration of mono- and diradicals may be obtained:

$$\frac{d}{dt}\left([R\cdot]V\right) = \left\{2k_i[\mathrm{St}]^3 + 4k_{fM}[\mathrm{St}][\cdot R\cdot] - k_{tc}[R\cdot]^2 + 2k_{d2}[\mathrm{Pe_P}]\right\}V \quad \text{(A.10)}$$

$$\frac{d}{dt}\left([\cdot R\cdot]V\right) = \left\{\left(2k_{i1}[\cdot I\cdot^{(2)}] - 2k_{fM}[\cdot R\cdot]\right)[\mathrm{St}] - 2k_{tc}[\cdot R\cdot]\left([R\cdot] + 2[\cdot R\cdot]\right) + 2k_{tc}[\cdot R\cdot]^2\right\}V \quad \text{(A.11)}$$

Balances for the polymeric species

$$\frac{d}{dt}\left([S_n{}^{(i)}]V\right) = \left\{k_{fM}[\mathrm{St}][S_n{}^{\cdot(i)}] + \frac{k_{tc}}{2}\sum_{j=0}^{i}\sum_{m=1}^{n-1}[S_{n-m}{}^{\cdot(i-j)}][S_m{}^{\cdot(j)}] - k_{d2}i[S_n{}^{(i)}]\right\}V$$
$$(n \geq 2, i = 0, 1, 2...) \quad \text{(A.12)}$$

Note that only polymers with peroxides ($i \neq 0$) can decompose.

The concentration of the polymer with i undecomposed peroxide groups can be defined as

$$[P^{(i)}] = \sum_{n=1}^{\infty} [{S_n}^{(i)}] \tag{A.13}$$

Define the total polymer concentration $[P]$

$$[P] = \sum_{i=0}^{\infty} [\mathrm{P}^{(i)}] = \sum_{i=0}^{\infty} \sum_{n=2}^{\infty} [{S_n}^{(i)}] \tag{A.14}$$

By adding up Equation A.12 over all$n$s and all is, the balance for the molar concentration of polymer can be written:

$$\frac{d}{dt}([P]V) = \left\{ k_{fM}[\mathrm{St}][R\cdot] + \frac{k_{tc}}{2}[R\cdot]^2 - k_{d2}[\mathrm{Pe_P}] \right\} V \tag{A.15}$$

Peroxide groups

The total concentration of peroxide groups is

$$[\mathrm{Pe}] = 3[\mathrm{I}^{(3)}] + 2[\cdot\mathrm{I}\cdot^{(2)}] + [\mathrm{Pe}_{R\cdot}] + [\mathrm{Pe}_{\cdot R\cdot}] + [\mathrm{Pe_P}] \tag{A.16}$$

with

$$[\mathrm{Pe}_{R\cdot}] = \sum_{i=1}^{\infty} \sum_{n=1}^{\infty} i[{S_n}\cdot^{(i)}] \tag{A.17a}$$

$$[\mathrm{Pe}_{\cdot R\cdot}] = \sum_{i=1}^{\infty} \sum_{n=1}^{\infty} i[\cdot{S_n}\cdot^{(i)}] \tag{A.17b}$$

$$[\mathrm{Pe_P}] = \sum_{i=1}^{\infty} \sum_{n=1}^{\infty} i[{S_n}^{(i)}] \tag{A.17c}$$

where [Pe], [Pe$_{\cdot R\cdot}$], and [Pe$_\mathrm{P}$] respectively represent the molar concentration of peroxide groups accumulated in monoradicals, diradicals and polymer species. From Equation A.16 and assuming pseudosteady-state for radical species, by which all time derivatives may be set to zero:

$$\frac{d[\mathrm{Pe}]}{dt} = 3\frac{d[\mathrm{I}^{(3)}]}{dt} + \frac{d[\mathrm{Pe_P}]}{dt} \tag{A.18}$$

Peroxide groups are consumed only by decomposition reactions in the initiator and the polymer chains. Therefore:

$$\frac{d[\mathrm{Pe}]}{dt} = -3k_{d1}[\mathrm{I}^{(3)}] - k_{d2}[\mathrm{Pe_P}] \tag{A.19}$$

By considering equations A.1 and A.19 and from Equation A.18, the total peroxide groups contained in the polymer chains can be calculated from the following equation:

$$\frac{d[\mathrm{Pe_P}]}{dt} = 6k_{d1}[\mathrm{I}^{(3)}] - k_{d2}[\mathrm{Pe_P}] \tag{A.20}$$

Conversion

$$x = \frac{[\mathrm{St}]_0 V_0 - [\mathrm{St}]V}{[\mathrm{St}]_0 V_0} \tag{A.21}$$

where the subscript "0" indicates initial conditions. In this model, the effect of volume contraction is neglected and therefore

$$x = \frac{[\mathrm{St}]_0 - [\mathrm{St}]}{[\mathrm{St}]_0} \tag{A.22}$$

Equations A.1, A.2, A.4, A.10, A.11, A.15, A.20, A.22 can be simultaneously solved to find the evolutions of $[I^{(3)}]$, [St], $[\cdot I^{\cdot(2)}]$, $[R\cdot]$, $[\cdot R\cdot]$, [P], $[\mathrm{Pe_P}]$ and x.

A.2 Distributions module

Consider equations A.7 and A.8. Assuming pseudosteady-state, all time derivatives may be set to zero and the following recurrence formulas can be obtained:

$$[\cdot S_n{}^{\cdot(i)}] = \frac{k_p[\mathrm{St}][\cdot S_{n-1}{}^{\cdot(i)}] + k_{tc}\sum_{j=1}^{i}\sum_{m=1}^{n-1}[\cdot S_{n-m}{}^{\cdot(i-j)}][\cdot S_m{}^{\cdot(j)}]}{k_p[\mathrm{St}] + k_{fM}[\mathrm{St}] + k_{tc}\left([R\cdot] + 2[\cdot R\cdot]\right)} \qquad (n \geq 2, i = 2, 4, 6...) \tag{A.23}$$

$$[S_n{}^{(i)}\cdot] = \frac{\left(k_p[S_{n-1}{}^{\cdot(i)}] + 2k_{fM}[\cdot S_n{}^{\cdot(i)}]\right)[\mathrm{St}] + 2k_{tc}\sum_{j=0}^{i}\sum_{m=1}^{n-1}[\cdot S_{n-m}{}^{\cdot(i-j)}][S_m{}^{\cdot(j)}]}{k_p[\mathrm{St}] + k_{fM}[\mathrm{St}] + k_{tc}\left([R\cdot] + 2[\cdot R\cdot]\right)} + \frac{k_{d2}\sum_{j=i+1}^{\infty}\sum_{m=n+1}^{\infty}p_{mj}(n,i)j[S_m^{(j)}]}{k_p[\mathrm{St}] + k_{fM}[\mathrm{St}] + k_{tc}\left([R\cdot] + 2[\cdot R\cdot]\right)} \qquad (n \geq 2, i = 0, 1, 2, 3...) \tag{A.24}$$

Define the following molar ratio:

$$\sigma_2 = \frac{[\cdot {S_1}^{(2)} \cdot]}{[R\cdot] + 2[\cdot R\cdot]} \tag{A.25}$$

and the following dimensionless kinetic parameters:

$$\tau = \frac{k_{fM}}{k_p} \tag{A.26}$$

$$\beta = \frac{k_{tc} R_p}{(k_p[\mathrm{St}])^2} = \frac{k_{tc}\left([R\cdot] + 2[\cdot R\cdot]\right)}{k_p[\mathrm{St}]} \tag{A.27}$$

$$\alpha = \tau + \beta \tag{A.28}$$

$$\gamma = \frac{k_{d2}}{k_p} \tag{A.29}$$

By replacing the definitions in A.25, A.26, A.27 and A.28 in Equation A.23 and solving the recurrence formula, the following explicit expression for diradicals MWD can be obtained:

$$[\cdot {S_n}^{(2k)} \cdot] = \frac{1}{(1+\alpha)^{n-1}} (\beta\sigma_2)^{k-1} \frac{(n+k-2)!}{(n-k)!k!(k-1)!} [\cdot {S_1}^{(2)} \cdot] \qquad (n \geq 2, k = 1, 2, 3...) \tag{A.30}$$

Equation A.24 can be written

$$[{S_n}^{(i)} \cdot] = \frac{1}{1+\alpha} \left([{S_{n-1}}^{\cdot (i)}] + 2\tau[\cdot {S_n}^{\cdot (i)}] + \frac{2\beta}{[R\cdot] + 2[\cdot R\cdot]} \sum_{j=0}^{i} \sum_{m=1}^{n-1} [\cdot {S_{n-m}}^{\cdot (i-j)}][{S_m}^{\cdot (j)}] + \frac{\gamma}{[\mathrm{St}]} \Psi(n,i) \right) (n \geq 2, i = 1, 2, 3...) \tag{A.31}$$

where

$$\Psi(n,i) = \sum_{j=i+1}^{\infty} \sum_{m=n+1}^{\infty} p_{mj}(n,i) j [S_m^{(j)}] \tag{A.32}$$

Equations A.30 and A.31 must be solved by using equations A.5 and A.6. The Number Chain Length Distribution (NCLD) for the PS species can then be found by integrating equations in A.12 with the expressions found for $[{S_n}^{(i)} \cdot]$.

The maximum chain length (maximum value of n) and number of peroxide groups (maximum value of i) simulated by resolution of the model are determined as follows: simulations are carried out with a large number for maximum undecomposed peroxide groups within the polymer chains (up to 30) and a very large number for maximum chain

length (up to 25 000 monomer units). The maximum chain length and number of peroxide groups simulated is then adapted in order to ensure that the system simulates the species that determine the molecular structure of the polymer and the average molecular weights values, and at the same time minimize the time required for the simulations.

In order to account for the formation of monoradicals from random scission of the polymer chains containing peroxide groups, consider a polymer chain with length n and i peroxide groups (where $i > 0$), all of which have the same thermal stability. It will be assumed that the peroxide groups are uniformly distributed within the polymer chain. when Let m be a uniformly distributed random variable whose value ranges from 1 to $n - 1$ and represents the position in which the peroxide group is located within the polymer chain, starting from either chain end. For a given instant, upon peroxide group decomposition, a polymer chain of length n generates 2 monoradicals, one of length m, and the other one with length $n - m$. These chains will have $i - j$ and $j - 1$ undecomposed peroxide groups respectively. If the hypothesis is made that peroxide groups are uniformly distributed in the formed monoradicals, the following relation must hold:

$$\frac{j-1}{n-m} = \frac{i-j}{m}$$

Therefore,

$$j = \left[\frac{i(n-m)+m}{n}\right]$$

where the brackets indicate the integer part of the expression.

The scission of $[S_n^{(i)}]$ generates two monoradicals, one with length m and $i - j$ peroxide groups, the other one with length $n - m$ and $j - 1$ peroxide groups, namely $[S_m^{(i-j)}]$ and $[S_{n-m}^{(j-1)}]$. Said monoradicals are generated at a rate given by $ik_{d2}[S_n^{(i)}]$.

Average molecular weights

The number average molecular weight, weight average molecular weight and polydispersity are calculated with:

$$\bar{M}_n = M_{\mathrm{St}} \frac{\sum_{i=0}^{\infty} \sum_{n=2}^{\infty} n[{S_n}^{(i)}]}{\sum_{i=0}^{\infty} \sum_{n=2}^{\infty} [{S_n}^{(i)}]} \tag{A.33a}$$

$$\bar{M}_w = M_{\mathrm{St}} \frac{\sum_{i=0}^{\infty} \sum_{n=2}^{\infty} n^2[{S_n}^{(i)}]}{\sum_{i=0}^{\infty} \sum_{n=2}^{\infty} n[{S_n}^{(i)}]} \tag{A.33b}$$

$$D = \frac{\bar{M}_w}{\bar{M}_n} \tag{A.33c}$$

where M_{St} is the molar mass of the repeating styrene unit.

Appendix B

Mathematical model for the bulk polymerization of styrene at 120–200 °C using DEKTP

The mathematical model is based on the kinetic mechanism of Table 3.1 and considers the mass balances for the chemical species in the reaction system.

B.1 Basic module

Balances for non-polymeric reagents and products

Initiator (DEKTP)

$$\frac{d}{dt}\left([I^{(3)}]V\right) = -3(k_{d1} + k_{dt})[I^{(3)}]V \tag{B.1}$$

Monomer (St)

Assuming the long chain hypothesis, by which propagation is the only monomer-consuming reaction:

$$\frac{d}{dt}\left([\mathrm{St}]V\right) = -R_pV = -k_p[\mathrm{St}]\left([R\cdot] + 2[\cdot R\cdot]\right)V \tag{B.2}$$

where R_p is the global St polymerization rate, and

$$[R\cdot] = \sum_{i=0}^{\infty}\sum_{n=1}^{\infty}[S_n\cdot^{(i)}] \tag{B.3a}$$

$$[\cdot R\cdot] = \sum_{i=0}^{\infty}\sum_{n=1}^{\infty}[\cdot S_n\cdot^{(i)}] \tag{B.3b}$$

represent the total concentrations of mono- and diradicals respectively.

Radical Species

Consider the mass balances of all free radicals appearing in the global kinetics. Such balances provide:

$$\frac{d}{dt}\left([\cdot I\cdot^{(2)}]V\right) = \left(3fk_{d1}[I^{(3)}] - 2k_{i1}[\cdot I\cdot^{(2)}][\mathrm{St}]\right)V \tag{B.4}$$

$$\frac{d}{dt}\left([\cdot I\cdot^{(0)}]V\right) = \left(6fk_{d1}[I^{(3)}] - 2k_{i1}[\cdot I\cdot^{(0)}][\mathrm{St}]\right)V \tag{B.5}$$

$$\frac{d}{dt}\left([S_1\cdot^{(0)}]V\right) = \Big\{2k_i[\mathrm{St}]^3 - \Big(k_p[S_1\cdot^{(0)}] - k_{fM}\left([R\cdot] + 2[\cdot R\cdot]\right) + k_{fM}[S_1\cdot^{(0)}]\Big)[\mathrm{St}] - k_{tc}[S_1\cdot^{(0)}]\left([R\cdot] + 2[\cdot R\cdot]\right)\Big\}V \tag{B.6}$$

$$\frac{d}{dt}\left([\cdot S_1\cdot^{(2)}]V\right) = \Big\{\Big(2k_{i1}[\cdot \mathrm{I}\cdot^{(2)}] - 2k_p[\cdot S_1\cdot^{(2)}] - 2k_{fM}[\cdot S_1\cdot^{(2)}]\Big)[\mathrm{St}] - 2k_{tc}[\cdot S_1\cdot^{(2)}]\left([R\cdot] + 2[\cdot R\cdot]\right)\Big\}V \tag{B.7}$$

$$\frac{d}{dt}\left([\cdot S_1\cdot^{(0)}]V\right) = \Big\{\Big(2k_{i1}[\cdot \mathrm{I}\cdot^{(0)}] - 2k_p[\cdot S_1\cdot^{(0)}] - 2k_{fM}[\cdot S_1\cdot^{(0)}]\Big)[\mathrm{St}] - 2k_{tc}[\cdot S_1\cdot^{(0)}]\left([R\cdot] + 2[\cdot R\cdot]\right)\Big\}V \tag{B.8}$$

$$\frac{d}{dt}\left([\cdot S_n\cdot^{(i)}]V\right) = \Big\{2k_p[\mathrm{St}]\left([\cdot S_{n-1}\cdot^{(i)}] - [\cdot S_n\cdot^{(i)}]\right) - 2k_{fM}[\mathrm{St}][\cdot S_n\cdot^{(i)}] - 2k_{tc}\left([R\cdot] + 2[\cdot R\cdot]\right)[\cdot S_n\cdot^{(i)}] + 2k_{tc}\sum_{j=0}^{i}\sum_{m=1}^{n-1}[\cdot S_{n-m}\cdot^{(i-j)}][\cdot S_m\cdot^{(j)}]\Big\}V \quad (n \geq 2, i = 2, 4, 6...) \tag{B.9}$$

$$\frac{d}{dt}\left([S_n{\cdot}^{(i)}]V\right) = \left\{\left(k_p\left([S_{n-1}{\cdot}^{(i)}] - [S_n{\cdot}^{(i)}]\right) + k_{fM}\left(2[{\cdot}S_n{\cdot}^{(i)}] - [S_n{\cdot}^{(i)}]\right)\right)[\mathrm{St}]\right.$$
$$- k_{tc}\left([R{\cdot}] + 2[{\cdot}R{\cdot}]\right)[S_n{\cdot}^{(i)}] + 2k_{tc}\sum_{j=0}^{i}\sum_{m=1}^{n-1}[{\cdot}S_{n-m}{\cdot}^{(i-j)}][S_m{\cdot}^{(j)}]$$
$$\left. + k_{d2}\sum_{j=i+1}^{\infty}\sum_{m=n+1}^{\infty} p_{mj}(n,i)j[S_m^{(j)}] + \delta_{i0}k_{dt}\sum_{j=i+1}^{\infty}\sum_{m=n+1}^{\infty} {p'}_{mj}(n,0)j[S_m^{(j)}]\right\} V$$
$$(n \geq 2, i = 0, 1, 2, 3...) \quad \text{(B.10)}$$

Where $p_{mj}(n,i)$ denotes the probability that a scission of a chain of dead polymer of length m and j peroxide groups yields a monoradical of chain length n with i peroxide groups. Adding this probability over all ns and is, the following can be proven:

$$\sum_{i=1}^{\infty}\sum_{n=1}^{\infty}\sum_{j=i+1}^{\infty}\sum_{m=n+1}^{\infty} p_{mj}(n,i)j[S_m^{(j)}] = 2\sum_{i=1}^{\infty}\sum_{n=1}^{\infty} i[S_n^{(i)}] = 2[\mathrm{Pe_P}] \quad \text{(B.11)}$$

where $[\mathrm{Pe_P}]$ is the concentration of peroxide groups in the polymer chains. The 2 in Equation A.16 arises from the fact that the scission of any polymer chain with peroxide groups produces 2 monoradicals.

Similarly, in Equation B.10 $p'_{mj}(n,0)$ is the probability that a scission of a chain of dead polymer of length m and j peroxide groups yields a monoradical of chain length n without peroxide groups, due to a total decomposition reaction. It is assumed that total decomposition reactions generate monoradicals without undecomposed peroxide groups. It should be noted that diradicals would also be generated when a polymeric chain with undecomposed peroxide groups suffers a total decomposition reaction. These probability coefficients will be related to the stoichiometric coefficients α_n and β_n in the kinetic mechanism of Table 3.1. However, this is expected to have little or no effect on the detailed polymer MWD, as polymeric chains with undecomposed peroxide groups in systems in which initiator decomposition is mostly total are expected to have very low concentrations, because in these systems the behavior of the initiator is close to the one of a traditional monofunctional initiator, and the MWD for temperatures at which initiator decomposition is not exclusively sequential is controlled by transfer to monomer reactions.

The generation of monoradicals from decomposition of peroxide groups within polymeric chains due to total decomposition must be considered only for monoradicals without undecomposed peroxide groups (i.e., species of the form $[S_n{\cdot}^{(0)}]$).

The following assumption is made:

$$\sum_{i=0}^{\infty}\sum_{n=1}^{\infty}\sum_{j=i+1}^{\infty}\sum_{m=n+1}^{\infty}\delta_{i0}{p'}_{mj}(n,0)j[\mathrm{S}_m^{(j)}] \approx 2[\mathrm{Pe_P}] \tag{B.12}$$

which is equivalent to asserting that the total decomposition of any polymer chain with undecomposed peroxide groups (without characterizing it by chain length) generates two monoradicals (which contain no undecomposed peroxide groups), which is in turn equivalent to stating that the polymer chains may have only one undecomposed peroxide group. This is a simplification since the total decomposition of a polymer chain generates as many radicals as undecomposed peroxide groups were within the chain, and the number of peroxide groups within the chains is a variable. However, it allows for a much more simple form for the equations in the Basic Module, and simulations show that, in the simulated conditions, this assumption has little effect on the values of the theoretical predictions that are of interest.

From equations B.6 through B.19 the total concentration of mono- and diradicals may be obtained:

$$\frac{d}{dt}\left([R\cdot]V\right) = \left\{2k_i[\mathrm{St}]^3 + 4k_{fM}[\mathrm{St}][\cdot R\cdot] - k_{tc}[R\cdot]^2 + 2(k_{d2}+k_{dt})[\mathrm{Pe_P}]\right\}V \tag{B.13}$$

$$\frac{d}{dt}\left([\cdot R\cdot]V\right) = \left\{\left(2k_{i1}([\cdot I\cdot^{(2)}] + [\cdot I\cdot^{(0)}]) - 2k_{fM}[\cdot R\cdot]\right)[\mathrm{St}] - 2k_{tc}[\cdot R\cdot]\left([R\cdot] + 2[\cdot R\cdot]\right) + 2k_{tc}[\cdot R\cdot]^2\right\}V \tag{B.14}$$

Balances for the polymeric species

$$\frac{d}{dt}\left([{S_n}^{(i)}]V\right) = \left\{k_{fM}[\mathrm{St}][{S_n}\cdot^{(i)}] + \frac{k_{tc}}{2}\sum_{j=0}^{i}\sum_{m=1}^{n-1}[{S_{n-m}}\cdot^{(i-j)}][{S_m}\cdot^{(j)}] - (k_{d2}+k_{dt})i[{S_n}^{(i)}]\right\}V$$

$$(n \geq 2, i = 0, 1, 2...) \tag{B.15}$$

The concentration of the polymer with i undecomposed peroxide groups can be defined as

$$[P^{(i)}] = \sum_{n=1}^{\infty}[{S_n}^{(i)}] \tag{B.16}$$

Define the total polymer concentration $[P]$

$$[P] = \sum_{i=0}^{\infty} [P^{(i)}] = \sum_{i=0}^{\infty} \sum_{n=2}^{\infty} [{S_n}^{(i)}] \tag{B.17}$$

By adding up Equation B.15 over all$n$s and all is, the balance for the molar concentration of polymer can be written:

$$\frac{d}{dt}([P]V) = \left\{ k_{fM}[\mathrm{St}][R\cdot] + \frac{k_{tc}}{2}[R\cdot]^2 - (k_{d2} + k_{dt})[\mathrm{Pe_P}] \right\} \tag{B.18}$$

Peroxide groups

The total concentration of peroxide groups is

$$[\mathrm{Pe}] = 3[\mathrm{I}^{(3)}] + 2[\cdot\mathrm{I}\cdot^{(2)}] + [\mathrm{Pe}_{R\cdot}] + [\mathrm{Pe}_{\cdot R\cdot}] + [\mathrm{Pe_P}] \tag{B.19}$$

with

$$[\mathrm{Pe}_{R\cdot}] = \sum_{i=1}^{\infty} \sum_{n=1}^{\infty} i[{S_n}\cdot^{(i)}] \tag{B.20a}$$

$$[\mathrm{Pe}_{\cdot R\cdot}] = \sum_{i=1}^{\infty} \sum_{n=1}^{\infty} i[\cdot{S_n}\cdot^{(i)}] \tag{B.20b}$$

$$[\mathrm{Pe_P}] = \sum_{i=1}^{\infty} \sum_{n=1}^{\infty} i[{S_n}^{(i)}] \tag{B.20c}$$

where [Pe], $[\mathrm{Pe}_{\cdot R\cdot}]$, and $[\mathrm{Pe_P}]$ respectively represent the molar concentration of peroxide groups accumulated in monoradicals, diradicals and polymer species. From Equation B.19 and assuming pseudosteady-state for radical species, by which all time derivatives may be set to zero:

$$\frac{d[\mathrm{Pe}]}{dt} = 3\frac{d[\mathrm{I}^{(3)}]}{dt} + \frac{d[\mathrm{Pe_P}]}{dt} \tag{B.21}$$

Peroxide groups are consumed only by decomposition reactions in the initiator and the polymer chains. Therefore:

$$\frac{d[\mathrm{Pe}]}{dt} = -3(k_{d1} + k_{dt})[\mathrm{I}^{(3)}] - (k_{d2} + k_{dt})[\mathrm{Pe_P}] \tag{B.22}$$

By considering equations B.1 and B.22 and from Equation B.21, the total peroxide groups contained in the polymer chains can be calculated from the following equation:

$$\frac{d[\mathrm{Pe_P}]}{dt} = 6(k_{d1} + k_{dt})[\mathrm{I}^{(3)}] - (k_{d2} + k_{dt})[\mathrm{Pe_P}] \tag{B.23}$$

Conversion

The monomer conversion can be calculated from

$$x = \frac{[\mathrm{St}]_0 V_0 - [\mathrm{St}]V}{[\mathrm{St}]_0 V_0} \tag{B.24}$$

where the subscript "0" indicates initial conditions. In this model, the effect of volume contraction is neglected and therefore

$$x = \frac{[\mathrm{St}]_0 - [\mathrm{St}]}{[\mathrm{St}]_0} \tag{B.25}$$

Equations B.1, B.2, B.4, B.13, B.14, B.18, B.23, B.25 can be simultaneously solved to find the evolutions of $[I^{(3)}]$, [St], $[\cdot I \cdot^{(2)}]$, $[R\cdot]$, $[\cdot R\cdot]$, $[P]$, $[\mathrm{Pe_P}]$ and x.

Average rate of polymerization

The average rate of polymerization can be defined, for a given value of conversion x as

$$\bar{R}_{px} = \frac{1}{t_x}\int_0^{t_x} R_p dt \tag{B.26}$$

where t_x is the time at which value for conversion is x. In view of Equation B.2, it may be written

$$\bar{R}_{px} = -\frac{1}{t_x}\int_0^{t_x} \frac{1}{V} d\left([\mathrm{St}]\, V\right) = \frac{1}{t_x}\left([\mathrm{St}]_0 - [\mathrm{St}]_{t_x}\right) \tag{B.27}$$

where constant volume is assumed. Considering the definition of conversion of B.25, the average rate of polymerization may be calculated as

$$\bar{R}_{px} = \frac{[\mathrm{St}]_0 x}{t_x} \tag{B.28}$$

The fraction of chemical initiation by total decomposition can be defined as

$$f_{td} = \frac{-3k_{dt}[I^{(3)}]}{-3\left(k_{d1} + k_{dt}\right)[I^{(3)}]} = \frac{k_{dt}}{k_{d1} + k_{dt}} \tag{B.29}$$

B.2 Distributions module

Consider equations B.13 and B.14. Assuming pseudosteady-state, all time derivatives may be set to zero and the following recurrence formulas can be obtained:

$$[\cdot S_n \cdot^{(i)}] = \frac{k_p[\mathrm{St}][\cdot S_{n-1} \cdot^{(i)}] + k_{tc} \sum_{j=1}^{i} \sum_{m=1}^{n-1} [\cdot S_{n-m} \cdot^{(i-j)}][\cdot S_m \cdot^{(j)}]}{k_p[\mathrm{St}] + k_{fM}[\mathrm{St}] + k_{tc}([R\cdot] + 2[\cdot R\cdot])} \quad (n \geq 2, i = 2, 4, 6...) \quad \text{(B.30)}$$

$$[S_n{}^{(i)}\cdot] = \frac{\left(k_p[S_{n-1} \cdot^{(i)}] + 2k_{fM}[\cdot S_n \cdot^{(i)}]\right)[\mathrm{St}] + 2k_{tc} \sum_{j=0}^{i} \sum_{m=1}^{n-1} [\cdot S_{n-m} \cdot^{(i-j)}][S_m \cdot^{(j)}]}{k_p[\mathrm{St}] + k_{fM}[\mathrm{St}] + k_{tc}([R\cdot] + 2[\cdot R\cdot])}$$
$$+ \frac{k_{d2} \sum_{j=i+1}^{\infty} \sum_{m=n+1}^{\infty} p_{mj}(n,i) j[S_m^{(j)}] + \delta_{i0} k_{dt} \sum_{j=i+1}^{\infty} \sum_{m=n+1}^{\infty} p'_{mj}(n,0) j[S_m^{(j)}]}{k_p[\mathrm{St}] + k_{fM}[\mathrm{St}] + k_{tc}([R\cdot] + 2[\cdot R\cdot])} \quad (n \geq 2, i = 0, 1, 2, 3...) \quad \text{(B.31)}$$

The Number Chain Length Distribution (NCLD) for the PS species can then be found by integrating equations in B.15 with the expressions found for $[S_n{}^{(i)}\cdot]$.

The maximum chain length (maximum value of n) and number of peroxide groups (maximum value of i) simulated by resolution of the model are determined as follows: simulations are carried out with a large number for maximum undecomposed peroxide groups within the polymer chains (up to 30) and a very large number for maximum chain length (up to 25 000 monomer units). The maximum chain length and number of peroxide groups simulated is then adapted in order to ensure that the system simulates the species that determine the molecular structure of the polymer and the average molecular weights values, and at the same time minimize the time required for the simulations.

In order to account for the formation of monoradicals from random scission of the polymer chains containing peroxide groups, consider a polymer chain with length n and i peroxide groups (where $i > 0$), all of which have the same thermal stability. It will be assumed that the peroxide groups are uniformly distributed within the polymer chain. when Let m be a uniformly distributed random variable whose value ranges from 1 to $n - 1$ and represents the position in which the peroxide group is located

within the polymer chain, starting from either chain end. For a given instant, upon peroxide group decomposition, a polymer chain of length n generates 2 monoradicals, one of length m, and the other one with length $n-m$. These chains will have $i-j$ and $j-1$ undecomposed peroxide groups respectively. If the hypothesis is made that peroxide groups are uniformly distributed in the formed monoradicals, the following relation must hold:

$$\frac{j-1}{n-m} = \frac{i-j}{m}$$

Therefore,

$$j = \left[\frac{i(n-m)+m}{n}\right]$$

where the brackets indicate the integer part of the expression.

The scission of $[S_n^{(i)}]$ generates two monoradicals, one with length m and $i-j$ peroxide groups, the other one with length $n-m$ and $j-1$ peroxide groups, namely $[S_m^{(i-j)}]$ and $[S_{n-m}^{(j-1)}]$. Said monoradicals are generated at a rate given by $ik_{d2}[S_n^{(i)}]$.

For the case of a total decomposition, it is assumed that the scission of a polymer with chain length n and i undecomposed peroxide groups generates $(i+1)$ monoradicals, each with a chain length of

$$m = \left[\frac{n}{i+1}\right]$$

which are generated at a rate given by $ik_{dt}[S_n^{(i)}]$.

Average molecular weights

The number average molecular weight, weight average molecular weight and polydispersity are calculated with:

$$\bar{M}_n = M_{\mathrm{St}} \frac{\sum_{i=0}^{\infty}\sum_{n=2}^{\infty} n[{S_n}^{(i)}]}{\sum_{i=0}^{\infty}\sum_{n=2}^{\infty}[{S_n}^{(i)}]} \tag{B.32a}$$

$$\bar{M}_w = M_{\mathrm{St}} \frac{\sum_{i=0}^{\infty}\sum_{n=2}^{\infty} n^2[{S_n}^{(i)}]}{\sum_{i=0}^{\infty}\sum_{n=2}^{\infty} n[{S_n}^{(i)}]} \tag{B.32b}$$

$$D = \frac{\bar{M}_w}{\bar{M}_n} \tag{B.32c}$$

where M_{St} is the molar mass of the repeating styrene unit.

Appendix C

Mathematical model for the bulk polymerization of styrene using multifunctional initiators

The mathematical model is based on the kinetic mechanism of Table 4.2 and considers the mass balances for the chemical species in the reaction system.

C.1 Basic module

Balances for non-polymeric reagents and products

Multifunctional initiators ($\phi = 1, 2, 3$)

$$\frac{d}{dt}\left([I^{(\phi)}]V\right) = -\phi k_{d1}[I^{(\phi)}]V \tag{C.1}$$

$$\frac{d}{dt}\left([\bar{I}^{(\phi)}]V\right) = -\phi k_{d1}[\bar{I}^{(\phi)}]V \tag{C.2}$$

Secondary initiator species ($\phi > i = 1, 2$)

$$\frac{d}{dt}\left([\bar{I}^{(i)}]V\right) = -ik_{d1}[\bar{I}^{(i)}]V + (1 - f_1)\sum_{j=i+1}^{\phi} jk_{d1}\left([I^{(j)}] + [\bar{I}^{(j)}]\right)V \tag{C.3}$$

Monomer (St)

Assuming the long chain hypothesis, by which propagation is the only monomer-consuming reaction:

$$\frac{d}{dt}\left([\mathrm{St}]V\right) = -R_pV = -k_p[\mathrm{St}]\left([R\cdot] + 2[\cdot R\cdot]\right)V \tag{C.4}$$

where R_p is the global St polymerization rate, and

$$[R\cdot] = \sum_{i=0}^{\infty}\sum_{n=1}^{\infty}[S_n\cdot^{(i)}] \tag{C.5a}$$

$$[\cdot R\cdot] = \sum_{i=0}^{\infty}\sum_{n=1}^{\infty}[\cdot S_n\cdot^{(i)}] \tag{C.5b}$$

represent the total concentrations of mono- and diradicals respectively.

Radical species ($i = 0, 1, ...; n = 2, 3, ...$)

Consider the mass balances of all free radicals appearing in the global kinetics. Such balances provide:

$$\frac{d}{dt}\left([\cdot I\cdot^{(i)}]V\right) = f_1(i+1)k_{d1}[I^{(i+1)}]V - 2k_{i1}[\mathrm{St}][\cdot I\cdot^{(i)}]V \tag{C.6}$$

$$\frac{d}{dt}\left([I\cdot^{(i)}]V\right) = \sum_{j=i+1}^{\phi} p_j(i)f_1 j k_{d1}[\bar{I}^{(j)}]V - k_{i1}[\mathrm{St}][I\cdot^{(i)}]V \tag{C.7}$$

Where $p_i(j)$ is the probability that the decomposition of the initiator of functionality j generates a monoradical with i undecomposed peroxide groups.

$$\frac{d}{dt}\left([\cdot S_1\cdot^{(i)}]V\right) = 2k_{i1}[\cdot I\cdot^{(i)}][\mathrm{St}]V - 2\left(k_p[\mathrm{St}] + k_{fM}[\mathrm{St}] + k_{tc}\left([R\cdot] + 2[\cdot R\cdot]\right)\right)[\cdot S_1\cdot^{(i)}]V \tag{C.8}$$

$$\frac{d}{dt}\left([S_1\cdot^{(i)}]V\right) = \left\{k_{i1}[I\cdot^{(i)}][\mathrm{St}] + \delta_{i0}\left(2k_{i0}[\mathrm{St}]^3 + k_{fM}[\mathrm{St}]\left([R\cdot] + 2[\cdot R\cdot]\right)\right)\right\}V - \left(k_p[\mathrm{St}] + k_{fM}[\mathrm{St}] + k_{tc}\left([R\cdot] + 2[\cdot R\cdot]\right)\right)[S_1\cdot^{(i)}]V \tag{C.9}$$

where δ_{i0} is the Kronecker Delta ($\delta_{i0} = 1$ if $i = 0$ and $\delta_{i0} = 0$ otherwise).

$$\frac{d}{dt}\left([\cdot S_n\cdot^{(i)}]V\right) = 2k_p[\mathrm{St}]\left([\cdot S_{n-1}\cdot^{(i)}] - [\cdot S_n\cdot^{(i)}]\right)V - 2\left(k_{fM}[\mathrm{St}] + k_{tc}\left([R\cdot] + 2[\cdot R\cdot]\right)\right)[\cdot S_n\cdot^{(i)}]V + 2k_{tc}\sum_{j=0}^{i}\sum_{m=1}^{n-1}[\cdot S_{n-m}\cdot^{(i-j)}][\cdot S_m\cdot^{(j)}]V \tag{C.10}$$

$$\frac{d}{dt}\left([S_n{\cdot}^{(i)}]V\right) = \left(k_p\left([S_{n-1}{\cdot}^{(i)}] - [S_n{\cdot}^{(i)}]\right) + 2k_{fM}[{\cdot}S_n{\cdot}^{(i)}]\right)[\mathrm{St}]V$$
$$- \left(k_{fM}[\mathrm{St}] + k_{tc}\left([R{\cdot}] + 2[{\cdot}R{\cdot}]\right)\right)[S_n{\cdot}^{(i)}]V + 2k_{tc}\sum_{j=0}^{i}\sum_{m=1}^{n-1}[{\cdot}S_{n-m}{\cdot}^{(i-j)}][S_m{\cdot}^{(j)}]V$$
$$+ f_2 k_{dp}\sum_{j=i+1}^{\infty}\sum_{m=n+1}^{\infty}\left(p_{mj}(n,i)j[S_m^{(j)}]\right)V \quad \text{(C.11)}$$

In Equation C.11, $p_{mj}(n,i)$ is the probability that a scission of a chain of dead polymer of length m and j peroxide groups yields a growing monoradical of chain length n with i peroxide groups. Adding this probability over all ns and is, the following can be proven:

$$\sum_{i=1}^{\infty}\sum_{n=1}^{\infty}\sum_{j=i+1}^{\infty}\sum_{m=n+1}^{\infty}p_{mj}(n,i)j[S_m^{(j)}] = 2\sum_{i=1}^{\infty}\sum_{n=1}^{\infty}i[S_n^{(i)}] = 2[\mathrm{Pe_P}] \quad \text{(C.12)}$$

where $[\mathrm{Pe_P}]$ is the concentration of peroxide groups in the polymer chains. The 2 in Equation C.12 arises from the fact that the scission of any polymer chain with peroxide groups produces 2 monoradicals.

From equations C.8 and C.10 the total concentration of diradicals may be obtained:

$$\frac{d}{dt}\left([{\cdot}R{\cdot}]V\right) = 2k_{i1}\sum_{j=0}^{\phi-1}[{\cdot}I{\cdot}^{(j)}][\mathrm{St}]V + 2k_{tc}[{\cdot}R{\cdot}]^2V - 2\left(k_{fM}[\mathrm{St}] + k_{tc}\left([R{\cdot}] + 2[{\cdot}R{\cdot}]\right)\right)[{\cdot}R{\cdot}]V \quad \text{(C.13)}$$

From Equation C.9 and C.11 and considering Equation C.12, the total concentration of monoradicals may be obtained:

$$\frac{d}{dt}\left([R{\cdot}]V\right) = k_{i1}\sum_{j=0}^{\phi-1}[{\cdot}I{\cdot}^{(j)}][\mathrm{St}]V + 4k_{fM}[{\cdot}R{\cdot}][\mathrm{St}]V + 2k_i[\mathrm{St}]^3V$$
$$- k_{tc}\left([R{\cdot}] + 2[{\cdot}R{\cdot}]\right)[R{\cdot}]V + 2f_2k_{dp}[\mathrm{Pe_{PS}}]V \quad \text{(C.14)}$$

The total radicals are calculated as $[R] + 2[{\cdot}R{\cdot}]$. Using Equations C.13 and C.14,

$$\frac{d}{dt}\left(\left([R{\cdot}] + 2[{\cdot}R{\cdot}]\right)V\right) = k_{i1}\sum_{j=0}^{\phi-1}\left(4[{\cdot}I{\cdot}^{(j)}] + [I{\cdot}^{(j)}]\right)[\mathrm{St}]V + 2k_i[\mathrm{St}]^3V$$
$$+ 2f_2k_{dp}[\mathrm{Pe_{PS}}]V - k_{tc}([R{\cdot}] + 2[{\cdot}R{\cdot}])^2V \quad \text{(C.15)}$$

Peroxide groups

Neglecting the concentration of peroxide groups in the radicals, the total concentration

of peroxide groups is

$$[\mathrm{Pe}] = \sum_{j=1}^{\phi} j \left([I^{(j)}] + [\bar{\mathrm{I}}^{(j)}] \right) + [\mathrm{Pe_{PS}}] \tag{C.16}$$

with

$$[\mathrm{Pe_{PS}}] = \sum_{i=0}^{\infty} \sum_{n=1}^{\infty} i \left[\mathrm{S}_n{}^{(i)} \right] \tag{C.17}$$

Peroxide groups are consumed only by decomposition reactions. Therefore:

$$\frac{d}{dt} \left([\mathrm{Pe}] V \right) = - \sum_{i=1}^{\phi} j k_{d1} \left([I^{(i)}] + [\bar{\mathrm{I}}^{(i)}] \right) V - k_{dp} [\mathrm{Pe_{PS}}] V \tag{C.18}$$

Using this result and Equation C.16, the molar concentration of undecomposed peroxide groups accumulated in the polymer can be calculated from the difference

$$\frac{d}{dt} \left([\mathrm{Pe_{PS}}] V \right) = \frac{d}{dt} \left([\mathrm{Pe}] V \right) - \sum_{j=1}^{\phi} j \frac{d}{dt} \left(\left([I^{(j)}] + [\bar{\mathrm{I}}^{(j)}] \right) V \right) \tag{C.19}$$

Conversion and volume

The monomer conversion can be calculated from

$$x = \frac{[\mathrm{St}]_0 V_0 - [\mathrm{St}] V}{[\mathrm{St}]_0 V_0} \tag{C.20}$$

where the subscript "0" indicates initial conditions. The evolution of the reaction volume V is obtained from

$$V = V_0^{\mathrm{St}} \left(1 - \varepsilon x \right) \tag{C.21}$$

with

$$\varepsilon = \frac{V_0^{\mathrm{St}} - V_f^{\mathrm{St}}}{V_0^{\mathrm{St}}} \tag{C.22}$$

Where ε is the St volume contraction factor, V_0^{St} is the initial St volume and V_f^{St} is the final volume at full conversion.

Equation C.1 to C.4, C.6, C.7, C.15, and C.12 to C.21 are solved simultaneously to find the evolution of species $[I^{(i)}]$, $[\bar{I}^{(i)}]$, [St], $[\cdot I.^{(i)}]$, $[I.^{(i)}]$ $([R\cdot] + 2[\cdot R\cdot])$, $[\mathrm{Pe_P}]$, x and V.

C.2 Moments module

Distribution moments equations

Define the k^{th} moment of the distribution of diradicals ($\sigma_k^{(i)}$), monoradicals ($\lambda_k^{(i)}$) and polymer ($\mu_k^{(i)}$) species, characterized by their number of undecomposed peroxide groups i:

$$\sigma_k^{(i)} = \sum_{n=1}^{\infty} n^k [\cdot S_n^{(i)} \cdot] \tag{C.23}$$

$$\lambda_k^{(i)} = \sum_{n=1}^{\infty} n^k [S_n^{(i)} \cdot] \tag{C.24}$$

$$\mu_k^{(i)} = \sum_{n=1}^{\infty} n^k [S_n^{(i)}] \tag{C.25}$$

The evolution of the 0^{th}, 1^{st} and 2^{nd} moments of the distributions of diradicals, monoradicals and polymer species are written:

$$\frac{d\left(\sigma_0^{(i)} V\right)}{dt} = 2k_{i1}[\cdot I\cdot^{(i)}][\text{St}]V + 2k_{tc}\sum_{j=0}^{i} \sigma_0^{(i-j)}\sigma_0^{(j)} V - 2\left(k_{fM}[\text{St}] + k_{tc}\sum_{i=0}^{\infty}\left(\lambda_0^{(i)} + 2\sigma_0^{(i)}\right)\right)\sigma_0^{(i)} V \tag{C.26}$$

$$\frac{d\left(\sigma_1^{(i)} V\right)}{dt} = 2k_{i1}[\cdot I\cdot^{(i)}][\text{St}]V + 2k_p[\text{St}]\sigma_0^{(i)} V + 2k_{tc}\sum_{j=0}^{i}\left(\sigma_0^{(i-j)}\sigma_1^{(j)} + \sigma_1^{(i-j)}\sigma_0^{(j)}\right) V - 2\left(k_{fM}[\text{St}] + k_{tc}\sum_{i=0}^{\infty}\left(\lambda_0^{(i)} + 2\sigma_0^{(i)}\right)\right)\sigma_1^{(i)} V \tag{C.27}$$

$$\frac{d\left(\sigma_2^{(i)} V\right)}{dt} = 2k_{i1}[\cdot I\cdot^{(i)}][\text{St}]V + 2k_p[\text{St}]\left(2\sigma_1^{(i)} + \sigma_0^{(i)}\right) V + 2k_{tc}\sum_{j=0}^{i}\left(\sigma_0^{(i-j)}\sigma_2^{(j)} + 2\sigma_1^{(i-j)}\sigma_1^{(j)} + \sigma_2^{(i-j)}\sigma_0^{(j)}\right) V - 2\left(k_{fM}[\text{St}] + k_{tc}\sum_{i=0}^{\infty}\left(\lambda_0^{(i)} + 2\sigma_0^{(i)}\right)\right)\sigma_2^{(i)} V \tag{C.28}$$

$$\frac{d\left(\lambda_0^{(i)}V\right)}{dt} = k_{i1}[I\cdot^{(i)}][\mathrm{St}]V + 2k_{fM}[\mathrm{St}]\sigma_0^{(i)}V + 2k_{tc}\sum_{j=0}^{i}\sigma_0^{(i-j)}\lambda_0^{(j)}V + 2k_{dp}\sum_{j=i+1}^{\infty}\mu_0^{(j)}V + k_{fM}[\mathrm{St}]\delta_{i0}\sum_{j=0}^{\infty}\lambda_0^{(j)}V - \left(k_{fM}[\mathrm{St}] + k_{tc}\sum_{j=0}^{\infty}\left(\lambda_0^{(j)} + 2\sigma_0^{(j)}\right)\right)\lambda_0^{(i)}V \quad \text{(C.29)}$$

$$\frac{d\left(\lambda_1^{(i)}V\right)}{dt} = k_{i1}[I\cdot^{(i)}][\mathrm{St}]V + k_p[\mathrm{St}]\lambda_0^{(i)}V + 2k_{fM}[\mathrm{St}]\sigma_1^{(i)}V + 2k_{tc}\sum_{j=0}^{i}\left(\lambda_0^{(i-j)}\sigma_1^{(j)} + \lambda_1^{(i-j)}\sigma_0^{(j)}\right)V + 2k_{dp}\sum_{j=i+1}^{\infty}\mu_1^{(j)}V + k_{fM}[\mathrm{St}]\delta_{i0}\sum_{j=0}^{\infty}\left(\lambda_0^{(j)} + 2\sigma_0^{(j)}\right)V - \left(k_{fM}[\mathrm{St}] + k_{tc}\sum_{j=0}^{\infty}\left(\lambda_0^{(j)} + 2\sigma_0^{(j)}\right)\right)\lambda_1^{(i)}V \quad \text{(C.30)}$$

$$\frac{d\left(\lambda_2^{(i)}V\right)}{dt} = k_{i1}[I\cdot^{(i)}][\mathrm{St}]V + k_p[\mathrm{St}]\left(2\lambda_1^{(i)} + \lambda_0^{(i)}\right)V + 2k_{fM}[\mathrm{St}]\sigma_2^{(i)}V + 2k_{tc}\sum_{j=0}^{i}\left(\lambda_0^{(i-j)}\sigma_2^{(j)} + 2\lambda_1^{(i-j)}\sigma_1^{(j)} + \lambda_2^{(i-j)}\sigma_0^{(j)}\right)V + 2k_{dp}\sum_{j=i+1}^{\infty}\mu_2^{(j)}V + k_{fM}[\mathrm{St}]\delta_{i0}\sum_{j=0}^{\infty}\left(\lambda_0^{(j)} + 2\sigma_0^{(j)}\right)V - \left(k_{fM}[\mathrm{St}] + k_{tc}\sum_{i=0}^{\infty}\left(\lambda_0^{(j)} + 2\sigma_0^{(j)}\right)\right)\lambda_2^{(i)}V \quad \text{(C.31)}$$

$$\frac{d\left(\mu_0^{(i)}V\right)}{dt} = k_{fM}[\mathrm{St}]\lambda_0^{(i)}V + \frac{1}{2}k_{tc}\sum_{j=0}^{i}\lambda_0^{(i-j)}\lambda_0^{(j)}V - ik_{dp}\mu_0^{(i)}V \quad \text{(C.32)}$$

$$\frac{d\left(\mu_1^{(i)}V\right)}{dt} = k_{fM}[\mathrm{St}]\lambda_1^{(i)}V + \frac{1}{2}k_{tc}\sum_{j=0}^{i}\left(\lambda_0^{(i-j)}\lambda_1^{(j)} + \lambda_1^{(i-j)}\lambda_0^{(j)}\right)V - ik_{dp}\mu_1^{(i)}V \quad \text{(C.33)}$$

$$\frac{d\left(\mu_2^{(i)}V\right)}{dt} = k_{fM}[\mathrm{St}]\lambda_2^{(i)}V + \frac{1}{2}k_{tc}\sum_{j=0}^{i}\left(\lambda_0^{(i-j)}\lambda_2^{(j)} + 2\lambda_1^{(i-j)}\lambda_1^{(j)} + \lambda_2^{(i-j)}\lambda_0^{(j)}\right)V - ik_{dp}\mu_2^{(i)}V \quad \text{(C.34)}$$

The average molecular weights and polydispersity can then be calculated from

$$\bar{M}_n = \frac{\sum_{i=0}^{\infty}\mu_1^{(i)}}{\sum_{i=0}^{\infty}\mu_0^{(i)}} \quad \text{(C.35)}$$

$$\bar{M}_w = \frac{\sum_{i=0}^{\infty} \mu_2^{(i)}}{\sum_{i=0}^{\infty} \mu_1^{(i)}} \tag{C.36}$$

$$D = \frac{\bar{M}_w}{\bar{M}_n} \tag{C.37}$$

C.3 Distributions module

Radical species $(i = 0, 1, ...; n = 2, 3, ...)$

Consider equations C.10 and C.11. Assuming pseudosteady-state, all time derivatives may be set to zero and the following recurrence formulas can be obtained:

$$[\cdot S_n \cdot^{(i)}] = \frac{k_p[\mathrm{St}][\cdot S_{n-1} \cdot^{(i)}] + k_{tc} \sum_{j=0}^{i} \sum_{m=1}^{n-1} [\cdot S_{n-m} \cdot^{(i-j)}][\cdot S_m \cdot^{(j)}]}{k_p[\mathrm{St}] + k_{fM}[\mathrm{St}] + k_{tc}\left([R\cdot] + 2[\cdot R\cdot]\right)} \tag{C.38}$$

$$\begin{aligned}[S_n \cdot^{(i)}] = {} & \frac{\left(k_p[S_{n-1} \cdot^{(i)}] + 2k_{fM}[\cdot S_n \cdot^{(i)}]\right)[\mathrm{St}]}{k_p[\mathrm{St}] + k_{fM}[\mathrm{St}] + k_{tc}\left([R\cdot] + 2[\cdot R\cdot]\right)} \\ & + \frac{2k_{tc} \sum_{j=0}^{i} \sum_{m=1}^{n-1} [\cdot S_{n-m} \cdot^{(i-j)}][S_m \cdot^{(j)}] + k_{dp} \sum_{j=i+1}^{\infty} \sum_{m=n+1}^{\infty} p_{mj}(n,i) j [S_m^{(j)}]}{k_p[\mathrm{St}] + k_{fM}[\mathrm{St}] + k_{tc}\left([R\cdot] + 2[\cdot R\cdot]\right)}\end{aligned} \tag{C.39}$$

Polystyrene species $(i = 0, 1, ...; n = 2, 3, ...)$

The mass balances for the PS species provide

$$\begin{aligned}\frac{d}{dt}\left([S_n{}^{(i)}]V\right) = {} & k_{fM}[\mathrm{St}][S_n \cdot^{(i)}]V + \frac{k_{tc}}{2} \sum_{j=0}^{i} \sum_{m=1}^{n-1} [S_{n-m} \cdot^{(i-j)}][S_m \cdot^{(j)}]V - i k_{dp}[S_n{}^{(i)}]V \\ & + (1 - f_2)\, k_{dp} \sum_{j=i+1}^{\infty} \sum_{m=n+1}^{\infty} p_{mj}(n,i) j [S_m^{(j)}]V\end{aligned} \tag{C.40}$$

In order to account for the generation of monoradicals from random scission polymer chains by sequential decomposition of peroxide groups within the chains, consider a polymer chain with length n and i peroxide groups, all of which have the same thermal stability. Let m be a uniformly distributed random variable whose value ranges 1 from 1 to $n-1$. The polymer chain may form 2 monoradicals, one with length m, and the other one with length $n - m$. These chains will have $i - j$ and $j - 1$ undecomposed peroxide

groups respectively. If the peroxide groups are assumed to be uniformly distributed within the polymer chains in the course of polymerization, the following relation must hold:

$$\frac{j-1}{n-m} = \frac{i-j}{m}$$

Therefore,

$$j = [\frac{i(n-m)+m}{n}]$$

where the brackets indicate the integer part of the expression.

The scission has then generated two monoradicals, one with length m and $i-j$ peroxide groups, the other one with length $n-m$ and $j-1$ peroxide groups.

Note that this chain scission algorithm can be modified for specific cases. For example, in the case of a linear bifunctional initiator, since all peroxide groups are located at a chain end, $m = 1$ for every scission.

The Number Chain Length Distribution (NCLD) for the PS species is

$$N_{\mathrm{PS}}^{(i)}(n) = [{S_n}^{(i)}]V \tag{C.41}$$

found by integrating Equation C.40 with equations C.38 and C.39 using also Equation C.8 and C.9 for species $[\cdot {S_1}^{\cdot(i)}]$ and $[{S_1}^{\cdot(i)}]$. The concentration of the total PS species characterized by the number of undecomposed peroxide groups can be calculated with

$$[P^{(i)}] = \sum_{n=1}^{\infty} [{S_n}^{(i)}] \tag{C.42}$$

The NCLD for the total polymer can be calculated using

$$P_n = \sum_{i=0}^{\infty} [{S_n}^{(i)}]V \tag{C.43}$$

The total moles of PS are

$$N_{\mathrm{PS}} = \sum_{i=0}^{\infty}\sum_{n=1}^{\infty} N_{\mathrm{PS}}^{(i)}(n) \tag{C.44}$$

To obtain the corresponding Weight Chain Length Distribution (WCLD), multiply the NCLD by sM_{St} and replace n by s to obtain

$$G_{\mathrm{PS}}^{(i)}(s) = sM_{\mathrm{St}}[{S_s}^{(i)}]V \tag{C.45}$$

The mass of PS can then be calculated as

$$G_{\mathrm{PS}} = \sum_{i=0}^{\infty} \sum_{s=1}^{\infty} G_{\mathrm{PS}}^{(i)}(s) \tag{C.46}$$

The average molecular weights and polydispersity can then be calculated from

$$\bar{M}_n = \frac{G_{\mathrm{PS}}}{N_{\mathrm{PS}}} = \frac{\sum_{i=0}^{\infty} \sum_{s=1}^{\infty} G_{\mathrm{PS}}^{(i)}(s)}{\sum_{i=0}^{\infty} \sum_{n=1}^{\infty} [{S_n}^{(i)}]V} \tag{C.47}$$

$$\bar{M}_w = \frac{\sum_{i=0}^{\infty} \sum_{s=1}^{\infty} s G_{\mathrm{PS}}^{(i)}(s)}{G_{\mathrm{PS}}} = \frac{\sum_{i=0}^{\infty} \sum_{s=1}^{\infty} s G_{\mathrm{PS}}^{(i)}(s)}{\sum_{i=0}^{\infty} \sum_{s=1}^{\infty} G_{\mathrm{PS}}^{(i)}(s)} \tag{C.48}$$

$$D = \frac{\bar{M}_w}{\bar{M}_n} \tag{C.49}$$

Appendix D

Mathematical model for the bulk polymerization of styrene in the presence of polybutadiene using multifunctional initiators

The mathematical model is based on the kinetic mechanism of Table 5.3 and considers the mass balances for the chemical species in the reaction system.

D.1 Basic module

Balances for non-polymeric reagents and products

Multifunctional initiators ($\phi = 1, 2, 3$)

$$\frac{d}{dt}\left([I^{(\phi)}]V\right) = -\phi k_{d1}[I^{(\phi)}]V \tag{D.1}$$

$$\frac{d}{dt}\left([\bar{I}^{(\phi)}]V\right) = -\phi k_{d1}[\bar{I}^{(\phi)}]V \tag{D.2}$$

Secondary initiator species ($\phi > i = 1, 2$)

$$\frac{d}{dt}\left([\bar{I}^{(i)}]V\right) = -ik_{d1}[\bar{I}^{(i)}]V + (1-f_1)\sum_{j=i+1}^{\phi} jk_{d1}\left([I^{(j)}] + [\bar{I}^{(j)}]\right)V \tag{D.3}$$

Monomer (St)

Assuming the long chain hypothesis, by which propagation is the only monomer-consuming reaction:

$$\frac{d}{dt}\left([\mathrm{St}]V\right) = -R_pV = -k_p[\mathrm{St}]\left([R\cdot] + 2[\cdot R\cdot]\right)V \tag{D.4}$$

where R_p is the global St polymerization rate, and

$$[R\cdot] = [S\cdot] + [P\cdot] = \sum_{i=0}^{\infty}\sum_{n=1}^{\infty}[S_n{}^{\cdot(i)}] + \sum_{i=0}^{\infty}\sum_{n=1}^{\infty}[P_n{}^{\cdot(i)}] \tag{D.5a}$$

$$[\cdot R\cdot] = \sum_{i=0}^{\infty}\sum_{n=1}^{\infty}[\cdot S_n{}^{\cdot(i)}] \tag{D.5b}$$

represent the total concentrations of mono- and diradicals respectively. In Equation D.5, an S species is a PS homoradical and a P species is a PB or copolymer radical.

Unreacted B units

Let us represent with $B*$ an unreacted B unit in the copolymer or in the initial (or purely crosslinked) PB. When a P molecule is attacked, a $B*$ unit is consumed, and a $B*$ unit is generated in transfer reactions of a $P_0\cdot$ radical. Therefore,

$$\frac{d}{dt}\left([B*]V\right) = -\left\{k_{i2}\left(2\sum_{j=0}^{\phi-1}[\cdot I^{\cdot(j)}] + \sum_{j=0}^{\phi-1}[I^{\cdot(j)}]\right) + k_{fG}\left([R\cdot] + 2[\cdot R\cdot]\right)\right\}[B*]V + k_{fM}[\mathrm{St}][P_0\cdot]V \tag{D.6}$$

with

$$[P_0\cdot] = \sum_{i=0}^{\infty}[P_0{}^{\cdot(i)}] \tag{D.7}$$

Radical species ($i = 0, 1, ...; n = 2, 3, ...$)

Consider the mass balances of all free radicals appearing in the global kinetics. Such balances provide:

$$\frac{d}{dt}\left([\cdot I^{\cdot(i)}]V\right) = f_1(i+1)k_{d1}[I^{(i+1)}]V - 2\left(k_{i1}[\mathrm{St}] + k_{i2}[B*]\right)[\cdot I^{\cdot(i)}]V \tag{D.8}$$

$$\frac{d}{dt}\left([I^{\cdot(i)}]V\right) = \sum_{j=i+1}^{\phi} p_j(i)f_1 j k_{d1}[\bar{I}^{(j)}]V + 2k_{i2}[B*][\cdot I^{\cdot(j)}]V - \left(k_{i1}[\mathrm{St}] + k_{i2}[B*]\right)[I^{\cdot(i)}]V \tag{D.9}$$

Where $p_i(j)$ is the probability that the decomposition of the initiator of functionality j generates a monoradical with i undecomposed peroxide groups.

For PS homoradicals,

$$\frac{d}{dt}\left([\cdot S_1\cdot^{(i)}]V\right) = 2k_{i1}[\cdot I\cdot^{(i)}][\mathrm{St}]V - 2\left(k_p[\mathrm{St}] + k_{fM}[\mathrm{St}] + k_{fG}[B*] + k_{tc}\left([R\cdot] + 2[\cdot R\cdot]\right) + k''_{tc}[P_0\cdot]\right)[\cdot S_1\cdot^{(i)}]V \quad \text{(D.10)}$$

$$\frac{d}{dt}\left([S_1\cdot^{(i)}]V\right) = \left\{k_{i1}[I\cdot^{(i)}][\mathrm{St}]+\right\}V + +\delta_{i0}\left(2k_{i0}[\mathrm{St}]^3 + k_{fM}\left([R\cdot] + 2[\cdot R\cdot]\right)[\mathrm{St}]\right)V - \left(k_p[\mathrm{St}] + k_{fM}[\mathrm{St}] + k_{fG}[B*] + k_{tc}\left([R\cdot] + 2[\cdot R\cdot]\right) + k''_{tc}[P_0\cdot]\right)[S_1\cdot^{(i)}]V \quad \text{(D.11)}$$

where δ_{i0} is the Kronecker Delta ($\delta_{i0} = 1$ if $i = 0$ and $\delta_{i0} = 0$ otherwise).

$$\frac{d}{dt}\left([\cdot S_n\cdot^{(i)}]V\right) = 2k_p[\mathrm{St}]\left([\cdot S_{n-1}\cdot^{(i)}] - [\cdot S_n\cdot^{(i)}]\right)V - 2\left(k_{fM}[\mathrm{St}] + k_{fG}[B*] + k_{tc}\left([R\cdot] + 2[\cdot R\cdot]\right) + k''_{tc}[P_0\cdot]\right)[\cdot S_n\cdot^{(i)}]V + 2k_{tc}\sum_{j=0}^{i}\sum_{m=1}^{n-1}[\cdot S_{n-m}\cdot^{(i-j)}][\cdot S_m\cdot^{(j)}]V \quad \text{(D.12)}$$

$$\frac{d}{dt}\left([S_n\cdot^{(i)}]V\right) = \left(k_p\left([S_{n-1}\cdot^{(i)}] - [S_n\cdot^{(i)}]\right) + 2k_{fM}[\cdot S_n\cdot^{(i)}]\right)[\mathrm{St}]V + 2k_{fG}[\cdot S_n\cdot^{(i)}][B*]V - \left(k_{fM}[\mathrm{St}] + k_{fG}[B*] + k_{tc}\left([R\cdot] + 2[\cdot R\cdot]\right) + k''_{tc}[P_0\cdot]\right)[S_n\cdot^{(i)}]V + 2k_{tc}\sum_{j=0}^{i}\sum_{m=1}^{n-1}[\cdot S_{n-m}\cdot^{(i-j)}][S_m\cdot^{(j)}]V + f_2k_{d2}\sum_{j=i+1}^{\infty}\sum_{m=n+1}^{\infty}\left(p_{mj}(n,i)j[S_m^{(j)}] + p'_{mj}(n,i)j[P_m^{(j)}]\right)V \quad \text{(D.13)}$$

In Equation D.13, $p_{mj}(n,i)$ is the probability that a scission of a chain of temporarily dead free PS of length m and j peroxide groups yields a growing monoradical of chain length n with i peroxide groups and $p'_{mj}(n,i)$ is the probability that a scission of a temporarily dead PS chain in the GC of length m and j peroxide groups yields a growing monoradical of chain length n with i peroxide groups.

Adding this probability over all ns and is, the following can be proven:

$$\sum_{i=1}^{\infty}\sum_{n=1}^{\infty}\sum_{j=i+1}^{\infty}\sum_{m=n+1}^{\infty}\left(p_{mj}(n,i)j[S_m^{(j)}] + {p'}_{mj}(n,i)j[{P_m}^{(j)}]\right)$$
$$= \sum_{i=1}^{\infty}\sum_{n=1}^{\infty}\left(2i[S_n^{(i)}] + i[P_n^{(i)}]\right) = 2[\mathrm{Pe_{PS}}] + [\mathrm{Pe_C}] \quad \text{(D.14)}$$

where $[\mathrm{Pe_{PS}}]$ is the concentration of peroxide groups in the free PS chains and $[\mathrm{Pe_C}]$ is the concentration of peroxides groups in the GC. Note that the scission of any free PS chain with peroxide groups produces 2 PS homoradicals, whereas the scission of a chain within the copolymer generates only one PS homoradical and one copolymer radical.

For PB radicals and copolymer radicals,

$$\frac{d}{dt}\left([{P_0}^{\cdot(i)}]V\right) = \left(k_{i2}\sum_{j=0}^{\phi-1}\left(2[\cdot I^{\cdot(j)}] + [I^{\cdot(j)}]\right) + k_{fG}\left([R\cdot] + 2[\cdot R\cdot]\right)\right)[B*^{(i)}]V$$
$$-\left(k_{p1}[\mathrm{St}] + {k'}_{fM}[\mathrm{St}] + {k'}_{tc}[P_0\cdot] + k_{tc}\left([R\cdot] + 2[\cdot R\cdot]\right)\right)[{P_0}^{\cdot(i)}]V \quad \text{(D.15)}$$

$$\frac{d}{dt}\left([{P_1}^{\cdot(i)}]V\right) = k_{i1}[\mathrm{St}][{P_0}^{\cdot(i)}]V + 2k_{tc}\sum_{j=0}^{i}[{P_0}^{\cdot(i-j)}][\cdot{S_1}^{(j)}\cdot]V$$
$$-\left(k_p[\mathrm{St}] + k_{fM}[\mathrm{St}] + k_{fG}[B*] + {k''}_{tc}[P_0\cdot] + k_{tc}\left([R\cdot] + 2[\cdot R\cdot]\right)\right)[{P_1}^{\cdot(i)}]V \quad \text{(D.16)}$$

$$\frac{d}{dt}\left([{P_n}^{\cdot(i)}]V\right) = k_p[\mathrm{St}][{P_{n-1}}^{\cdot(i)}]V$$
$$+ f_2k_{d2}\sum_{j=i+1}^{\infty}\sum_{m=n+1}^{\infty}{p'}_{mj}(n,i)j[P_m^{(j)}]V + 2k_{tc}\sum_{j=0}^{i}\sum_{m=1}^{n-1}[{P_{n-m}}^{\cdot(i-j)}][\cdot{S_m}^{\cdot(j)}]V$$
$$-\left(k_p[\mathrm{St}] + k_{fM}[\mathrm{St}] + k_{fG}[B*] + {k''}_{tc}[P_0\cdot] + k_{tc}\left([R\cdot] + 2[\cdot R\cdot]\right)\right)[{P_n}^{\cdot(i)}]V \quad \text{(D.17)}$$

where $[B*^{(i)}]$ is the molar concentration of total B units in PB or copolymer molecules with i undecomposed peroxide groups and

$$[B*] = \sum_{i=0}^{\infty}[B*^{(i)}] \quad \text{(D.18)}$$

Note that $i = 0$ for PB.

Summing Equation D.15 all over is,

$$\frac{d}{dt}\left([P_0\cdot]V\right) = \left(k_{i2}\sum_{j=0}^{\phi-1}\left(2[\cdot I\cdot^{(j)}] + [I\cdot^{(j)}]\right) + k_{fG}\left([R\cdot] + 2[\cdot R\cdot]\right)\right)[B*]V$$
$$- \left(k_{i1}[\mathrm{St}] + k'_{fM}[\mathrm{St}] + k'_{tc}[P_0\cdot] + k_{tc}\left([R\cdot] + 2[\cdot R\cdot]\right)\right)[P_0\cdot]V \quad \text{(D.19)}$$

From Equations D.16 and D.17, summing all over ns and is, the total concentration of PB and copolymer radicals may be obtained:

$$\frac{d}{dt}\left([P\cdot]V\right) = k_{i1}[\mathrm{St}][P_0\cdot]V + k_{fG}\left([S\cdot] + 2[\cdot R\cdot]\right)[B*]V$$
$$+ k_{d2}[\mathrm{Pe_C}]V - \left(k_{fM}[\mathrm{St}] + k''_{tc}[P_0\cdot] + k_{tc}\left([S\cdot] + [P\cdot]\right)\right)[P\cdot]V \quad \text{(D.20)}$$

From Equations D.10 and D.12, the total concentration of diradicals (which are only PS homoradicals) may be obtained: obtained:

$$\frac{d}{dt}\left([\cdot R\cdot]V\right) = k_{i2}\sum_{j=0}^{\phi-1}2[\cdot I\cdot^{(j)}][\mathrm{St}]V + 2k_{tc}[\cdot R\cdot]^2V$$
$$- 2\left(k_{fM}[\mathrm{St}] + k_{fG}[B*] + k_{tc}\left([R\cdot] + 2[\cdot R\cdot]\right) + k''_{tc}[P_0\cdot]\right)[\cdot R\cdot]V \quad \text{(D.21)}$$

From Equation D.11 and D.13 and considering Equation D.14, the total concentration of PS monoradicals may be obtained:

$$\frac{d}{dt}\left([S\cdot]V\right) = \left(k_{i2}\sum_{j=0}^{\phi-1}[I\cdot^{(j)}] + k_{fM}\left([P\cdot] + 4[\cdot R\cdot]\right)\right)[\mathrm{St}]V + 2k_i[\mathrm{St}]^3V + 2k_{fG}[B*][\cdot R\cdot]V$$
$$- \left(k_{tc}\left([S\cdot] + [P\cdot] + 2[\cdot R\cdot]\right) + k_{fG}[B*] + k''_{tc}[P_0\cdot]\right)[S\cdot]V + f_2k_{d2}\left(2[\mathrm{Pe_{PS}}] + [\mathrm{Pe_C}]\right)V \quad \text{(D.22)}$$

The total radicals are calculated as $[R\cdot] + 2[\cdot R\cdot] = [S\cdot] + [P\cdot] + 2[\cdot R\cdot]$. Using Equations D.20 trough D.22,

$$\frac{d}{dt}\left(\left([R\cdot] + 2[\cdot R\cdot]\right)V\right) = k_{i1}\sum_{j=0}^{\phi-1}\left(4[\cdot I\cdot^{(j)}] + [I\cdot^{(j)}]\right)[\mathrm{St}]V + 2k_i[\mathrm{St}]^3V + k_{i1}[\mathrm{St}][P_0\cdot]V$$
$$+2f_2k_{d2}\left([\mathrm{Pe_{PS}}] + [\mathrm{Pe_C}]\right)V - k_{tc}([R\cdot] + 2[\cdot R\cdot])^2V - k''_{tc}\left([R\cdot] + 2[\cdot R\cdot]\right)[P_0\cdot]V \quad \text{(D.23)}$$

Peroxide groups

Neglecting the concentration of peroxide groups in the radicals, the total concentration of peroxide groups is

$$[\mathrm{Pe}] = \sum_{j=1}^{\phi} j \left([I^{(j)}] + [\bar{\mathrm{I}}^{(j)}] \right) + [\mathrm{Pe_{PS}}] + [\mathrm{Pe_C}] \tag{D.24}$$

with

$$[\mathrm{Pe_{PS}}] = \sum_{i=0}^{\infty} \sum_{n=1}^{\infty} i[{S_n}^{(i)}] \tag{D.25a}$$

$$[\mathrm{Pe_C}] = \sum_{i=0}^{\infty} i[\mathrm{P}^{(i)}] \tag{D.25b}$$

Peroxide groups are consumed only by decomposition reactions. Therefore:

$$\frac{d}{dt}\left([\mathrm{Pe}]V\right) = -\sum_{i=1}^{\phi} j k_{d1} \left([I^{(i)}] + [\bar{\mathrm{I}}^{(i)}] \right) V - k_{d2} \left([\mathrm{Pe_{PS}}] + [\mathrm{Pe_C}] \right) V \tag{D.26}$$

Using this result and Equation D.24, the molar concentration of peroxide groups accumulated in the free PS and the GC can be calculated from the following difference

$$\frac{d}{dt}\left(\{[\mathrm{Pe_{PS}}] + [\mathrm{Pe_C}]\} V\right) = \frac{d}{dt}\left([\mathrm{Pe}]V\right) - \sum_{j=1}^{\phi} j \frac{d}{dt} \left(\left([I^{(j)}] + [\bar{\mathrm{I}}^{(j)}] \right) V \right) \tag{D.27}$$

Conversion and volume

The monomer conversion can be calculated from

$$x = \frac{[\mathrm{St}]_0 V_0 - [\mathrm{St}]V}{[\mathrm{St}]_0 V_0} \tag{D.28}$$

where the subscript "0" indicates initial conditions. The evolution of the reaction volume V is obtained from

$$V = V_0^{\mathrm{St}} \left(1 - \varepsilon x\right) + V_0^{\mathrm{PB}} \tag{D.29}$$

with

$$\varepsilon = \frac{V_0^{\mathrm{St}} - V_f^S}{V_0^{\mathrm{St}}} \tag{D.30}$$

Where ε is the St volume contraction factor, V_0^{St} and V_0^{PB} are the initial St and PB volumes respectively and V_f^S is the final volume of free and grafted St at full conversion.

Equation D.1 to D.6, D.8, D.9, D.19, D.23, and D.24 to D.29 are solved simultaneously to find the evolution of species $[I^{(i)}]$,$[\bar{I}^{(i)}]$, [St], $[B*]$, $[\cdot I\cdot^{(i)}]$, $[I\cdot^{(i)}]$, $[P_0\cdot]$, $([R\cdot]+2[\cdot R\cdot])$, $([\mathrm{Pe_{PS}}]+[\mathrm{Pe_C}])$, x and V.

D.2 Distributions module

D.2.1 Free PS

Radical species $(i=0,1,...;\ n=2,3,...)$

Consider equations D.12 and D.13. Assuming pseudosteady-state, all time derivatives may be set to zero and the following recurrence formulas can be obtained:

$$[\cdot S_n\cdot^{(i)}]=\frac{k_p[\mathrm{St}][\cdot S_{n-1}\cdot^{(i)}]+k_{tc}\sum_{j=0}^{i}\sum_{m=1}^{n-1}[\cdot S_{n-m}\cdot^{(i-j)}][\cdot S_m\cdot^{(j)}]}{k_p[\mathrm{St}]+k_{fM}[\mathrm{St}]+k_{fG}[B*]+k_{tc}\left([R\cdot]+2[\cdot R\cdot]\right)+k''_{tc}[P_0\cdot]} \tag{D.31}$$

$$\begin{aligned}[S_n\cdot^{(i)}]=&\frac{\left(k_p[S_{n-1}\cdot^{(i)}]+2k_{fM}[\cdot S_n\cdot^{(i)}]\right)[\mathrm{St}]+2k_{fG}[\cdot S_n\cdot^{(i)}][B*]}{k_p[\mathrm{St}]+k_{fM}[\mathrm{St}]+k_{fG}[B*]+k_{tc}\left([R\cdot]+2[\cdot R\cdot]\right)+k''_{tc}[P_0\cdot]}\\ &+\frac{2k_{tc}\sum_{j=0}^{i}\sum_{m=1}^{n-1}[\cdot S_{n-m}\cdot^{(i-j)}][S_m\cdot^{(j)}]+k_{d2}\sum_{j=i+1}^{\infty}\sum_{m=n+1}^{\infty}\left(p_{mj}(n,i)j[S_m^{(j)}]+{p'}_{mj}(n,i)j[\mathrm{P}_m^{(j)}]\right)}{k_p[\mathrm{St}]+k_{fM}[\mathrm{St}]+k_{fG}[B*]+k_{tc}\left([R\cdot]+2[\cdot R\cdot]\right)+k''_{tc}[P_0\cdot]}\end{aligned} \tag{D.32}$$

Polystyrene species $(i=0,1,...;\ n=2,3,...)$

The mass balances for the PS species provide

$$\begin{aligned}\frac{d}{dt}\left([S_n{}^{(i)}]V\right)=&\,k_{fM}[\mathrm{St}][S_n\cdot^{(i)}]V+\frac{k_{tc}}{2}\sum_{j=0}^{i}\sum_{m=1}^{n-1}[S_{n-m}\cdot^{(i-j)}][S_m\cdot^{(j)}]V-i[S_n{}^{(i)}]V\\ &+(1-f_2)\,k_{d2}\sum_{j=i+1}^{\infty}\sum_{m=n+1}^{\infty}\left(p_{mj}(n,i)j[S_m^{(j)}]+{p'}_{mj}(n,i)j[\mathrm{P}_m^{(j)}]\right)V\end{aligned} \tag{D.33}$$

In order to account for the generation of monoradicals from random scission of the free PS or graft copolymer chains by sequential decomposition of peroxide groups within the chains, consider a PS chain with length n and i peroxide groups, all of which have the same thermal stability. Let m be a uniformly distributed random variable whose value ranges 1 from 1 to $n-1$. The polymer chain may form 2 monoradicals, one with

length m, and the other one with length $n-m$. These chains will have $i-j$ and $j-1$ undecomposed peroxide groups respectively. If the peroxide groups are assumed to be uniformly distributed within the polymer chains in the course of polymerization, the following relation must hold:

$$\frac{j-1}{n-m} = \frac{i-j}{m}$$

Therefore,

$$j = \left[\frac{i(n-m)+m}{n}\right]$$

where the brackets indicate the integer part of the expression.

The scission has then generated two monoradicals, one with length m and $i-j$ peroxide groups, the other one with length $n-m$ and $j-1$ peroxide groups.

Note that this chain scission algorithm can be modified for specific cases. For example, in the case of a linear bifunctional initiator, since all peroxide groups are located at a chain end, $m=1$ for every scission.

The Number Chain Length Distribution (NCLD) for the free PS species is

$$N_{\mathrm{PS}}^{(i)}(n) = [{S_n}^{(i)}]V \tag{D.34}$$

found by integrating Equation D.33 with Equations D.31 and D.32 using also Equation D.10 and D.11 for species $[\cdot {S_1}\cdot^{(i)}]$ and $[{S_1}\cdot^{(i)}]$. The concentration of the total PS species characterized by the number of undecomposed peroxide groups can be calculated with

$$[P^{(i)}] = \sum_{n=1}^{\infty} [{S_n}^{(i)}] \tag{D.35}$$

The NCLD for the total polymer can be calculated using

$$P_n = \sum_{i=0}^{\infty} [{S_n}^{(i)}]V \tag{D.36}$$

The total moles of PS are

$$N_{\mathrm{PS}} = \sum_{i=0}^{\infty}\sum_{n=1}^{\infty} N_{\mathrm{PS}}^{(i)}(n) \tag{D.37}$$

To obtain the corresponding Weight Chain Length Distribution (WCLD), multiply the NCLD by sM_{St} and replace n by s to obtain

$$G_{\mathrm{PS}}^{(i)}(s) = sM_{\mathrm{St}}[{S_s}^{(i)}]V \tag{D.38}$$

The mass of free PS can then be calculated as

$$G_{\mathrm{PS}} = \sum_{i=0}^{\infty}\sum_{s=1}^{\infty} G_{\mathrm{PS}}^{(i)}(s) \tag{D.39}$$

The average molecular weights can then be calculated from

$$\bar{M}_{n,\mathrm{PS}} = \frac{G_{\mathrm{PS}}}{N_{\mathrm{PS}}} = \frac{\sum_{i=0}^{\infty}\sum_{s=1}^{\infty} G_{\mathrm{PS}}^{(i)}(s)}{\sum_{i=0}^{\infty}\sum_{n=1}^{\infty}[{S_n}^{(i)}]V} \tag{D.40a}$$

$$\bar{M}_{w,\mathrm{PS}} = \frac{\sum_{i=0}^{\infty}\sum_{s=1}^{\infty} sG_{\mathrm{PS}}^{(i)}(s)}{G_{\mathrm{PS}}} = \frac{\sum_{i=0}^{\infty}\sum_{s=1}^{\infty} sG_{\mathrm{PS}}^{(i)}(s)}{\sum_{i=0}^{\infty}\sum_{s=1}^{\infty} G_{\mathrm{PS}}^{(i)}(s)} \tag{D.40b}$$

D.2.2 Residual PB

Let $N_{\mathrm{PB}}(b)$ denote the moles of PB with b units of B ($b \geq 1$). Consider only the reactions involving the unreacted PB and the reactions at each chain length b, $bN_{\mathrm{PB}}(b)$ is therefore the molar concentrations of $B*$ at each chain length. Assuming that the number of attacked $B*$ is proportional to the $B*$ contents of each chain length class, the fraction of $P_0\cdot$ radicals that are primary PB radicals of chain length b is therefore $bN_{\mathrm{PB}}(b)/[B*]$. Then, from the kinetic mechanism,

$$\frac{d}{dt}N_{\mathrm{PB}}(b) = -\left(k_{i2}\sum_{j=0}^{\phi-1}\left(2[\cdot I\cdot^{(j)}] + [I\cdot^{(j)}]\right) + k_{fG}\left([R\cdot] + 2[\cdot R\cdot]\right)\right) bN_{\mathrm{PB}}(b) + k'_{fM}[\mathrm{St}][P_0\cdot]\frac{bN_{\mathrm{PB}}(b)}{[B*]} \tag{D.41}$$

where $N_{\mathrm{PB}}(b)$ at $t = 0$ is *a priori* known from experimental data. The corresponding WCLD for the residual PB can be obtained from

$$G_{\mathrm{PB}}(b) = bM_B N_{\mathrm{PB}}(b) \tag{D.42}$$

The total moles and mass of residual PB are

$$N_{\mathrm{PB}} = \sum_{b=1}^{\infty} N_{\mathrm{PB}}(b) \tag{D.43}$$

$$G_{\mathrm{PB}} = \sum_{b=1}^{\infty} G_{\mathrm{PB}}(b) \tag{D.44}$$

Grafting efficiency and average number of St branches

The grafted St mass can be calculated from

$$G_{\mathrm{GS}} = M_{\mathrm{St}}[\mathrm{St}]_0 V_0 x - G_{\mathrm{PS}} \tag{D.45}$$

The St grafting efficiency is calculated from

$$E_{\mathrm{GS}} = \frac{G_{\mathrm{GS}}}{G_{\mathrm{PS}} + G_{\mathrm{GS}}} \tag{D.46}$$

The average number of St branches per reacted PB molecule is

$$J = \frac{G_{\mathrm{GS}} / \bar{M}_{n,\mathrm{PS}}}{N_{PB_0} - N_{\mathrm{PB}}} \tag{D.47}$$

Phase volumes

The volume of the individual phases, considered completely immiscible, is obtained from

$$V_{\mathrm{I}} = \frac{G_{PB} + G_{GS}}{\rho_{PB}} \tag{D.48a}$$

$$V_{\mathrm{II}} = \frac{M_{\mathrm{St}}[\mathrm{St}]\mathrm{V}_{\mathrm{II}}\rho_{\mathrm{St}} + \mathrm{G}_{\mathrm{PS}}}{\rho_{PS}} \tag{D.48b}$$

where ρ_k is the density of chemical species k.

D.2.3 Graft copolymer

The complete copolymer distribution, characterized by grafted St and B units in the copolymer and number of undecomposed peroxide groups, is derived from the detailed kinetic mechanism in Table for copolymer radicals and copolymer species. The following nomenclature was used:

$P^{(i)}(s,b)$	Copolymer with s styrene units, b butadiene units and i undecomposed peroxide groups in the grafted chains
$P_0\,.^{(i)}\,(s,b)$	Primary radical produced by attack to a butadiene repetitive unit (B) present in $P^{(i)}(s,b)$
$P_n\,.^{(i)}\,(s,b)$	Copolymer radical with i undecomposed peroxide groups, s styrene units, b butadiene units and n units of St in the active branch

Initiation$(\phi = 1,2,3; i < \phi; j = 0,1,...; s,b = 1,2,...)$

$$\cdot I.^{(i)} + P^{(j)}(s,b) \xrightarrow{2k_{i2}} P_0.^{(j)}(s,b) + I.^{(i)}$$
$$I.^{(i)} + P^{(j)}(s,b) \xrightarrow{k_{i2}} P_0.^{(j)}(s,b) + \bar{I}^{(i)}$$

Propagation $(n,s,b = 1,2,3...; i = 0,1,2...)$

$$P_0.^{(i)}(s,b) + \mathrm{St} \xrightarrow{k_p} P_1.^{(i)}(s,b)$$
$$P_n.^{(i)}(s,b) + \mathrm{St} \xrightarrow{k_p} P_{n+1}.^{(i)}(s,b)$$

Transfer to monomer $(n,s,b = 1,2,3...; i = 0,1,2...)$

$$P_0.^{(i)}(s,b) + \mathrm{St} \xrightarrow{k'_{fM}} P^{(i)}(s,b) + S_1.^{(0)}$$
$$P_n.^{(i)}(s-n,b) + \mathrm{St} \xrightarrow{k_{fM}} P^{(i)}(s,b) + S_1.^{(0)}$$

Transfer to rubber $(n,s,b,c,t = 1,2,3...; i,j = 0,1,2...)$

$$S_n.^{(i)} + P^{(j)}(s,b) \xrightarrow{k_{fG}} S_n{}^{(i)} + P_0.^{(j)}(s,b)$$
$$\cdot S_n.^{(i)} + P^{(j)}(s,b) \xrightarrow{2k_{fG}} S_n\,.^{(i)} + P_0.^{(j)}(s,b)$$
$$P_0.^{(i)}(s,b) + P^{(j)}(t,c) \xrightarrow{k_{fG}} P^{(i)}(s,b) + P_0.^{(j)}(t,c)$$
$$P_n.^{(i)}(s-n,b) + P^{(j)}(t,c) \xrightarrow{k_{fG}} P^{(i)}(s,b) + P_0.^{(j)}(t,c)$$

Re-initiation $(s,b = 1,2,3,...; n = 1,2,...,s-1; m = 1,2,...,n-1; i = 1,2...; j = 0,1,...,i-1)$

$$P^{(i)}(s,b) \xrightarrow{ik_{dp}} P_{n-m}.^{(i-j)}(s-n-m,b) + S_m{}^{(j-1)}\,.$$

Combination termination $(n,m,s,b,c,t = 1,2,3...; i,j = 0,1,2...)$

$$P_0.^{(i-j)}(s-t,b-c) + P_0.^{(j)}(t,c) \xrightarrow{k'_{tc}} P^{(i)}(s,b)$$
$$P_0.^{(i-j)}(s-t-m,b) + P_m.^{(j)}(t,c) \xrightarrow{k'_{tc}} P^{(i)}(s,b)$$
$$P_n.^{(i-j)}(s-n-m-t,b-c) + P_m.^{(j)}(t,c) \xrightarrow{k'_{tc}} P^{(i)}(s,b)$$
$$P_0.^{(i-j)}(s,b) + \cdot S_m.^{(j)} \xrightarrow{2k''_{tc}} P_m.^{(i)}(s,b)$$
$$P_n.^{(i-j)}(s,b) + \cdot S_m.^{(j)} \xrightarrow{2k''_{tc}} P_{n+m}.^{(i)}(s,b)$$
$$P_0.^{(i-j)}(s-m,b) + S_m.^{(j)} \xrightarrow{k''_{tc}} P^{(i)}(s,b)$$
$$P_n.^{(i-j)}(s-n-m,b) + S_m.^{(j)} \xrightarrow{k''_{tc}} P^{(i)}(s,b)$$

TABLE D.1: Detailed kinetic mechanism for graft copolymer bivariate distribution.

Copolymer radicals

For deriving the equations, it was considered that $[B*^{(i)}(s,b)] \approx b[P^{(i)}(s,b)]$. From the detailed kinetic mechanism of Table and using the pseudosteady-state hypothesis,

$$\left(k_{i2} \sum_{j=0}^{\phi-1} \left(2[\cdot I^{(j)} \cdot] + [I^{(j)} \cdot] \right) + k_{fG} \left([R\cdot] + 2[\cdot R\cdot] \right) \right) b[P^{(i)}(s,b)]$$
$$- \left(k_{i1}[\mathrm{St}] + k'_{fM}[\mathrm{St}] + k'_{tc}[P_0\cdot] + k''_{tc} \left([R\cdot] + 2[\cdot R\cdot] \right) \right) [P_0\cdot^{(i)}(s,b)] = 0 \quad \text{(D.49)}$$

$$k_{i1}[\mathrm{St}][P_0\cdot^{(i)}(s,b)] + 2k''_{tc} \sum_{j=0}^{i} [P_0\cdot^{(i-j)}(s,b)][\cdot S_1{}^{(j)} \cdot]$$
$$- \left(k_p[\mathrm{St}] + k_{fM}[\mathrm{St}] + k_{fG}[B*] + k'_{tc}[P_0\cdot] + k''_{tc} \left([R\cdot] + 2[\cdot R\cdot] \right) \right) [P_1\cdot^{(i)}(s,b)]V = 0 \quad \text{(D.50)}$$

$$k_p[\mathrm{St}][P_{n-1}\cdot^{(i)}(s,b)] + f_2 k_{d2} \sum_{j=i+1}^{\infty} \sum_{m=n+1}^{\infty} \sum_{t=s+1}^{\infty} \sum_{c=b}^{\infty} p''_{mjtc}(n,i,s,b) j [P_m^{(j)}(t,c)]$$
$$+ 2k''_{tc} \sum_{j=0}^{i} \sum_{m=1}^{n-1} [P_{n-m}\cdot^{(i-j)}(s,b)][\cdot S_m\cdot^{(j)}]V + 2k''_{tc} \sum_{j=0}^{i} [P_0\cdot^{(i-j)}(s,b)][\cdot S_n\cdot^{(j)}]$$
$$- \left(k_p[St] + k_{fM}[St] + k_{fG}[B*] + k'_{tc}[P_0\cdot] + k''_{tc} \left([R\cdot] + 2[\cdot R\cdot] \right) \right) [P_n\cdot^{(i)}(s,b)] = 0 \quad \text{(D.51)}$$

In Equation D.51, $p''_{mjtc}(n,i,s,b)$ is the probability that a scission of a temporarily dead PS chain from $P^{(j)}(t,c)$ having m repetitive units of St and j peroxide groups yields a growing PS monoradical of chain length n with i peroxide groups, with the resulting copolymer radical having s units of St and b units of B.

Copolymer bivariate distribution

$$\begin{aligned}
\frac{d}{dt}\Big([P^{(i)}(s,b)]V\Big) = &-k_{i2}\sum_{j=0}^{\phi-1}\Big(2[\cdot I^{(j)}\cdot] + [I^{(j)}\cdot]\Big)b[P^{(i)}(s,b)]V \\
&- k_{fG}\left([R\cdot] + 2[\cdot R\cdot] + [P_0\cdot]\right)b[P^{(i)}(s,b)]V - ik_{d2}f_2[P^{(i)}(s,b)]V \\
&+ (1-f_2)k_{d2}\sum_{j=i+1}^{\infty}\sum_{t=s+1}^{\infty}{p'}_{jt}(i,s)j[P^{(j)}(t,b)]V \\
&+ k_{fG}[B*]\sum_{n=1}^{s}[P_n^{(i)}\cdot(s-n,b)]V + k_{fG}[B*][P_0^{(i)}\cdot(s,b)]V \\
&+ k_{fM}[\mathrm{St}]\sum_{n=1}^{s}[P_n^{(i)}\cdot(s-n,b)]V + k_{fM}[\mathrm{St}][P_0^{(i)}\cdot(s,b)]V \\
&+ \frac{1}{2}{k'}_{tc}\sum_{j=0}^{i}\sum_{t=0}^{s}\sum_{c=1}^{b-1}[P_0^{(i-j)}\cdot(s-t,b-c)][P_0^{(j)}\cdot(t,c)]V \\
&+ {k'}_{tc}\sum_{j=0}^{i}\sum_{t=0}^{s-1}\sum_{m=1}^{s-t}\sum_{c=1}^{b-1}[P_0^{(i-j)}\cdot(s-t-m,b-c)][P_m^{(j)}\cdot(t,c)]V \\
&+ \frac{1}{2}{k'}_{tc}\sum_{j=0}^{i}\sum_{n=1}^{s-t-m}\sum_{m=1}^{s-t}\sum_{t=0}^{s-1}\sum_{c=1}^{b-1}[P_n^{(i-j)}\cdot(s-t-m-n,b-c)][P_m^{(j)}\cdot(t,c)]V \\
&+{k''}_{tc}\sum_{j=0}^{i}\sum_{n=1}^{s}[P_0^{(i-j)}\cdot(s-n,b)][S_n^{(j)}\cdot]V + {k''}_{tc}\sum_{j=0}^{i}\sum_{n=1}^{s-m}\sum_{m=1}^{s-1}[P_m^{(i-j)}\cdot(s-n-m,b)][S_n^{(j)}\cdot]V
\end{aligned} \tag{D.52}$$

The total copolymer NCLD can be obtained from

$$N(s,b) = \sum_{i=0}^{\infty}P^{(i)}(s,b)V \tag{D.53}$$

and the corresponding WCLD from

$$G(s,b) = (sM_{\mathrm{St}} + bM_{\mathrm{B}})N(s,b) \tag{D.54}$$

Copolymer average composition and molecular weights

The average chemical composition of the graft copolymer is estimated with the mass fraction of St

$$\bar{\omega}_{\mathrm{St}} = \frac{\sum_{i=0}^{\infty}\sum_{s=1}^{\infty}\sum_{b=1}^{\infty}[P^{(i)}(s,b)]sM_{\mathrm{St}}}{\sum_{i=0}^{\infty}\sum_{s=1}^{\infty}\sum_{b=1}^{\infty}[P^{(i)}(s,b)](sM_{\mathrm{St}} + bM_{\mathrm{Bd}})} \tag{D.55}$$

The copolymer average molecular weights are calculated with

$$\bar{M}_{n,\mathrm{C}} = \frac{\sum_{i=0}^{\infty}\sum_{b=1}^{\infty}\sum_{s=1}^{\infty}[P^{(i)}(s,b)](sM_{\mathrm{St}} + bM_{\mathrm{B}})}{\sum_{i=0}^{\infty}\sum_{b=1}^{\infty}\sum_{s=1}^{\infty}[P^{(i)}(s,b)]} \tag{D.56a}$$

$$\bar{M}_{w,\mathrm{C}} = \frac{\sum_{i=0}^{\infty}\sum_{b=1}^{\infty}\sum_{s=1}^{\infty}[P^{(i)}(s,b)](sM_{\mathrm{St}} + bM_{\mathrm{B}})^2}{\sum_{i=0}^{\infty}\sum_{b=1}^{\infty}\sum_{s=1}^{\infty}[P^{(i)}(s,b)](sM_{\mathrm{St}} + bM_{\mathrm{B}})} \tag{D.56b}$$

D.3 Melt flow index module

The Melt Flow Index (MFI) is the mass flow rate, in units of g/10 min, of a HIPS melt that flows through a plastometer capillary when forced by a piston loaded with constant weight. The polymer accumulates in a barrel, prior to entering the capillary. Between the barrel and the capillary there is an abrupt contraction or "entrance" zone. First, the apparent shear viscosity $\eta(\dot{\gamma})$ is related to the apparent shear rate $\dot{\gamma}$ by means of a three-parameter Carreau expression [120, 121].

$$\eta(\dot{\gamma}) = \frac{\eta_0}{\left[1 + (\tau_r\dot{\gamma})^2\right]^{n'/2}} \tag{D.57}$$

where η_0 is the zero-shear viscosity, τ_r the relaxation time and n' is a rheological parameter [122]. The relaxation time of the polymer is calculated as:

$$\tau_r = \frac{6\eta_{0,P}\bar{M}_{w,\mathrm{PS}}}{\pi^2\rho RT} \tag{D.58}$$

For $\eta_{0,P}$, the polymer shear-viscosity, the following expression is used

$$\eta_{0,\mathrm{P}} = \eta_{0,\mathrm{PS}} e^{\frac{A\phi_D}{1-B\phi_D}} \tag{D.59}$$

where $\eta_{0,\mathrm{PS}}$ is the zero-shear viscosity of the free PS, A and B are constants taken from the literature [115] and ϕ_D is the volume fraction of the dispersed phase, which is estimated as $\phi_D \approx \phi_R$ where ϕ_R is the total rubber in the final product, calculated as

$$\phi_R = \frac{\sum_{i=\mathrm{PB,GC}} G_i/\rho_i}{\sum_{i=\mathrm{PS,PB,GC}} G_i/\rho_i} \tag{D.60}$$

This approximation estimates ϕ_D by defect, since ϕ_R does not include the occluded PS contained in the rubber particles [57]. Finally, $\eta_{0,\mathrm{PS}}$ is estimated from

$$\ln \eta_{0,\mathrm{PS}} = -20.95 + 3.4 \ln \left(\frac{\bar{M}_{w,\mathrm{PS}}}{33000} \right) + \frac{11000}{T} \tag{D.61}$$

The MFI is estimated using the model proposed by Seavey et al. [98]. The model assumes: a) steady-state flow; b) zero velocity at the capillary wall; and c) the elongational viscosity can be estimated using Trouton's ratio. While assumption b) is valid for homogeneous systems [120], it is extended here to an heterogeneous one. The following nomenclature was used:

R_b	Barrel radius
L_b	Barrel length
R_c	Capillary radius
L_c	Capillary length
R_p	Piston radius
ΔP_b	Pressure drop in the barrel
ΔP_c	Pressure drop in the capillary
ΔP_e	Pressure drop in the entrance zone
m	Piston weight
g	Acceleration of gravity
$\dot{\gamma}_{R_b}$	Shear rate at the barrel wall
$\dot{\gamma}_{R_c}$	Shear rate at the capillary wall
$\dot{\epsilon}_a$	Apparent elongational rate in the capillary
η_{R_b}	Apparent viscosity at the barrel wall
η_{R_c}	Apparent viscosity at the capillary wall
η_{e_c}	Apparent elongational viscosity in the capillary

The MFI is calculated as

$$\mathrm{MFI} = \rho \dot{Q} \tag{D.62}$$

where $\dot{Q}$ is the volumetric flow rate through the plastometer, and ρ is the density of the final HIPS, calculated as

$$\rho = \sum_{i=\mathrm{PS,PB,GC}} \omega_i \rho_i \tag{D.63}$$

where the ω_i are the mass fractions of the different polymer species. The volumetric flow $\dot{Q}$ is calculated from the relation between η and $\cdot\gamma$ given by Equation and the following mass and momentum balances in the plastometer [98, 123]:

$$\dot{Q} = \frac{\pi R_b^3 \dot{\gamma}_{R_b}}{3} - \frac{\pi}{3}\left(\frac{2L_b}{\Delta P_b}\right)^3 \int_0^{\dot{\gamma}_{R_b}} [\eta(\dot{\gamma})\dot{\gamma}]^3 d\dot{\gamma} \tag{D.64}$$

$$\dot{Q} = \frac{\pi R_c^3 \dot{\gamma}_{R_c}}{3} - \frac{\pi}{3}\left(\frac{2L_c}{\Delta P_c}\right)^3 \int_0^{\dot{\gamma}_{R_c}} [\eta(\dot{\gamma})\dot{\gamma}]^3 d\dot{\gamma} \tag{D.65}$$

$$\dot{\gamma}_{R_b}\eta_{R_b} = \frac{\Delta P_b R_b}{2L_b} \tag{D.66}$$

$$\dot{\gamma}_{R_c}\eta_{R_c} = \frac{\Delta P_c R_c}{2L_c} \tag{D.67}$$

The total pressure drop is given by

$$\Delta P_b + \Delta P_e + \Delta P_c = \frac{mg}{\pi R_p^2} \tag{D.68}$$

where ΔP_e is estimated as in the work of Rohlfing and Janzen [123]:

$$\Delta P_e = \frac{4\sqrt{2}\dot{\gamma}_a}{3(n'+1)}\left(\frac{4n'}{3n'+1}\right)^{(1+n'/2)} \sqrt{\eta_{a,c}\eta_{e,c}} \tag{D.69}$$

The expressions for $\dot{\gamma}_a$ and $\dot{\epsilon}_a$ are

$$\dot{\gamma}_a = \left(\frac{4}{3+1/n'}\right)\dot{\gamma}_{R_c} \tag{D.70}$$

$$\dot{\epsilon}_a = \frac{4\eta_{a,c}\dot{\gamma}_a}{3(n'+1)\Delta P_e}\left(\frac{4n'}{3n'+1}\right)^{n'+1} \tag{D.71}$$

where the Trouton ratio is used to relate the elongational viscosity to the shear viscosity

$$\eta_e(\dot{\epsilon}) = 3\eta(\dot{\gamma}) \tag{D.72}$$

with $\dot{\gamma} = \epsilon_a$ [98].

The values for the numerical parameters related to plastometer geometry are: $R_b = 4.78$ mm, $R_c = 1.05$ mm, $R_p = 4.74$ mm, $L_b = 46$ mm, $L_c = 8$ mm, $m = 5$ kg and $g = 9,81$ m/s^2 with an essay temperature of $T = 200$ °C. Equations D.64 to D.71 are simultaneously solved in order to evaluate the MFI with Equation D.62.

Bibliography

[1] R.E. Kirk, D.F. Othmer, J.I. Kroschwitz, and M. Howe-Grant. *Kirk-Othmer Encyclopedia of Chemical Technology, Pigments to Powders, Handling*. Encyclopedia of Chemical Technology. Wiley, 1996. ISBN 9780471526889.

[2] J. Scheirs and D. Priddy. *Modern styrenic polymers: Polystyrenes and Styrenic Copolymers*. 2003. ISBN 978-0-471-49752-3. doi: 10.1002/0470867213.

[3] Merchant Research and Consulting Ltd. Styrene: 2015 World Market Outlook and Forecast up to 2019. 2015.

[4] U.S. Department of Energy. SBIR Advances: New Process for Producing Styrene Cuts Costs , Saves Energy , and Reduces Greenhouse Gas Emissions. 2012.

[5] Ceresana. Market Study: Styrene. 2013. URL http://www.ceresana.com/en/Market-Studies/Chemicals/Styrene.

[6] J. Maul, B. G. Frushour, J. R. Kontoff, H. E., K.H. Ott, and C. Schade. Polystyrene and Styrene Copolymers. In *Ullmann's Encyclopedia of Industrial Chemistry*, pages 475–522. Wiley-VCH Verlag GmbH & Co. KGaA, Weinheim, Germany, July 2007. ISBN 9783527306732. doi: 10.1002/14356007.a21_615.pub2. URL http://doi.wiley.com/10.1002/14356007.a21_615.pub2.

[7] A. Rudin. *The Elements of Polymer Science and Engineering*. 3 edition, 2012. ISBN 978-0-12-382178-2.

[8] H. Weber, I. De Grave, and E. Röhrl. Foamed Plastics. In *Ullmann's Encyclopedia of Industrial Chemistry*, pages 73–198. Wiley-VCH Verlag GmbH & Co. KGaA, Weinheim, Germany, June 2000. ISBN 3527306730, 9783527306732. doi: 10.1002/14356007.a11_435. URL http://doi.wiley.com/10.1002/14356007.a11_435.

[9] J. Edenbaum. *Plastics additives and modifiers handbook*. Van Nostrand Reinhold, 1992. ISBN 9780442234508.

[10] C. V. Luciani. *Poliestireno de Alto Impacto. Modelado matemático del proceso productivo, predicción de la estructura molecular, la morfología, y las propiedades finales*. PhD thesis, Universidad Nacional del Litoral, 2006.

[11] D. A. Estenoz and G. R. Meira. Mathematical model of a continuous industrial high-impact polystyrene process. *AIChE Journal*, 44(2):427–441, February 1998. ISSN 00011541. doi: 10.1002/aic.690440219. URL http://doi.wiley.com/10.1002/aic.690440219.

[12] G. Soto, E. Nava, M. Rosas, M. Fuenmayor, I. M. Gonza, G. R. Meira, and H. M. Oliva. Bulk Polymerization of Styrene in the Presence of Polybutadiene : Effect of Initiator Type and Prepolymerization Conditions on Particle Morphology. *Journal of Applied Polymer Science*, 91:1397–1412, 2004.

[13] G.; Acuña P.; Olivo J. ; Ramos-DeValle L.F. Diaz de Leon, R.; Morales. Mechanical behavior of high impact polystyrene based on sbr copolymers: Part i. *Polymer Engineering & Science*, 45(9):1288–1296, 2005. ISSN 1548-2634. doi: 10.1002/pen.20404. URL http://dx.doi.org/10.1002/pen.20404.

[14] A. Echte. *Rubber-Toughened Styrene Polymers*, chapter 3, pages 15–64. doi: 10.1021/ba-1989-0222.ch002. URL http://pubs.acs.org/doi/abs/10.1021/ba-1989-0222.ch002.

[15] Ceresana. Market Study: Engineering Plastics. 2013. URL http://www.ceresana.com/en/market-studies/plastics/engineering-plastics/.

[16] J. M. Asua, editor. *Polymer Reaction Engineering*. Blackwell Publishing Ltd, Oxford, UK, January 2007. ISBN 9780470692134. doi: 10.1002/9780470692134. URL http://doi.wiley.com/10.1002/9780470692134.

[17] A. W. Hui and A. E. Hamielec. Thermal Polymerization of Styrene at High Conversion and Temperatures. An Experimental Study. *Journal of Applied Polymer Science*, 16(3):749–769, 1972.

[18] S. Zhu and A. E. Hamielec. Polymerization Kinetic Modeling and Macromolecular Reaction Engineering. In *Polymer Science: A Comprehensive Reference*, volume 4, pages 779–831. Elsevier B.V., 2012. ISBN 9780444533494. doi: 10.1016/B978-0-444-53349-4.00127-8. URL http://dx.doi.org/10.1016/B978-0-444-53349-4.00127-8.

[19] T. Meyer and J. Keurentjes, editors. *Handbook of Polymer Reaction Engineering*. Wiley, 2005. ISBN 3-527-31014-2.

[20] C. Kotoulas and C. Kiparissides. A generalized population balance model for the prediction of particle size distribution in suspension polymerization reactors. *Chemical Engineering Science*, 61(2):332–346, January 2006. ISSN 00092509. doi: 10.1016/j.ces.2005.07.013. URL http://linkinghub.elsevier.com/retrieve/pii/S0009250905006202.

[21] G. Odian. *Principles of Polymerization*. 2004. ISBN 9780470754368.

[22] G. Moad and D. Solomon. *The Chemistry of Radical Polymerization*. Elsevier Science, 2 edition, 2006. ISBN 9780080442860.

[23] W. A. Pryor and L. D. Lasswell. An excellent review on the subject of spontaneous polymerization of styrene. *Advanced Free Radical Chemistry*, 5:27–99, 1975.

[24] K. S. Khuong, W. H. Jones, W. A Pryor, and K. N. Houk. The mechanism of the self-initiated thermal polymerization of styrene. Theoretical solution of a classic problem. *Journal of the American Chemical Society*, 127(4):1265–77, February 2005. ISSN 0002-7863. doi: 10.1021/ja0448667. URL http://www.ncbi.nlm.nih.gov/pubmed/15669866.

[25] Jorge R. Cerna Cortez. *Uso de peróxidos cíclicos multifuncionales como iniciadores de la polimerización*. Tesis de doctorado, Centro de Investigación en Química Aplicada, 2002.

[26] A. E. Hamielec and H. Tobita. Polymerization Processes, 1. Fundamentals. In *Ullmann's Encyclopedia of Industrial Chemistry*, pages 317–388. Wiley-VCH Verlag GmbH & Co. KGaA, Weinheim, Germany, October 2011. ISBN 9783527306732. doi: 10.1002/14356007.a21_305.pub2. URL http://doi.wiley.com/10.1002/14356007.a21_305.pub2.

[27] Carbon-carbon bond-type macromolecular radical initiator and preparation method thereof, July 8 2015. URL https://www.google.ch/patents/CN103342765B?cl=en. CN Patent 103,342,765.

[28] J.M. Sosa and C. Chevillard. Use of accelerators in free-radical polymerizations of styrene, August 3 2004. URL http://www.google.com/patents/US6770716. US Patent 6,770,716.

[29] D. Bertin, B. Boutevin, and M. Destarac. Fabrication process for copolymers of controlled architecture via the use of functional radical initiators in a living radical polymerisation, and initiator compositions and corresponding copolymers, April 28 1999. URL https://www.google.ch/patents/EP0911350A1?cl=en. EP Patent App. EP19,980,402,624.

[30] R.A. Koster, D.B. Priddy, and I. Li. Difunctional living free radical polymerization initiators, October 14 1997. URL https://www.google.ch/patents/US5677388. US Patent 5,677,388.

[31] R. Seltzer, R.A.E. Winter, and P.J. Schirmann. Peroxide free radical initiators containing hindered amine moieties with low basicity, August 18 1992. URL https://www.google.ch/patents/US5140081. US Patent 5,140,081.

[32] W.H. Tong and D.B. Priddy. Multifunctional cyclobutarene peroxide polymerization initiators, January 7 1992. URL http://www.google.ch/patents/US5079322. US Patent 5,079,322.

[33] C.S. Sheppard and R.E. MacLeay. Peroxide free radical initiators containing ultraviolet light stabilizing groups, December 12 1978. URL http://www.google.ch/patents/US4129586. US Patent 4,129,586.

[34] Organic Peroxide Market by Type, Applications & Geography - Global Industry Trends & Forecasts to 2020. Technical report, Markets and Markets, 2015. URL http://www.researchandmarkets.com/research/ll67hm/organic_peroxide.

[35] R.E. Drumright, P. E. Kastl, and D. B Priddy. Cycloalkane perketal initiators for styrene polymerization. 1. Decomposition chemistry of 1,1-bis(tert-butylperoxy)cyclohexane. *Macromolecules*, 26(9):2246–2252, 1993. URL http://pubs.acs.org/doi/abs/10.1021/ma00061a017.

[36] A. V. Castañeda Facio. *Estudio de la Descomposición Térmica del Diperóxido de Pinacolona: Formación de Oligómeros y Polímeros a base de Estireno con estructura definida*. PhD thesis, Instituto Teconlógico de la Laguna, 2007.

[37] C. Volga, B. Hazer, and O. Torul. Kinetic study of vinyl polymerization with a new oligo azo peroxidic initiator. *European polymer journal*, 33(6):907–912, 1997. URL http://www.sciencedirect.com/science/article/pii/S0014305796001814.

[38] Ba. Pabin-szafko, E. Wisniewska, B. Hefczyc, and J. Zawadiak. New Azo-Peroxidic Initiators in the Radical Polymerization of Styrene and Methyl mMethacrylate. *European Polymer Journal*, 45(5):1476–1484, 2009. ISSN 0014-3057. doi: 10.1016/j.eurpolymj.2009.02.001. URL http://dx.doi.org/10.1016/j.eurpolymj.2009.02.001.

[39] M. A. Villalobos, A. E. Hamielec, and P. E. Wood. Kinetic Model for Short-Cycle Bulk Styrene Polymerization through Bifunctional Initiators. *Journal of Applied Polymer Science*, 42:629–641, 1991.

[40] K. Shanmugananda Murthy, K. Kishore, and V. Krishna Mohan. Vinyl Monomer Based Polyperoxides as Potential Initiators for Radical Polymerization: An Exploratory Investigation with Poly(.alpha.-methylstyrene peroxide). *Macromolecules*, 27(24):7109–7114, November 1994. ISSN 0024-9297. doi: 10.1021/ma00102a017. URL http://pubs.acs.org/doi/abs/10.1021/ma00102a017.

[41] D. A. Estenoz, G. R. Leal, Y. R. Lopez, Ha. M. Oliva, and G. R. Meira. Bulk polymerization of styrene in the presence of polybutadiene. The use of bifunctional initiators. *Journal of Applied Polymer Science*, 62(6):917–939, November 1996. ISSN 00218995. doi: 10.1002/(SICI)1097-4628(19961107)62:6⟨917::AID-APP8⟩3.3.CO;2-W. URL http://doi.wiley.com/10.1002/(SICI)1097-4628(19961107)62:6<917::AID-APP8>3.3.CO;2-W.

[42] W. Sheng, J. Wu, G. Shan, Z. Huang, and Z. Weng. Free-radical bulk polymerization of styrene with a new trifunctional cyclic peroxide initiator. *Journal of Applied Polymer Science*, 94(3):1035–1042, November 2004. ISSN 0021-8995. doi: 10.1002/app.20937. URL http://doi.wiley.com/10.1002/app.20937.

[43] L. Cavin, A. Rouge, T. Meyer, and A. Renken. Kinetic modeling of free radical polymerization of styrene initiated by the bifunctional initiator 2,5-dimethyl-2,5-bis (2-ethyl hexanoyl peroxy)hexane. *Polymer*, 41:3925–3935, 2000.

[44] I. Piirma and L. H. Chou. Block copolymers obtained by free-radical mechanism. I. Methyl methacrylate and styrene. *Journal of Applied Polymer Science*, 24(9): 2051–2070, November 1979. ISSN 00218995. doi: 10.1002/app.1979.070240913. URL http://doi.wiley.com/10.1002/app.1979.070240913.

[45] B. Z. Gunesin and I. Piirma. Block copolymers obtained by free radical mechanism. II. Butyl acrylate and methyl methacrylate. *Journal of Applied Polymer Science*, 26:3103–3115, 1981. URL http://onlinelibrary.wiley.com/doi/10.1002/app.1981.070260924/abstract.

[46] A. I. Prisyazhnyuk and S. S. Ivanchev. Diperoxides with differing thermal stabilities of the peroxide groups as initiators of radical polymerization and block copolymerization. *Polymer Science USSR*, (2):450–458, 1970. URL http://www.sciencedirect.com/science/article/pii/003239507090167X.

[47] N. S. Tsvetkov and R. F. Markovskaya. Polyfunctional initiators of radical polymerization and the molecular weight distribution of polymers. *Polymer Science USSR*, (9):1936–1939, 1974. URL http://www.sciencedirect.com/science/article/pii/0032395074902226.

[48] Y. L. Zherebin, S. S. Ivanchev, and N. M. Domareva. Preparation of block copolymers using oligoperoxide initiators containing peroxide groups of different heat stabilities. *Polymer Science USSR*, (4):893–901, 1974. URL http://www.sciencedirect.com/science/article/pii/0032395074902159.

[49] J. Brandrup, E. H. Immergut, and E. A. Grulke, editors. *Polymer Handbook*. Wiley, 4 edition, 2003. ISBN 97804714793-9.

[50] G. R. Meira, C. V. Luciani, and D. A. Estenoz. Continuous Bulk Process for the Production of High-Impact Polystyrene: Recent Developments in Modeling and Control. *Macromolecular Reaction Engineering*, 1(1):25–39, January 2007. ISSN 1862832X. doi: 10.1002/mren.200600010. URL http://doi.wiley.com/10.1002/mren.200600010.

[51] A. Penlidis, S.R. Ponnuswamy, C. Kiparissides, and K.F. O'Driscoll. Polymer reaction engineering: Modelling considerations for control studies. *The Chemical Engineering Journal*, 50(2):95–107, 1992. ISSN 03009467. doi: 10.1016/0300-9467(92)80013-Z.

[52] C. Kiparissides. Polymerization reactor modeling: a review of recent developments and future directions. *Chemical Engineering Science*, 51(10):1637–1659, 1996. URL http://www.sciencedirect.com/science/article/pii/0009250996000243.

[53] W. J. Yoon, Y. S. Kim, I. S. Kim, and K. Y. Choi. Recent advances in polymer reaction engineering: Modeling and control of polymer properties. *Korean Journal of Chemical Engineering*, 21(1):147–167, 2004. ISSN 0256-1115. doi: 10.1007/BF02705393.

[54] C. Kiparissides. Challenges in particulate polymerization reactor modeling and optimization: A population balance perspective. *Journal of Process Control*, 16(3):205–224, March 2006. ISSN 09591524. doi: 10.1016/j.jprocont.2005.06.004. URL http://linkinghub.elsevier.com/retrieve/pii/S0959152405000624.

[55] I. L. Gamba, S. Marquez Damian, D. A. Estenoz, N. Nigro, M. A. Storti, and D. Knoeppel. Residence Time Distribution Determination of a Continuous Stirred Tank Reactor using Computational Fluid Dynamics and its Application on the Mathematical Modeling of Styrene Polymerization. *International Journal of Chemical Reactor Engineering*, 10(1), January 2012. ISSN 1542-6580. doi: 10.1515/1542-6580.3057. URL http://www.degruyter.com/view/j/ijcre.2012.10.issue-1/1542-6580.3057/1542-6580.3057.xml.

[56] J. R. Vega, L. M. Gugliotta, and Gregorio R. M. Continuous Emulsion Polymerization of Styrene and Butadiene. Reduction of Off-Spec Product between Steady-States. *Latin American Applied Research*, 25:77–82, 1995.

[57] V. Luciani, C, D. A. Estenoz, R. Meira, G, and H. M. Oliva. Reduction of Transients between Steady States in the Continuous Production of High-Impact Polystyrene. *Industrial & Engineering Chemistry Research*, 44(22):8354–8367, October 2005. ISSN 0888-5885. doi: 10.1021/ie050657z. URL http://pubs.acs.org/doi/abs/10.1021/ie050657z.

[58] A. Flores-Tlacuahuac, L. T. Biegler, and E. Saldívar-Guerra. Dynamic Optimization of HIPS Open-Loop Unstable Polymerization Reactors. *Industrial & Engineering Chemistry Research*, 44(8):2659–2674, April 2005. ISSN 0888-5885. doi: 10.1021/ie049534p. URL http://pubs.acs.org/doi/abs/10.1021/ie049534p.

[59] D. S. Achilias and C. Kiparissides. Development of a general mathematical framework for modeling diffusion-controlled free-radical polymerization reactions. *Macromolecules*, pages 3739–3750, 1992. URL http://pubs.acs.org/doi/abs/10.1021/ma00040a021.

[60] D. S. Achilias and G. D. Verros. Modeling of diffusion-controlled reactions in free radical solution and bulk polymerization: Model validation by DSC experiments. *Journal of Applied Polymer Science*, 2010. doi: 10.1002/app. URL http://onlinelibrary.wiley.com/doi/10.1002/app.31675/full.

[61] J. H. Duerksen, A. E. Hamielec, and J. W. Hodgins. Polymer reactors and molecular weight distribution: Part I. Free radical polymerization in a continuous stirred-tank reactor. *AIChE Journal*, 13(6):1081–1086, 1967. URL http://onlinelibrary.wiley.com/doi/10.1002/aic.690130609/abstract.

[62] A. E. Hamielec, J. W. Hodgins, and K. Tebbens. Polymer reactors and molecular weight distribution: Part II. Free radical polymerization in a batch reactor. *AIChE Journal*, 13(6):1087–1091, 1967. URL http://onlinelibrary.wiley.com/doi/10.1002/aic.690130610/abstract.

[63] A. Husain and A. E. Hamielec. Thermal Polymerization of Styrene. *Journal of Applied Polymer Science*, 22(5):1207–1223, 1978.

[64] F. López-Serrano, J. E. Puig, and J. Alvarez. On the modeling assessment of thermal styrene polymerization. *AIChE Journal*, 50(9):2246–2257, September 2004. ISSN 0001-1541. doi: 10.1002/aic.10239. URL http://doi.wiley.com/10.1002/aic.10239.

[65] W. J. Yoon and K. Y. Choi. Free-Radical Polymerization of Styrene with a Binary Mixture of Symmetrical Bifunctional Initiators. *Journal of applied polymer science*, 46:1353–1367, 1992. URL http://onlinelibrary.wiley.com/doi/10.1002/app.1992.070460804/abstract.

[66] K. J. Kim, W. Liang, and K. Y. Choi. Bulk free radical polymerization of styrene with unsymmetrical bifunctional initiators. *Industrial & engineering chemistry ...*, 0(I):131–138, 1989. URL http://pubs.acs.org/doi/abs/10.1021/ie00086a001.

[67] K. Y. Choi, W. R. Liang, and G. D. Lei. Kinetics of bulk styrene polymerization catalyzed by symmetrical bifunctional initiators. *Journal of Applied Polymer Science*, 35(6):1547–1562, May 1988. ISSN 00218995. doi: 10.1002/app.1988.070350612. URL http://doi.wiley.com/10.1002/app.1988.070350612.

[68] K. J. Kim and K. Y. Choi. Modeling of free radical polymerization of styrene catalyzed by unsymmetrical bifunctional initiators. *Chemical engineering science*, 44(2):297–312, 1989. URL http://www.sciencedirect.com/science/article/pii/0009250989850663.

[69] K. Y. Choi and G. D. Lei. Modeling of free-radical polymerization of styrene by bifunctional initiators. *AIChE Journal*, 33(12):2067–2076, 1987. URL http://onlinelibrary.wiley.com/doi/10.1002/aic.690331217/abstract.

[70] I. M. Gonzalez, G. R. Meira, and H. M. Oliva. Synthesis of Polystyrene with Mixtures of Mono- and Bifunctional Initiators. *Journal of Applied Polymer Science*, 59(3000):1015–1026, 1996.

[71] K. J. Kim and K. Y. Choi. Steady state behavior of a continuous stirred tank reactor for styrene polymerization with bifunctional free radical initiators. *Chemical engineering science*, 43(4):965–977, 1988. URL http://www.sciencedirect.com/science/article/pii/0009250988800927.

[72] M. Benbachir and D. Benjelloun. Investigation of free radical polymerization using diperoxyesters as bifunctional initiators. *Polymer*, 42:7727–7738, 2001.

[73] M. Asteasuain, A. Brandolin, and C. Sarmoria. Molecular weight distributions in styrene polymerization with asymmetric bifunctional initiators. *Polymer*, 45(1): 321–335, January 2004. ISSN 00323861. doi: 10.1016/j.polymer.2003.10.083. URL http://linkinghub.elsevier.com/retrieve/pii/S0032386103010164.

[74] M. J Scorah. *Experimental and modeling investigation of a novel tetrafunctional initiator in free radical polymerization*. Doctoral thesis, University of Waterloo, 2005.

[75] M. J. Scorah, R. Dhib, and A. Penlidis. Modelling of free radical polymerization of styrene and methyl methacrylate by a tetrafunctional initiator. *Chemical Engineering Science*, 61(15):4827–4859, August 2006. ISSN 00092509. doi: 10.1016/j.ces.2006.03.018. URL http://linkinghub.elsevier.com/retrieve/pii/S000925090600162X.

[76] P. Acuña, G. Morales, and R. Díaz de León. Synthesis and Characterization of High-Impact Polystyrene Using a Multifunctional Cyclic Peroxide as the Initiator. *Journal of Applied Polymer Science*, 114:3198–3210, 2009. doi: 10.1002/app.

[77] E. Galhardo, P. Magalhães Bonassi Machado, and L. M. Ferrareso Lona. Living free radical polymerization using cyclic trifunctional initiator. *Journal of Applied Polymer Science*, 124:3900–3904, 2012. doi: 10.1002/app. URL http://onlinelibrary.wiley.com/doi/10.1002/app.35507/full.

[78] E. Berkenwald, C. Spies, J. R. Cerna Cortez, G. Morales, and D. A. Estenoz. Mathematical model for the bulk polymerization of styrene using the symmetrical cyclic trifunctional initiator diethyl ketone triperoxide. I. Chemical initiation by sequential decomposition. *Journal of Applied Polymer Science*, 128(1):776–786, April 2013. ISSN 00218995. doi: 10.1002/app.38221. URL http://doi.wiley.com/10.1002/app.38221.

[79] E. Berkenwald, C. Spies, G. Morales, and D. A. Estenoz. Mathematical model for the bulk polymerization of styrene chemically initiated by sequential and total decomposition of the trifunctional initiator diethyl ketone. *Polymer Engineering and Science*, pages 1–11, 2014. doi: 10.1002/pen. URL http://onlinelibrary.wiley.com/doi/10.1002/pen.23876/full.

[80] M. Asteasuain, A. Brandolin, and C. Sarmoria. Recovery of molecular weight distributions from transformed domains . Part II . Application of numerical inversion methods. *Polymer*, 43, 2002.

[81] M. Asteasuain, C. Sarmoria, and A. Brandolin. Recovery of molecular weight distributions from transformed domains. Part I. Application of pgf to mass balances describing reactions involving free radicals. *Polymer*, 43, 2002. URL http://www.sciencedirect.com/science/article/pii/S0032386102000344.

[82] K. F. O'Driscoll and J. C. Bevington. The effect of multifunctional initiators on molecular weight in free radical polymerization. *European polymer journal*, 21(12):1039–1043, 1985. URL http://www.sciencedirect.com/science/article/pii/0014305785902113.

[83] J. Lu, H. Zhang, and Y. Yang. Monte Carlo simulation of kinetics and chain-length distribution in radical polymerization. *Die Makromolekulare Chemie, Theory and Simulations*, 2(5):747–760, September 1993. ISSN 10185054. doi: 10.1002/mats.1993.040020511. URL http://doi.wiley.com/10.1002/mats.1993.040020511.

[84] I. M. Maafa, J. B. P. Soares, and A. Elkamel. Prediction of Chain Length Distribution of Polystyrene Made in Batch Reactors with Bifunctional Free-Radical Initiators Using Dynamic Monte Carlo Simulation. *Macromolecular Reaction Engineering*, 1(3):364–383, May 2007. ISSN 1862832X. doi: 10.1002/mren.200700007. URL http://doi.wiley.com/10.1002/mren.200700007.

[85] D. A. Estenoz and G. R. Meira. Grafting of styrene onto polybutadiene: Calculation of the molecular macrostructure. *Journal of applied polymer science*, 50: 1081–1098, 1993. URL http://onlinelibrary.wiley.com/doi/10.1002/app.1993.070500617/abstract.

[86] D. A. Estenoz, E. Valdez, H. M. Oliva, and G. R. Meira. Bulk polymerization of styrene in presence of polybutadiene: Calculation of molecular macrostructure. *Journal of Applied Polymer Science*, 59(5):861–885, January 1996. ISSN 00218995. doi: 10.1002/(SICI)1097-4628(19960131)59:5⟨861::AID-APP12⟩3.3.CO;2-J. URL http://doi.wiley.com/10.1002/(SICI)1097-4628(19960131)59:5<861::AID-APP12>3.3.CO;2-J.

[87] S. I. Kuchanov, N. G. Ivanova, and S. S. Ivanchev. Molecular weight distribution of products of radical polymerization initiated using polyfunctional initiators. *Polymer Science USSR*, 1970(8):1870–1877, 1976. URL http://www.sciencedirect.com/science/article/pii/0032395076904032.

[88] V. A. Ivanov, S. I. Kuchanov, and S.S. Ivanchev. The theory of radical polymerization with polyfunctional initiators. *Polymer Science USSR*, 1974 (8):1923–1932, 1977. URL http://www.sciencedirect.com/science/article/pii/0032395077904051.

[89] J. R. Cerna, G. Morales, G. N. Eyler, and A. I. Cañizo. Bulk polymerization of styrene catalyzed by bi- and trifunctional cyclic initiators. *Journal of Applied Polymer Science*, 83(1):1–11, January 2002. ISSN 0021-8995. doi: 10.1002/app.2225. URL http://doi.wiley.com/10.1002/app.2225.

[90] I. C. Núñez. *Estudio del efecto de un iniciador trifuncional en la copolimerización estireno-alfametilestireno*. Tesis de maestría, Universidad Iberoamericana, 2006.

[91] M. J. Scorah, R. Dhib, and A. Penlidis. Recent Advances in the Study of Multifunctional Initiators in Free Radical Polymerizations. *Macromolecular Reaction Engineering*, 1(2):209–221, February 2007. ISSN 1862832X. doi: 10.1002/mren.200600040. URL http://doi.wiley.com/10.1002/mren.200600040.

[92] J. H. Duerksen and A. E. Hamielec. Polymer reactors and molecular weight distribution. IV. Free-radical polymerization in a steady-state stirred-tank reactor train. *Journal of Polymer Science Part C: Polymer Symposia*, 25(1): 155–166, March 2007. ISSN 04492994. doi: 10.1002/polc.5070250118. URL http://doi.wiley.com/10.1002/polc.5070250118.

[93] N. Casis, D. A. Estenoz, L. M. Gugliotta, H. M. Oliva, and G. R. Meira. Heterogeneous bulk polymerization of styrene in the presence of polybutadiene: Calculation of the macromolecular structure. *Journal of Applied Polymer Science*, 99(6):3023–3039, March 2006. ISSN 0021-8995. doi: 10.1002/app.22902. URL http://doi.wiley.com/10.1002/app.22902.

[94] Fred M. Peng. Polybutadiene Grafting and Crosslinking in High-Impact Polystyrene Bulk Thermal Process. *Journal of Applied Polymer Science*, 40:1289–1302, 1990.

[95] B. J. Meister and A. E. Platt. Evaluation of the performance of a commercial polystyrene devolatilizer. *Industrial & Engineering Chemistry Research*, 28(11): 1659–1664, November 1989. ISSN 0888-5885. doi: 10.1021/ie00095a014. URL http://pubs.acs.org/doi/abs/10.1021/ie00095a014.

[96] A. V. Tobolsky. Dead-End Radical Polymerization. *Journal of the American Chemical Society*, 80(1):5927–5929, 1958.

[97] A. V. Tobolsky, C. E. Rogers, and R. D. Brickman. Dead-End Radical Polymerization. II. *Journal of Process Control*, 82(1):1277–1280, 1960.

[98] K. C. Seavey, Y. A. Liu, N. P. Khare, T. Bremner, and C. Chen. Quantifying Relationships among the Molecular Weight Distribution, Non-Newtonian Shear Viscosity, and Melt Index for Linear Polymers. *Industrial & Engineering Chemistry Research*, 42(21):5354–5362, October 2003. ISSN 0888-5885. doi: 10.1021/ie021003i. URL http://pubs.acs.org/doi/abs/10.1021/ie021003i.

[99] E. Berkenwald, L. Laganá, P. Acuña, G. Morales, and D. Estenoz. Bulk Polymerization of Styrene using Multifunctional Initiators in a Batch Reactor : A Comprehensive Mathematical Model. *International Journal of Chemical Reactor Engineering*, 14(1):315–329, 2016. doi: 10.1515/ijcre-2015-0102.

[100] K. Delgado Rodriguez, Graciela Morales, J. Enríquez, and G. Barreto. Thermal decomposition of PDP and DEKTP in methyl methacrylate and its further polymerization kinetic study. In *Macromex 2014*, 2014.

[101] G. Dagli, A.S. Argon, and R.E. Cohen. Particle-size effect in craze plasticity of high-impact polystyrene. *Polymer*, 36(11):2173–2180, 1995.

[102] S. Joseph and S. Thomas. Morphology, morphology development and mechanical properties of polystyrene/polybutadiene blends. *European Polymer Journal*, 39 (1):115–125, January 2003. ISSN 00143057. doi: 10.1016/S0014-3057(02)00180-5. URL http://linkinghub.elsevier.com/retrieve/pii/S0014305702001805.

[103] W. A. Ludwico and S. L. Rosen. The kinetics of two-phase bulk polymerization. I. Monomer and initiator distribution. *Journal of Applied Polymer Science*, 19(3): 757–768, 1975. ISSN 00218995. doi: 10.1002/app.1975.070190313. URL http://doi.wiley.com/10.1002/app.1975.070190313.

[104] M. Fischer and G. P. Hellmann. On the Evolution of Phase Patterns during the High-Impact-Modified Polystyrene Process. *Macromolecules*, 29(7):2498–2509, January 1996. ISSN 0024-9297. doi: 10.1021/ma950779a. URL http://pubs.acs.org/doi/abs/10.1021/ma950779a.

[105] A Brydon, G. M. Burnett, and G. G. Cameron. Free-Radical Grafting of Monomers to Polydienes . I . Effect of Reaction Conditions on Grafting of Styrene to Polybutadiene. 11(1):3255–3269, 1973.

[106] G. F. Freeguard and M. Karmarkar. The production of rubber-modified polystyrene. II. The significance of shear in the phase inversion. *Journal of Applied*

Polymer Science, 15(7):1657–1663, July 1971. ISSN 00218995. doi: 10.1002/app.1971.070150709. URL http://doi.wiley.com/10.1002/app.1971.070150709.

[107] S. Zhiqiang, Y. Huigen, and P. Zuren. Studies on the rheological behavior of high-impact polystyrene prepolymerizing systems. *Journal of Applied Polymer Science*, 32(2):3349–3369, August 1986. ISSN 00218995. doi: 10.1002/app.1986.070320201. URL http://doi.wiley.com/10.1002/app.1986.070320201.

[108] J. Y. Park and O. O. Park. Secondary phase inversion induced by addition of polystyrene during prepolymerization of high-impact polystyrene in a batch reactor. *Advances in Polymer Technology*, 15:145–150, 1996. URL http://onlinelibrary.wiley.com/doi/10.1002/(SICI)1098-2329(199622)15:2%3C145::AID-ADV4%3E3.0.CO;2-V/abstract.

[109] G. P. Leal and J. M. Asua. Evolution of the morphology of HIPS particles. *Polymer*, 50(1):68–76, January 2009. ISSN 00323861. doi: 10.1016/j.polymer.2008.10.035. URL http://linkinghub.elsevier.com/retrieve/pii/S003238610800952X.

[110] R. Díaz de León and G. Morales. Phenomenon of phase inversion in high impact polystyrene: Physico-chemical, rheological and morphological study in the presence of chain transfer agent and using different tapered block copolymers. *Polymer Engineering & ...*, 2010. doi: 10.1002/pen. URL http://onlinelibrary.wiley.com/doi/10.1002/pen.21523/abstract.

[111] M. Vonka and J. Kosek. Modelling the morphology evolution of polymer materials undergoing phase separation. *Chemical Engineering Journal*, 207-208:895–905, October 2012. ISSN 13858947. doi: 10.1016/j.cej.2012.06.091. URL http://linkinghub.elsevier.com/retrieve/pii/S1385894712008121.

[112] F. Soriano-Corral, G. Morales, P. Acuña, E. Díaz-Barriga, B. Arellano, C. Vargas, and O. De la Paz. Synthesis and Characterization of High Impact Polystyrene from a Heterogeneous Styrene-Rubber-Polystyrene Solution: Influence of PS Concentration on the Phase Inversion, Morphology and Impact Strength. *Macromolecular Symposia*, 325-326(1):177–183, March 2013. ISSN 10221360. doi: 10.1002/masy.201200059. URL http://doi.wiley.com/10.1002/masy.201200059.

[113] R. López-Negrete de la Fuente, J. Lopez-Rubio, A. Flores-Tlacuahuac, and E. Saldívar-Guerra. Steady-State Multiplicity Behavior Analysis of a High-Impact Polystyrene Continuous Stirred Tank Reactor Using a Bifunctional Initiator. *Industrial & Engineering Chemistry Research*, 45(5):1689–1707, March 2006. ISSN 0888-5885. doi: 10.1021/ie0487383. URL http://pubs.acs.org/doi/abs/10.1021/ie0487383.

[114] D. A. Estenoz, I. M. González, H. M. Oliva, and G. R. Meira. Polymerization of styrene in the presence of polybutadiene: determination of the molecular structure. *Journal of Applied Polymer Science*, 74:1950–1961, 1999. URL http://onlinelibrary.wiley.com/doi/10.1002/(SICI)1097-4628(19991121)74:8%3C1950::AID-APP9%3E3.0.CO;2-L/abstract.

[115] R. L. Kruse. Viscosities and Normal Stress Coefficients of High Impact Polystyrene Fluids, 1980. ISSN 01486055.

[116] R. J. Albalak, Z. Tadmor, and Y. Talmon. Polymer Melt Devolatilization Mechanisms. *AIChE Journal*, 36(9):1313–1320, 1990.

[117] J. D. Stein, G. Fahrbach, and H. Adler. Crosslinking Reactions in High Impact Polystyrene Rubber Particles. *Advances in Chemistry Series*, 1975.

[118] K. Kirchner and K. Riederle. Thermal Polymerization of Styrene - The Formation of Oligomers and Intermediates, I. *Die Angewandte Makromolekulare Chemie*, 111(1703):1–16, 1983. URL http://onlinelibrary.wiley.com/doi/10.1002/apmc.1983.051110101/abstract.

[119] J. D. Campbell, F. Teymour, and M. Morbidelli. High Temperature Free Radical Polymerization. 1. Investigation of Continuous Styrene Polymerization. *Macromolecules*, 36(15):5491–5501, July 2003. ISSN 0024-9297. doi: 10.1021/ma0206422. URL http://pubs.acs.org/doi/abs/10.1021/ma0206422.

[120] D. C.; Chhabra R. P. Carreau, P. J.; De Kee. Rheology of polymeric systems, principles and applications. *AIChE Journal*, 45(8):1836–1837, 1999. ISSN 1547-5905. doi: 10.1002/aic.690450819. URL http://dx.doi.org/10.1002/aic.690450819.

[121] B. Elbirli and M. T. Shaw. Time Constants from Shear Viscosity Data. *Journal of Rheology*, 22(5):561, 1978. ISSN 01486055. doi: 10.1122/1.549489. URL http://link.aip.org/link/?JORHD2/22/561/1.

[122] J. Z. Liang and J. N. Ness. Effect of die angle on flow behaviour for high impact polystyrene melt. *Polymer Testing*, 16(4):403–412, 1997. URL http://www.scopus.com/inward/record.url?eid=2-s2.0-0031199333&partnerID=40&md5=bb1b84d8592278c7969f28c2411fd80a.

[123] J. Rohlfing, C. D.; Janzen. What's happening in the melt-flow plastometer: The role of elongational viscosity. *Society of Plastics Engineers, Inc. (SPE)*, 1997.